PNL-5818
UC-94e

18L

An Initial Study of Thermal Energy Storage in Unconfined Aquifers

April 1986

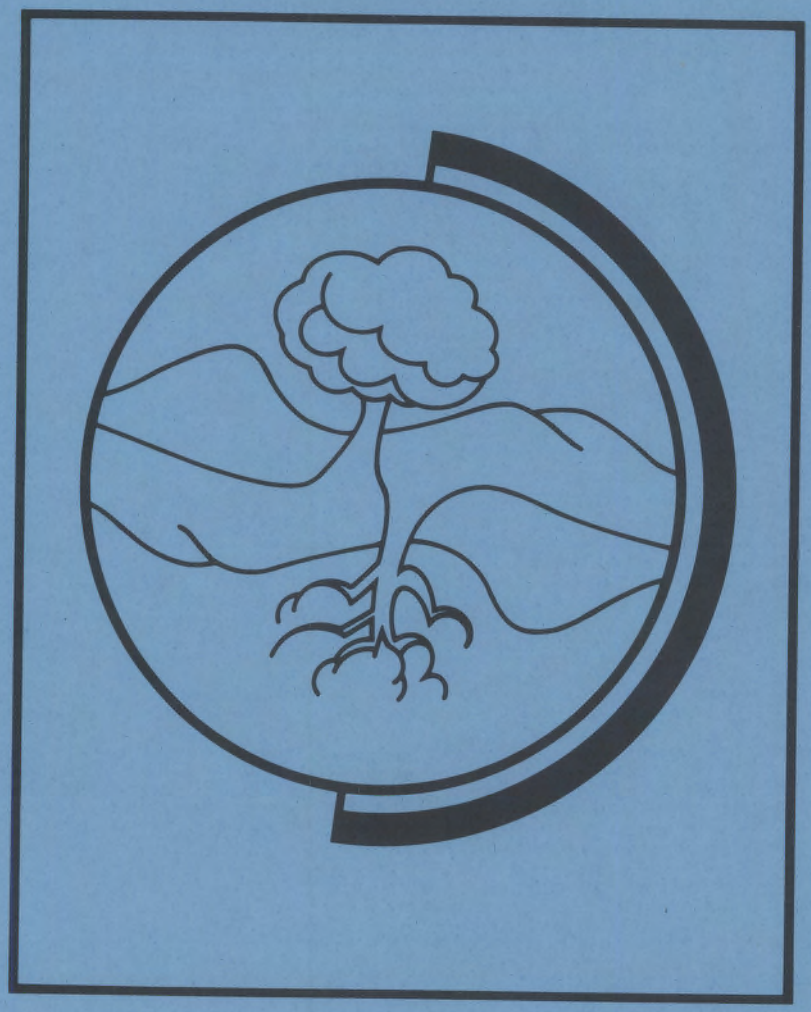

Prepared by the University of Minnesota
for Pacific Northwest Laboratory under
Contract DE-AC06-76RLO 1830
with the U.S. Department of Energy

Pacific Northwest Laboratory
Operated for the U.S. Department of Energy
by Battelle Memorial Institute

Battelle

PNL-5818

DISCLAIMER

This report was prepared as an account of work sponsored by an agency of the United States Government. Neither the United States Government nor any agency thereof, nor any of their employees, makes any warranty, express or implied, or assumes any legal liability or responsibility for the accuracy, completeness, or usefulness of any information, apparatus, product, or process disclosed, or represents that its use would not infringe privately owned rights. Reference herein to any specific commercial product, process, or service by trade name, trademark, manufacturer, or otherwise, does not necessarily constitute or imply its endorsement, recommendation, or favoring by the United States Government or any agency thereof. The views and opinions of authors expressed herein do not necessarily state or reflect those of the United States Government or any agency thereof.

PACIFIC NORTHWEST LABORATORY
operated by
BATTELLE
for the
UNITED STATES DEPARTMENT OF ENERGY
under Contract DE-AC06-76RLO 1830

Printed in the United States of America
Available from
National Technical Information Service
United States Department of Commerce
5285 Port Royal Road
Springfield, Virginia 22161

NTIS Price Codes
Microfiche A01

Printed Copy

Pages	Price Codes
001-025	A02
026-050	A03
051-075	A04
076-100	A05
101-125	A06
126-150	A07
151-175	A08
176-200	A09
201-225	A010
226-250	A011
251-275	A012
276-300	A013

3 3679 00058 6711

PNL-5818
UC-94e

AN INITIAL STUDY OF THERMAL ENERGY STORAGE IN UNCONFINED AQUIFERS

H. M. Haitjema
O. D. L. Strack

University of Minnesota
Minneapolis, Minnesota

April 1986

Prepared by
the University of Minnesota
for Pacific Northwest Laboratory
under Contract DE-AC06-76RLO 1830
with the U.S. Department of Energy
Subcontract No. B-E1234-A-0

Pacific Northwest Laboratory
Richland, Washington 99352

FOREWORD

Seasonal thermal energy storage (STES) involves storing thermal energy, such as winter chill, summer heat, and industrial waste heat for future use in heating and cooling buildings or for industrial processes. Widespread development and implementation of STES would significantly reduce the need to generate primary energy in the U.S. In fact, 198D data indicate that STES is technically suitable for providing 5 to 10% of the nation's energy with major contributions in the commercial, industrial, and residential sectors.

Aquifer thermal energy storage (ATES) is predicted to be the most cost-effective technology for seasonal storage of low-grade thermal energy. Approximately 60% of the U.S. is underlain with aquifers potentially suitable for underground energy storage. Under sponsorship of the U.S. Department of Energy, Pacific Northwest Laboratory (operated by Battelle Memorial Institute) has managed numerical modeling, laboratory studies, evaluation of environmental and institutional issues, and field testing of ATES at several sites.

This report describes the computer program UCATES, developed by Dr. H. Haitejema as a first step toward developing a comprehensive screening tool for ATES systems in unconfined aquifers. The program is capable of predicting the relative effects of regional flow on the efficiency of ATES systems, as well as predicting the effects of water table variation due to ATES pumping and injection. The code can be applied in its present form to virtually any unconfined ATES analysis. The model described here uses a somewhat unrealistic treatment of heat loss to overburden and underlaying soil. Inclusion of a more realistic heat loss mechanism within UCATES would improve the code making more reliable predictions of absolute ATES efficiencies possible. However, the predictions of the code described in this document should be adequate for preliminary design, evaluation, and optimization of unconfined ATES systems.

Landis D. Kannberg, Manager
Underground Energy Storage Program

SUMMARY

Convective heat transport in unconfined aquifers is modeled in a semi-analytic way. The transient groundwater flow is modeled by superposition of analytic functions, whereby changes in the aquifer storage are represented by a network of triangles, each with a linearly varying sink distribution. This analytic formulation incorporates the nonlinearity of the differential equation for unconfined flow and eliminates numerical dispersion in modeling heat convection.

The thermal losses through the aquifer base and vadose zone are modeled rather crudely. Only vertical heat conduction is considered in these boundaries, whereby a linearly varying temperature is assumed at all times. The latter assumption appears reasonable for thin aquifer boundaries. However, assuming such thin aquifer boundaries may lead to an overestimation of the thermal losses when the aquifer base is regarded as infinitely thick in reality.

The approach, indicated above, is implemented in the computer program UCATES, which serves as a first step toward the development of a comprehensive screening tool for ATES systems in unconfined aquifers. In its present form, the program is capable of predicting the relative effects of regional flow on the efficiency of ATES systems. However, only after a more realistic heatloss mechanism is incorporated in UCATES will reliable predictions of absolute ATES efficiencies be possible.

ACKNOWLEDGEMENTS

This research, supported by the Underground Energy Storage (UES) program, was conducted by the University of Minnesota for Pacific Northwest Laboratory (PNL). PNL is managed by Battelle Memorial Institute for the Department of Energy (DOE) under contract DE-AC06-76RLO 1830. The research has been conducted under subcontract B-E1234-A-0.

Strack developed the triangular areal sinks and also suggested its use for modeling transient unconfined groundwater flow.

Initial work on programming and validating the triangular areal sink distributions, applied in this study, has been done by Christine Detournay.

CONTENTS

	Page
SUMMARY	v
ACKNOWLEDGEMENTS	vii
LIST OF FIGURES	xi
LIST OF TABLES	xii
LIST OF SYMBOLS	xiii
1.0 INTRODUCTION	1
2.0 HEAT BALANCE EQUATION FOR CONVECTIVE HEAT TRANSPORT IN UNCONFINED AQUIFERS	3
2.1 THREE-DIMESNIONAL HEAT FLOW EQUATION	3
2.2 TWO-DIMENSIONAL HEAT FLOW EQUATION FOR UNCONFINED AQUIFERS	4
3.0 ANALYSIS OF HEAT LOSS THROUGH THE UPPER AND LOWER AQUIFER BOUNDARY	7
3.1 APPROXIMATE HEAT LOSS MECHANISM	7
3.2 TRANSIENT HEAT LOSS THROUGH A THIN AQUIFER TOP	9
Numerical Inversion of the Laplace Transform	13
3.3 COMPARISON OF THE EXACT AND APPROXIMATE SOLUTION	14
Improved Approximate Heat Loss Mechanism	15
3.4 HEAT LOSS THROUGH AN INFINITELY THICK AQUIFER BASE AND A THIN AQUIFER TOP	20
4.0 THERMAL ENERGY STORAGE FOR THE CASE OF RADIAL FLOW	25
4.1 CONFINED FLOW CONDITIONS	25
End of Injection	26
End of Storage	27
End of Recovery	27
Temperature Distribution in the Well	28
Thermal Efficiency	29
4.2 UNCONFINED FLOW CONDITIONS	30
End of Injection	34
End of Storage	35
End of Recovery	36
Temperature Distribution in the Well	38
Thermal Efficiency	38
4.3 REMARKS	39

5.0 MODELING THERMAL ENERGY STORAGE IN UNCONFINED AQUIFERS 41
5.1 SOLVING THE HEAT TRANSPORT PROBLEM 41
Temperature Distribution in the Aquifer 42
5.2 SOLVING THE TRANSIENT GROUNDWATER FLOW PROBLEM 43
Alternative Solution Procedure 45

6.0 PROGRAM UCATES 49
6.1 MATRIX EQUATIONS 49
6.2 THERMAL MARKERS 51

7.0 VALIDATIONS 53
7.1 WELL AT THE CENTER OF A CIRCULAR ISLAND 53
7.2 WELL NEAR A CANAL 56
7.3 THERMAL ENERGY STORAGE FOR THE CASE OF RADIAL FLOW 59

8.0 EXAMPLES 65
8.1 A SINGLE WELL ATES SYSTEM IN A UNIFORM FLOW FIELD 65
8.2 A SINGLE WELL ATES SYSTEM NEAR CREEKS AND A DOMESTIC WELL 67
8.3 REMARKS 69

REFERENCES R.1

APPENDIX A FLOW DUE TO A TRIANGULAR AREAL SOURCE WITH LINEARLY VARYING STRENGTH A.1

APPENDIX B MANUAL FOR PROGRAM UCATES B.1

FIGURES

3.1. Linear Temperature Distribution in the Aquifer Boundaries 8

3.2. Steady Radial Flow with Heat Injection for $r = 0$ at $t \geq 0$ 10

3.3. Temperature Distribution in the Aquifer for $H/\hat{d} = 10$, with Both the Exact and the Approximate Heat Loss Mechanisms 16

3.4. Temperature Distribution in the Aquifer for $H/\hat{d} = 10$, with Both the Exact and the Approximate Improved Heat Loss Mechanisms 18

3.5. Temperature Distribution in the Aquifer for $H/d^2 = 10$ Plotted as a Function of the Dimensionless Radial Distance $\tilde{r}$ 18

3.6. Comparison between Exact and Approximate Heat Loss Mechanism for $H/\hat{d} = 5$ 19

3.7. Comparison between Exact and Approximate Heat Loss Mechenism for $H/\hat{d} = 20$ 19

3.8. Confined Aquifer with an Infinitely Thick Aquifer Base and Insulated Aquifer Top 21

3.9. Confined Aquifer with a Thin Upper Boundary and Insulated Base 21

3.10. Temperature Distribution in the Aquifer for a Thin Aquifer Top and Both a Thin ($H/\hat{d} = 10$) and an Infinitely Thick Aquifer Base 23

3.11. Temperature Distibution in the Aquifer for a Thin Aquifer Top and Both a Thin ($H/\hat{d} = 5$) and an Infinitely Thick Aquifer Base 23

4.1. Temperature Distribution in a Confined Aquifer at the End of Injection 27

4.2 Temperature Distribution in a Confined Aquifer at the End of Storage 28

4.3. Temperature Distribution in the Well During Recovery of Thermal Energy from a Confined Aquifer 29

4.4. Thermal Efficiency for a Storage System in a Confined Aquifer 30

4.5. Temperature Distribution in an Unconfined Aquifer at the End of Injection 36

4.6. Temperature Distribution in an Unconfined Aquifer at the End of Storage 37

4.7. Temperature Distribution iu the Well During Recovery of Thermal Energy from an Unconfined Aquifer 38

7.1. Well at the Center of a Triangle Network 54

7.2. Drawdowns Obtained with Program UCATES Compared with Finite Difference Solutions 56

7.3. Well near a Finite Canal 57

7.4. Contour Plots of Piezometric Heads for $t = 2$ 58

7.5. Contour Plots of Piezometric Heads for $t = 10$ 59

7.6. Isotherms at the End of Injection Obtained with UCATES for the

Radial Flow Case 61
7.7. Isotherms at the End of Storage Obtained with UCATES for the Radial Flow Case 62
7.8. Temperature Distribution in the Well During Recovery Obtained with UCATES 63
8.1. Predicted Isotherms at the End of the ATES Phases for the Case of a Zero Uniform Flow Rate 66
8.2. Predicted Temperatures in the Well During Recovery for the Case of a Zero Uniform Flow 67
8.3. Predicted Isotherms at the End of the ATES Phases for the Case of Uniform Flow 68
8.4. Predicted Temperatures in the Well During Recovery for the Case of Uniform Flow 69
8.5. Predicted Isotherms at the End of Recovery and Temperatures in the Well for the Case of a Separate Recovery Well in a Uniform Flow Field 70
8.6. Predicted Isotherms at a Site Surrounded by Creeks and Canals, and Including a Domestic Well 71
8.7. Predicted Isotherms at the End of the Storage and Recovery Phases at a Site Surrounded by Creeks, Canals, and Including a Domestic Well 72
8.8. Predicted Temperatures in the Recovery Well at a Site Surrounded by Creeks and Canals, and Inclnding Domestic Well 73
A.1. Linearly Varying Source Distribution Over a Triangle A.1
A.2. Local Coordinate System for a Triangle A.2
A.3. Local Coordinate Systems at Normalized Triangle Sides A.3

TABLES

4.1. Thermal Efficiency for Storage in an Unconfined Aquifer 38

LIST OF SYMBOLS

A_{ij}	matrix coefficients (various dimensions)
c, c_s, c_w	specific heat of the aquifer, solids and water, respectively [m^2/s^2K^0]
C, C_s, C_w	heat capacity of the aquifer, solids and water, respectively [$kg/m\ s^2K^0$]
$\overset{1}{C}, \overset{2}{C}$	heat capacity of the lower and upper aquifer boundary, respectively
C'	heat capacity of the aquifer including the upper aquifer boundary
C^*	heat capacity of the aquifer, including the upper and lower aquifer boundary
$\tilde{C}, \tilde{C}_1, \tilde{C}_2$	dimensionless heat capacities of the aquifer and its lower and upper boundary, respectively
$\overset{1}{d}, \overset{2}{d}$	thickness of the lower and upper aquifer boundary, respectively [m]
E_1	exponential integral [-]
$\overset{1}{F}, \overset{2}{F}$	heat flux through the lower and upper aquifer boundary, respectively [kg/s^3]
$\overset{ls}{F}$	influence function for line sinks [m]
$\overset{tr}{F}$	influence function for triangular areal sinks [m^2]
g	acceleration of gravity [m/s^2]
G	given contribution to the potential function [m^3/s]
H	thickness of a confined aquifer [m]
k	Darcian permeability (hydraulic conductivity) [m/s]
n	aquifer porosity

p	pore pressure [kg/ms^2] Laplace inversion parameter
q_i	specific discharge vector [m/s]
Q_i	discharge vector [m^2/s]
$Q_{(i)}$	discharge of ith well [m^3]
$Q_m^{(t)}$	discharge of mth line sink at time t [m^2/s]
$\tilde{Q}$	dimensionless well discharge
r	radial distance [m]
r_o	well radius [m]
$\bar{r}$	dimensionless radial distance in a confined aquifer
$\tilde{r}$	dimensionless radial distance in an unconfined aquifer
$\tilde{r}_o$	dimensionless well radius
$\hat{S}$	rate of heat storage in upper aquifer boundary [kg/s^3]
t	time since start of injection
t^*	residence time of a thermal front [s]
$t_{(i)}$	time at which the ith well starts pumping
$\bar{t}$	dimensionless form of t in a confined aquifer
$\tilde{t}$	dimensionless form of t in an unconfined aquifer
t'	time since start of recovery
$\tilde{t}'$	dimensionless form of t involving C'
Δt_i	injection period
Δt_s	storage period
Δt_r	recovery period
Δt	injection, storage and recovery period

	time step
$\Delta\tilde{t}$	dimensionless form of Δt.
T	temperature in the aquifer measured with respect to the initial temperature [K°]
$\overset{1}{T},\overset{2}{T}$	temperature in the lower and upper aquifer boundary, respectively
T_0	injection temperature
$\tilde{T},\tilde{T}_1,\tilde{T}_2$	dimensionless form of T, $\overset{1}{T}$ and $\overset{2}{T}$, respectively
u^2	argument of the exponential integral E_1 for injection phase
u_1^2	argument of the exponential integral E_1 for storage phase
u_2^2	argument of the exponential integral E_1 for recovery phase
u_i^2	argument of E_1 for the ith well
U	Heaviside's unit step formation
v_i	average groundwater velocity [m/s]
v_r	average radial groundwater velocity
v_i^*	velocity of a thermal front
v_r^*	radial velocity of a thermal front
x,y	coordinates in a right-handed Cartesian coordinate system [m]
$\tilde{x},\tilde{y}$	dimensionless form of x and y
x_i	coordinates in a right-handed Cartesian coordinate system solution vector in a matrix equation
$x_{i\alpha}^w$	coordiuates of the ith well
y_i	known vector in a matrix equation

$z = x_1 + ix_2$	complex coordinate in two-dimensional space
z_1, z_2	endpoints of a line sink
z	vertical coordinate
$\tilde{z}$	dimensionless vertical coordinate
α	index used for vectors in two-dimensional space dimensionless coefficient involving heat condnctivities
α_o	dimensionless constant involving heat capacities
β	proportionality constant relating heat flux through the aquifer boundaries to temperature in the aquifer $[s^{-1}]$
$\bar{\beta}$	average value of β
$\tilde{\beta}$	dimensionless form of β
γ	dimensionless constant involving heat capacities and heat conductivities
γ_o	dimensionless constant involving heat capacities and the thicknesses of the aquifer and its confining layers.
δ_{ij}	Kronecker delta
η	thermal efficiency
θ	$\hat{C}/C$
ϕ	piezometric head [m]
$\tilde{\phi}$	dimensionless form of ϕ
$\bar{\phi}, \phi'$	constant (reference) piezometric head
ϕ_o	initial head in the aquifer
$\tilde{\phi}'$	dimensionless form of ϕ'
$\bar{\phi}_{(i)}$	head at the ith well at the onset of pumping
Φ	groundwater flow discharge potential $[m^3/s]$

Φ_0	constant reference potential
$\Phi_i^{(t)}$	potential at the ith control point at time t
$\overset{c}{\Phi}(t)$	constant potential at time t
$\overset{w}{\Phi}(t)_{(i)}$	potential at time t generated by the ith transient well
$\overset{e}{\Phi}(t)$	potential due to all flow features in the aquifer except transient wells
χ_i	coefficients of the heat flow equation
Ω	complex potential function
$\lambda, \lambda_s, \lambda_w$	heat conductivity of the aquifer, solids and water, respectively [kgm/s^3K^0]
$\overset{1}{\lambda}, \overset{2}{\lambda}$	heat conductivity of the lower and upper aquifer boundary, respectively
ρ_s, ρ_w	density of the solids and water, respectively [kg/m^3]
ρ_w	density of water
σ	areal sink density distribution representing changes in aquifer storage [m/s]
$\sigma_i^{(t)}$	strength at the ith nodal point in the triangle network at time t
$\overset{w}{\sigma}$	areal sink density distribution associated with $\partial\overset{w}{\Phi}/\partial t$
$\overset{e}{\sigma}$	areal sink density distribution associated with $\partial\overset{e}{\Phi}/\partial t$

1.0 INTRODUCTION

Most studies on Aquifer Thermal Energy Storage (ATES) deal with heat or chill storage in confined aquifers (Tsang et al. 1980; Mercer et al. 1982). Particularly for the case of deep confined aquifers, relatively high recovery rates of thermal energy seem possible. For such deep aquifers, the design of a thermal energy system may be based on a single well to be used for both injection and recovery of hot water. If existing groundwater flow velocities are small, it is often sufficient to study radial groundwater flow and heat transport in the vicinity of the injection/recovery well (Doughty et al. 1982; Sauty et al. 1982). Nonsymmetrical flow cases have been investigated by Gringarten and Sauty (1975) among others, who studied a well doublet in a uniform regional flow field. One well was used for the production of geothermal energy and the other well for disposal of the heat-depleted water. The authors investigated the effects of breakthrough on the production temperatures by application of Lauwerier's solution for transient heat flow in aquifers with infinitely thick upper and lower boundaries. Multiple well systems have been modeled by Vail and Kincaid (1983), who applied their computer program to a hypothetical 25 well ATES system. Vail and Kincaid solved heat convection in the horizontal plane by integrating analytical expressions for velocity. They solved heat conduction in the vertical plane by use of a finite-difference algorithm. All of the studies mentioned above dealt with confined aquifers and assumed steady groundwater flow. Indeed, even under transient flow conditions in confined aquifers, solutions to steady groundwater flow are often acceptable because of the small storage coefficient involved.

The costs associated with installing an ATES system in deep confined aquifers form an incentive to study the use of shallow unconfined aquifers, where installment costs for wells are relatively low. There are some complicating factors, however, which may be summarized as follows:

- The maximum possible injection and recovery rate of a single well in a shallow unconfined aquifer is usually significantly less than that of a well in a deep aquifer.
- Unconfined aquifers often exhibit complex flow conditions, which are caused by such features as rainfall, creeks and canals.
- Transient flow conditions cannot be ignored because of the relatively large storage coefficient for unconfined aquifers.

In view of these factors, feasibility studies for thermal energy storage in shallow unconfined aquifers should not be limited to the case of radial heat transport near a single well. It may be anticipated that multiple well systems are needed and that the natural, transient flow conditions have a large impact on the performance of the system. Furthermore, ATES studies in unconfined aquifers require solutions to transient groundwater flow.

The present study focusses on the develpment of a model to simulate ATES systems in unconfined aquifers under regional flow conditions. As a first approximation, heat transport in the aquifer is modeled as purely convective. Horizontal heat conduction is disregarded and heat loss through the aquifer base and vadose zone is treated in a highly simplified manner. The heat loss is based solely on vertical heat conduction through the aquifer boundaries, whereby a linear temperature distribution is assumed at all times. Ignoring the transient effects of the heat conduction in these aquifer boundaries seems acceptable, provided they are relatively thin. To solve the heat transport equation, a solution to the nonlinear transient groundwater flow problem is sought by superposition of analytic functions. The latter approach has been applied earlier in modeling steady flow in a double aquifer system (Strack and Haitjema 1981). The groundwater flow problem, in this study, is uncoupled from the heat flow problem, ignoring such effects as buoyancy and varying permeabilities. As presented in this study, the solution procedure for transient groundwater flow involves an approach, suggested by Strack, whereby newly developed areal source distributions are used to model changes in the aquifer storage. The analytic formulation of the groundwater flow problem makes it possible to solve the heat transport equation along its characteristics, avoiding the numerical dispersion problems frequently associated with numerical models, as reported for instance by Hellström and Claesson (1978).

The computer model UCATES, developed during this initial study, is intended as a first step toward a comprehensive screening tool for projected ATES systems in unconfined aquifers. The present version of UCATES may be improved upon by including a more sophisticated heat loss mechanism that should incorporate the effects of transient heat conduction in the aquifer base and vadose zone. Another improvement may be obtained by incorporating infiltration due to rainfall, which may significantly affect the thermal efficiency of an ATES system.

The following sections are included in this report. In Section 2 the heat balance equation is preaented for the case of heat transport in unconfined aquifers, whereby the Dupuit-Forchheimer assumption is adopted. In Section 3 a simplified heat loas mechanism is developed and compared to more sophisticated solutions for the case of steady confined groundwater flow. In Section 4 a simple ATES simulation is discussed for the case of radial flow. The simulation is based on heat convection only and incorporates the simplified heat losa mechanism developed in Section 3. In Section 5, the solution procedures for the heat transport equation and for the transient groundwater flow problem are outlined. The implementation of these procedures in program UCATES is briefly discussed in Section 6. Program validation is carried out in Section 7 followed by two examples of ATES simulations in Section 8.

It is noted that throughont this report, reference is made to heat flow and heat storage, but the results of this study apply equally well to ATES systems for chill storage.

2.0 HEAT BALANCE EQUATION FOR CONVECTIVE HEAT TRANSPORT IN UNCONFINED AQUIFERS

In this section the differential equation for heat flow in unconfined aquifers will be derived by integrating the three-dimensional heat flow equation over the saturated thickness of the aquifer.

2.1 THREE-DIMENSIONAL HEAT FLOW EQUATION

The differential equation for the temperature, T, in a porous medium is given by (Sauty et al. 1982)

$$\lambda \nabla^2 T = C_w q_i \frac{\partial T}{\partial x_i} + C\frac{\partial T}{\partial t} \qquad (i = 1,2,3) \tag{2.1}$$

where λ is the thermal conductivity of the aquifer and where q_i are the components of the specific discharge vector. In writing (2.1) it is assumed that the groundwater is incompressible, so that $\partial q_i/\partial x_i = 0$. Throughout this report the Einstein summation convention is used. The coefficients C_w and C are the heat capacities of the groundwater and the saturated soil in the aquifer, respectively. The parameters λ, C_w and C are defined as follows:

$$\lambda = n\lambda_w + (1-n)\lambda_s \tag{2.2}$$

$$C = nC_w + (1-n)C_s \tag{2.3}$$

$$C_w = \rho_w c_w \tag{2.4}$$

$$C_s = \rho_s c_s \tag{2.5}$$

where

λ_w	thermal conductivity of water
λ_s	thermal conductivity of solids (aquifer formation)
ρ_w	density of water
ρ_s	density of solids
c_w	specific heat of water
c_s	specific heat of solids
n	porosity of the aquifer

The dimensions, in SI units, of the various parameters are:

$$\lambda \quad \left[\frac{kg\ m}{s^3 K^0}\right]$$

$$\rho \quad \left[\frac{kg}{m^3}\right]$$

$$c \quad \left[\frac{m^2}{s^2 K^0}\right] \qquad (2.6)$$

$$C \quad \left[\frac{kg}{m\, s^2 K^0}\right]$$

$$n \quad [\ -\ ]$$

Note that in this analysis no distinction is made between the effective porosity and the total porosity. For sandy aquifers, the effective porosity may be assumed equal to the total porosity n of the formation (Olsthoorn, 1977).

The left-hand term in (2.1) represents heat conduction in the aquifer, the first term on the right-hand side of (2.1) represents heat convection and the remaining term accounts for heat storage. In this analysis the heat conduction in the horizontal direction will be disregarded with respect to the heat convection. This assumption has been validated for the case of steady heat transport by Verruijt (1969).

2.2 TWO-DIMENSIONAL HEAT FLOW EQUATION FOR UNCONFINED AQUIFERS

82quation (2.1) may be applied to unconfined aquifers, whereby the Dupuit-Forchheimer assumption is adopted; the piezometric head is constant over the aquifer height. If the head, ϕ, is measured with respect to the aquifer base, which is assumed horizontal, the saturated thickness of the aquifer equals ϕ. Integrating expression (2.1) over the aquifer thickness yields

$$\int_0^{\phi} \lambda \frac{\partial^2 T}{\partial x_3^2} dx_3 = \int_0^{\phi} C_w q_i \frac{\partial T}{\partial x_i} dx_3 + \int_0^{\phi} C \frac{\partial T}{\partial t} dx_3 \qquad (i = 1,2,3) \qquad (2.7)$$

or

$$\lambda \frac{\partial T}{\partial x_3}\Big|_{x_3=\phi} - \lambda \frac{\partial T}{\partial x_3}\Big|_{x_3=0} = C_w \int_0^{\phi} q_\alpha \frac{\partial T}{\partial x_\alpha} dx_3 + C_w \int_0^{\phi} q_3 \frac{\partial T}{\partial x_3} dx_3 + C \int_0^{\phi} \frac{\partial T}{\partial t} dx_3$$

$$(\alpha = 1,2) \qquad (2.8)$$

The vector q_α is the specific discharge vector for horizontal two-dimensional groundwater flow; $\alpha = 1,2$. The left-hand side of (2.8) represents the heat

fluxes across the bottom and top of the aquifer and may be represented by the symbols $\overset{1}{F}$ and $\overset{2}{F}$, respectively, whereby

$$\overset{1}{F} = -\lambda \frac{\partial T}{\partial x_3}\Big|_{x_3=0} = -\overset{1}{\lambda}\frac{\partial \overset{1}{T}}{\partial x_3}\Big|_{x_3=0}$$

$$\overset{2}{F} = \lambda \frac{\partial T}{\partial x_3}\Big|_{x_3=\phi} = \overset{2}{\lambda}\frac{\partial \overset{2}{T}}{\partial x_3}\Big|_{x_3=\phi} \tag{2.9}$$

The superscripts 1 and 2 in (2.9) refer to the lower and upper boundaries, respectively. The first integral on the right-hand side of (2.8) may be written as

$$\int_0^{\phi} q_\alpha \frac{\partial T}{\partial x_\alpha} dx_3 = q_\alpha \frac{\partial}{\partial x_\alpha}\int_0^{\phi} T dx_3 - q_\alpha \frac{\partial \phi}{\partial x_\alpha} T\Big|_{x_3=\phi} = q_\alpha \frac{\partial}{\partial x_\alpha}[\bar{T}\phi] - q_\alpha \frac{\partial \phi}{\partial x_\alpha} T\Big|_{x_3=\phi} \tag{2.10}$$

where use has been made of Leibnitz's Rule and where q_α is considered independent of x_3, a consequence of the Dupuit-Forchheimer assumption. The temperature $\bar{T}$ is the average temperature over the aquifer height.
The second integral on the right-hand side of (2.8) may be written as

$$\int_0^{\phi} q_3 \frac{\partial T}{\partial x_3} dx_3 = q_3 T\Big|_{x_3=0}^{x_3=\phi} - \int_0^{\phi} T \frac{\partial q_3}{\partial x_3} dx_3 \tag{2.11}$$

The vertical component of flow q_3, in a groundwater flow model based on the Dupuit-Forchheimer assumption, may be found from continuity considerations as (see Strack 1983)

$$q_3 = \left[q_\alpha \frac{\partial \phi}{\partial x_\alpha} + n\frac{\partial \phi}{\partial t} \right] \frac{x_3}{\phi} \tag{2.12}$$

so that

$$\frac{\partial q_3}{\partial x_3} = \left[q_\alpha \frac{\partial \phi}{\partial x_\alpha} + n\frac{\partial \phi}{\partial t} \right] \frac{1}{\phi} \tag{2.13}$$

With (2.12) and (2.13) the integral (2.11) becomes

$$\int_0^{\phi} q_3 \frac{\partial T}{\partial x_3} dx_3 = \left[q_\alpha \frac{\partial \phi}{\partial x_\alpha} + n\frac{\partial \phi}{\partial t} \right] T\Big|_{x_3=\phi} - q_\alpha \frac{\partial \phi}{\partial x_\alpha}\bar{T} - n\frac{\partial \phi}{\partial t}\bar{T} \tag{2.14}$$

where use has been made of $q_3 = 0$ for $x_3 = 0$. The last integral of (2.8) becomes with Leibnitz's Rule,

$$\int_0^{\phi} \frac{\partial T}{\partial t} dx_3 = \frac{\partial}{\partial t} \int_0^{\phi} T dx_3 - T\frac{\partial \phi}{\partial t}\Big|_{x_3=\phi} = \frac{\partial}{\partial t}\left[\phi \bar{T}\right] - T\frac{\partial \phi}{\partial t}\Big|_{x_3=\phi} \tag{2.15}$$

Combining (2.9), (2.10), (2.14) and (2.15) yields for (2.8)

$$\overset{1}{F} + \overset{2}{F} = C_w \Bigg[q_\alpha \phi \frac{\partial}{\partial x_\alpha}\bar{T} + q_\alpha \frac{\partial \phi}{\partial x_\alpha}\bar{T} - q_\alpha \frac{\partial \phi}{\partial x_\alpha} T\Big|_{x_3=\phi} + q_\alpha \frac{\partial \phi}{\partial x_\alpha} T\Big|_{x_3=\phi} +$$

$$n\frac{\partial \phi}{\partial t} T\Big|_{x_3=\phi} - q_\alpha \frac{\partial \phi}{\partial x_\alpha}\bar{T} - n\frac{\partial \phi}{\partial t}\bar{T}\Bigg] + C\frac{\partial \phi}{\partial t}\bar{T} + C\phi\frac{\partial \bar{T}}{\partial t} - C\frac{\partial \phi}{\partial t} T\Big|_{x_3=\phi} \tag{2.16}$$

The temperature at the top of the aquifer will be assumed equal to the average temperature in the aquifer, so that

$$T\Big|_{x_3=\phi} = \bar{T} \tag{2.17}$$

With (2.17), and writing T for $\bar{T}$, expression (2.16) reduces to

$$\overset{1}{F} + \overset{2}{F} = nC_w \phi v_\alpha \frac{\partial T}{\partial x_\alpha} + C\phi\frac{\partial T}{\partial t} \tag{2.18}$$

where v_α is the average horizontal groundwater velocity, which is obtained from q_α as

$$v_\alpha = \frac{q_\alpha}{n} \tag{2.19}$$

Equation (2.18) is the heat balance equation for convective heat transport in unconfined aquifers, whereby the Dupuit-Forchheimer assumption is adopted. It is noted that, for this case of convective heat transport only, the temperature gradient coincides with the direction of flow. The temperature T is assumed constant over the saturated aquifer thickness and the terms $\overset{1}{F}$ and $\overset{2}{F}$ represent the heat flux through the aquifer base and the upper aquifer boundary, the vadose zone, respectively. In general, the coefficients ϕ and v_α are functions of position x_α and time t. The heat fluxes $\overset{1}{F}$ and $\overset{2}{F}$ are generally functions of x_α, t and the temperature T in the aquifer.

3.0 ANALYSIS OF HEAT LOSS THROUGH THE UPPER AND LOWER AQUIFER BOUNDARY

The differential equation (2.18) for heat transport in an unconfined aquifer contains the terms $\overset{1}{F}$ and $\overset{2}{F}$, which represent heat conduction through the aquifer base and aquifer top, respectively. In general, these heat fluxes are functions of both location and time. Based on a number of simplifying assumptions, however, the heat fluxes $\overset{1}{F}$ and $\overset{2}{F}$ may be expressed exclusively in terms of the average temperature in the aquifer. The assumptions made are:

- The aquifer boundary, vadose zone or aquifer base, is of constant thickness and has constant thermal properties.
- The temperature at the ontside of the aquifer boundaries is constant.
- Heat convection and horizontal heat conduction in the aquifer boundary is neglected.
- The temperature distribution in the aquifer boundary is linear.

In this report the phrase 'aquifer boundary' refers to the aquifer base and vadose zone, unless specified otherwise. The fourth assumption, listed above, is clearly in violation with reality. A linear temperature distribution in the aquifer boundary will be approached only if the temperature in the aquifer has remained constant for some time. To verify the importance of the fourth assumption, the temperature distribution in the aquifer, obtained with the above assumptions, will be compared with a distribution that is obtained with transieut heat conduction through the aquifer boundary. The latter solution will be referred to as an exact one, althongh it is still based on the first three assumptions. Furthermore, it will be demonstrated that the approximate heat loss mechanism may be improved by incorporating (instantaneous) heat storage in the aquifer boundaries.

Finally, the first assumption, an aquifer base of finite thickness, is investigated. The temperature distribution in a confined aquifer with both a thin aquifer top and a thin aquifer base is compared with a solution for the case of a thin aquifer top and an infinitely thick aquifer base. Similar to the previous comparison, steady groundwater flow is assumed.

It is remarked that the phrase 'aquifer boundary' in this report refers to the aquifer base and vadose zone, unless specified otherwise.

3.1 APPROXIMATE HEAT LOSS MECHANISM

As indicated in Fig. 3.1, the vadose zone and aquifer base are of constant

thickness $\overset{2}{d}$ and $\overset{1}{d}$, respectively. The thermal properties of the vadose zone are $\overset{2}{\lambda}$ and $\overset{2}{C}$. The thermal properties of the aquifer base are $\overset{1}{\lambda}$ and $\overset{1}{C}$. The temperature on the ontside of the aquifer boundaries is assumed constant and

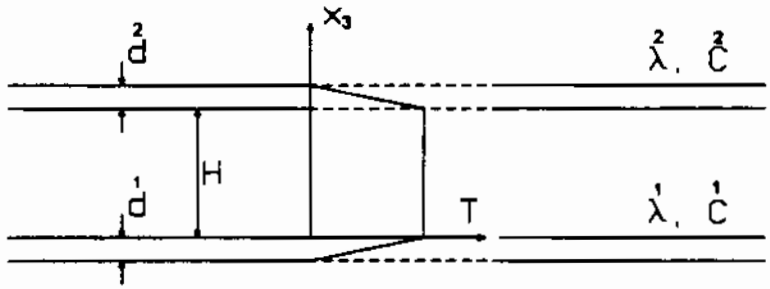

Fig. 3.1. Linear Temperature Distribution in the Aquifer Boundaries

taken to be zero. The heat fluxes $\overset{1}{F}$ and $\overset{2}{F}$ become, with (2.9),

$$\overset{1}{F} = -\overset{2}{\lambda}\frac{\partial \overset{1}{T}}{\partial x_3}\Big|_{x_3=0} = -\overset{2}{\lambda}\frac{T}{\overset{1}{d}}$$

$$\overset{2}{F} = \overset{2}{\lambda}\frac{\partial \overset{2}{T}}{\partial x_3}\Big|_{x_3=\phi} = -\overset{2}{\lambda}\frac{T}{\overset{1}{d}} \tag{3.1}$$

The differential equation (2.18) becomes, with (3.1),

$$nC_w\phi v_\alpha\frac{\partial T}{\partial x_\alpha} + C\phi\frac{\partial T}{\partial t} = -\left[\frac{\overset{1}{\lambda}\overset{1}{d} + \overset{2}{\lambda}\overset{2}{d}}{\overset{1}{d}\overset{2}{d}}\right]T \qquad (\alpha = 1,2) \tag{3.2}$$

where T is measured with respect to the temperature outside the aquifer. Expression (3.2) may be further evaluated by introducing the velocity v^*_α as

$$v^*_\alpha = \frac{nC_w}{C}v_\alpha \tag{3.3}$$

The velocity v^*_α is termed the thermal velocity (Hellström and Claesson, 1978), and may be interpreted as the velocity with which a temperature discontinuity (thermal front) travels through the aquifer. With (3.3) the differential equation (3.2) becomes

$$v^*_\alpha\frac{\partial T}{\partial x_\alpha} + \frac{\partial T}{\partial t} = -\left[\frac{\overset{1}{\lambda}\overset{2}{d} + \overset{2}{\lambda}\overset{1}{d}}{C\phi\overset{1}{d}\overset{2}{d}}\right]T \tag{3.4}$$

The first term in (3.4) may be expressed in terms of the residence time t^* of a thermal front, so that

$$\frac{\partial T}{\partial t^*} + \frac{\partial T}{\partial t} = -\beta T \tag{3.5}$$

For the case of confined flow, the head ϕ in (3.4) may be replaced by the aquifer thickness H, so that β is constant,

$$\beta = \frac{\overset{12}{\lambda d} + \overset{21}{\lambda d}}{CH\overset{12}{d}} \tag{3.6}$$

The solution to (3.5) is found to be (using standard Laplace transform pairs)

$$T = T_0 \, e^{-\beta t^*} \, U(t - t^*) \tag{3.7}$$

where T_0 is the temperature at the point of injection, where t^* is the residence time of a thermal front since injection and where $U(t - t^*)$ is Heaviside's unit step function and defined as

$$\begin{aligned} U(t - t^*) &= 1 \qquad (t > t^*) \\ U(t - t^*) &= 0 \qquad (t < t^*) \end{aligned} \tag{3.8}$$

It is noted that the flow path of a thermal front, in general, does not coincide with the flow path of a water particle. However, for the case of steady flow and for some special cases of transient flow (e.g., radial flow) a thermal front does travel along the flow path of a water particle. The velocity of a thermal front is a constant fraction of the water velocity [see (3.3)] so that, for the case of coinciding flow paths of thermal front and water, the temperature may be expressed as

$$T = T_0 \, e^{-\beta \frac{C}{nC_w} \tau} \, U\left[t - \frac{C}{nC_w} \tau \right] \tag{3.9}$$

where τ is the residence time of a water particle; the time that elapsed since the water particle was injected. This result conforms with the findings of Dietz and Lehner (1969) and Verruijt (1969).

3.2 TRANSIENT HEAT LOSS THROUGH A THIN AQUIFER TOP

With the heat loss mechanism expressed by (3.1), the proper transient effects in the heat conduction through the aquifer boundary are disregarded. To estimate the error that results from this approximation, a comparison will be made between the temperature distribution given by (3.7) and a temperature distribution obtained by incorporating transient heat loss through the aquifer boundaries. This comparison will be carried out by solving a non-steady heat flow problem for steady radial groundwater flow in a confined aquifer (see Fig. 3.2). The aquifer has a thickness H and has an upper aquifer boundary of

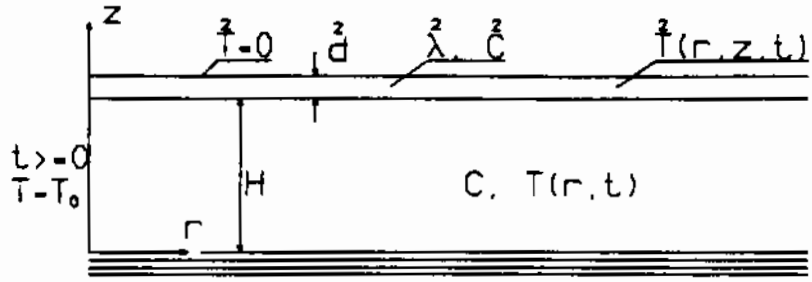

Fig. 3.2. Steady Radial Flow with Heat Injection for r=0 at $t \geqq 0$.

constant thickness $\hat{d}$. For simplicity, the aquifer base will be considered a thermal insulator. The temperature T in the aquifer is assumed constant over the aquifer height, but depends on the radial distance r from the heat source (and water source) and on the time t that has elapsed since heat injection;

$$T = T(r,t) \tag{3.10}$$

The temperature $\hat{T}$ in the aquifer boundary depends not only on r and t, but also on the vertical coordinate z;

$$\hat{T} = \hat{T}(r,z,t) \tag{3.11}$$

The temperature T in the aquifer satisfies the following differential equation [see (2.18)] :

$$\frac{nC_w}{C} v_r \frac{\partial T}{\partial r} - \frac{\hat{\lambda}}{CH} \frac{\partial \hat{T}}{\partial z}\bigg|_{z=H} + \frac{\partial T}{\partial t} = 0 \qquad (0 \leqq z \leqq H) \tag{3.12}$$

where the groundwater velocity v_r is independent of time. The temperature $\hat{T}$ in the aquifer boundary satisfies

$$\hat{\lambda} \frac{\partial^2 \hat{T}}{\partial z^2} = \hat{C} \frac{\partial \hat{T}}{\partial t} \qquad (H \leqq z \leqq H + \hat{d}) \tag{3.13}$$

The differential equations (3.12) and (3.13) are similar to those presented by Lauwerier (1955) for the case of linear flow. Lauwerier, however, solved the problem assuming an infinitely thick aquifer boundary. The analysis may be pursued in terms of the residence time τ of the injected water, as suggested by Dietz and Lehner (1969), rather than the radial coordinate r, so that (3.12) becomes

$$\frac{nC_w}{C} \frac{\partial T}{\partial \tau} - \frac{\hat{\lambda}}{CH} \frac{\partial \hat{T}}{\partial z}\bigg|_{z=H} + \frac{\partial T}{\partial t} = 0 \qquad (0 \leqq z \leqq H) \tag{3.14}$$

The following dimensionless parameters are introduced:

$$\tilde{T} = \frac{T}{T_o} \tag{3.15}$$

$$\tilde{T}_2 = \frac{\hat{T}}{T_0} \tag{3.16}$$

$$\tilde{z} = \frac{z}{H} \tag{3.17}$$

$$\tilde{\tau} = \frac{\hat{\lambda}}{nC_w H^2}\tau \tag{3.18}$$

$$\tilde{t} = \frac{\hat{\lambda}}{CH^2}t \tag{3.19}$$

With expressions (3.15) through (3.19), the differential equations (3.13) and (3.14) become

$$\frac{\partial^2 \tilde{T}_2}{\partial \tilde{z}^2} = \theta \frac{\partial \tilde{T}_2}{\partial \tilde{t}} \qquad (1 \leqq \tilde{z} \leqq 1 + \frac{\hat{d}}{H}) \tag{3.20}$$

and

$$\frac{\partial \tilde{T}_2}{\partial \tilde{\tau}} - \frac{\partial \tilde{T}_2}{\partial \tilde{z}} + \frac{\partial \tilde{T}_2}{\partial \tilde{t}} = 0 \qquad (\tilde{z} = 1) \tag{3.21}$$

respectively, where use has been made of

$$T = \hat{T} \qquad (z = H) \tag{3.22}$$

and where θ is defined as

$$\theta = \frac{\hat{C}}{C} \tag{3.23}$$

The boundary conditions and initial conditions for (3.20) and (3.21) are

$$\tilde{T}_2 = 1 \qquad (\tilde{t} \geqq 0,\ \tilde{\tau} = 0,\ \tilde{z} = 1) \tag{3.24}$$

$$\tilde{T}_2 = 0 \qquad (\tilde{t} = 0,\ \tilde{\tau} > 0,\ \tilde{z} = 1) \tag{3.25}$$

$$\tilde{T}_2 = 0 \qquad (\tilde{t} \geqq 0,\ \tilde{\tau} \geqq 0,\ \tilde{z} = 1 + \frac{\hat{d}}{H}) \tag{3.26}$$

The solution to (3.20) with (3.21) and (3.24) through (3.26) is obtained by use of the same double Laplace transform as employed by Lauwerier (1955):

$$v(\tilde{z}, s, p) = \int_0^\infty e^{-s\tilde{t}} \int_0^\infty (1 - \tilde{T}_2)\, e^{-p\tilde{\tau}}\, d\tilde{\tau} d\tilde{t} \tag{3.27}$$

Using (3.27), the differential equations (3.20) and (3.21) become

$$\frac{\partial^2 v}{\partial \tilde{z}^2} - \theta s v + \frac{\theta}{p} = 0 \qquad (1 \leqq \tilde{z} \leqq 1 + \frac{\hat{d}}{H}) \tag{3.28}$$

$$(s+p)v - \frac{\partial v}{\partial \tilde{z}} - \frac{1}{p} = 0 \qquad (\tilde{z} = 1) \tag{3.29}$$

The general solution to (3.28) is given by

$$v = A\, e^{\tilde{z}\sqrt{\theta s}} + B e^{-\tilde{z}\sqrt{\theta s}} + \frac{1}{sp} \tag{3.30}$$

The constants A and B are found from the boundary conditions $\tilde{z} = 1$ and $\tilde{z} = 1 + \hat{d}/H$. It follows from (3.26) with (3.27) that, for $\tilde{z} = 1 + \hat{d}/H$,

$$v = \frac{1}{sp} \qquad (\tilde{z} = 1 + \hat{d}/H) \tag{3.31}$$

so that B may be expressed in terms of A as [see (3.30)]

$$B = -A\, e^{2(1+\hat{d}/H)\sqrt{s\theta}} \tag{3.32}$$

Applying the boundary condition (3.29) and using (3.32) yields, after some elaborate but straightforward algebra,

$$v = \frac{1}{sp} - \frac{1}{s} \frac{\sinh\{(\tilde{z} - 1 - \hat{d}/H)\sqrt{s\theta}\}}{(s+p)\sinh\{-\hat{d}/H)\sqrt{s\theta}\} - \sqrt{s\theta}\cosh\{(\hat{d}/H)\sqrt{s\theta}\}} \tag{3.33}$$

A solution for v is sought at the upper aquifer boundary $(\tilde{z} = 1)$, so that (3.33) reduces to

$$v = \frac{1}{sp} - \frac{1}{s} \frac{1}{(s+p) + \sqrt{s\theta}\coth\{(\hat{d}/H)\sqrt{s\theta}\}} \tag{3.34}$$

The inverse transformation of v, with respect to p, becomes

$$\underset{p}{L^{-1}}\{v\} = \frac{1}{s} - \frac{1}{s}\, e^{-[s + \sqrt{s\theta}\coth\{(\hat{d}/H)\sqrt{s\theta}\}]\tilde{\tau}} \tag{3.35}$$

The inverse transformation with respect to s may be written in the form

$$\tilde{T} = \underset{s}{L^{-1}}\left[e^{-s\tilde{\tau}} f(s)\right] \tag{3.36}$$

where f(s) is defined as

$$f(s) = \frac{1}{s}\, e^{-\sqrt{\theta s}\coth\{(\hat{d}/H)\sqrt{\theta s}\}\tilde{\tau}} \tag{3.37}$$

It is noted that, because the solution is valid at $\tilde{z} = 1$, the temperature

parameter $\tilde{T}_2$ has been replaced by $\tilde{T}$, the temperature parameter for the aquifer. If $F(\tilde{t})$ is the inverse of $f(s)$,

$$F(\tilde{t}) = L^{-1}[f(s)] \tag{3.38}$$

then (3.36) becomes

$$\tilde{T} = F(\tilde{t})\,U(\tilde{t}-\tilde{\tau}) \tag{3.39}$$

where the 'function' U is defined as [see (3.8)]

$$\begin{aligned} U(\tilde{t}-\tilde{\tau}) &= 0 \qquad \tilde{t} < \tilde{\tau} \\ U(\tilde{t}-\tilde{\tau}) &= 1 \qquad \tilde{t} > \tilde{\tau} \end{aligned} \tag{3.40}$$

It may be observed from (3.37) that, for small values of s (i.e., large values of the time $\tilde{t}$), the function $f(s)$ can be approximated by

$$f(s) \simeq \frac{1}{s}\, e^{-\sqrt{\theta s}\,[H/(d^2\sqrt{\theta s})]\tilde{\tau}} = \frac{1}{s}\, e^{-(H/d^2)\tilde{\tau}} \qquad (s \ll 1) \tag{3.41}$$

The inverse of (3.41) is

$$F(\tilde{t}) = e^{-(H/d^2)\tilde{\tau}} \qquad (\tilde{t} \gg 1) \tag{3.42}$$

It appears that (3.39), with (3.42), (3.18) and (3.19) equals the approximate solution (3.9) with (3.6), if heat loss through the aquifer base is ignored:

$$T = T_0\, e^{-\{\lambda^2/(nC_w H d^2)\}\tau}\, U\left[t - \frac{C}{nC_w}\tau\right] \qquad (t \gg 1) \tag{3.43}$$

where τ is the residence time of the water. That (3.43) is indeed the same as (3.9) may be seen by replacing β in (3.9) by

$$\beta = \frac{\lambda^2}{CHd^2} \tag{3.44}$$

Numerical Inversion of the Laplace Transform

A solution to (3.38) must be obtained for those (relatively larger) values of s where the approximation (3.41) fails. This solution is obtained by numerically inverting (3.38) for ten different values of s, yielding a solution for ten different values of $\tilde{t}$. The inversion is carried out using a standard procedure described by Bellman (1966), and is not further discussed here. As appears from (3.39) and (3.40), a solution is needed only for values of $\tilde{t}$ larger than $\tilde{\tau}$, which may be accomplished as follows (see also Bellman 1966). The solution (3.36) is written in the form

$$\tilde{T}(\tilde{t}) = L^{-1}\{g(s)\} \tag{3.45}$$

where $g(s)$ is given by

$$g(s) = e^{-s\tilde{\tau}} f(s) \tag{3.46}$$

A solution is sought for $\tilde{T}(\tilde{\tau}+\tilde{t})$, where $\tilde{t} \geqq 0$. The function $\tilde{T}(\tilde{\tau}+\tilde{t})$ has the Laplace transform $g^*(s)$,

$$g^*(s) = \int_0^\infty e^{-s\tilde{t}}\, T(\tilde{\tau}+\tilde{t})d\tilde{t} = e^{s\tau} \int_0^\infty e^{-s(\tilde{t}+\tilde{\tau})}\, T(\tilde{\tau}+\tilde{t})d(\tilde{t}+\tilde{\tau}) \tag{3.47}$$

so that [see (3.45) and (3.46)]

$$g^*(s) = e^{s\tilde{\tau}} g(s) = f(s) \tag{3.48}$$

Thus, the inverse of $f(s)$ will give $\tilde{T}$ for times $\tilde{\tau}+\tilde{t}$,

$$\tilde{T}(\tilde{\tau}+\tilde{t}) = L^{-1}\{f(s)\} \quad (\tilde{t} \geqq 0) \tag{3.49}$$

3.3 COMPARISON OF THE EXACT AND APPROXIMATE SOLUTION

The temperature distribution in the aquifer, based on the approximate solution (3.43), may be expressed in terms of the dimensionless parameters $\tilde{T}$, $\tilde{t}$ and $\tilde{\tau}$ [see (3.15), (3.18), (3.19), (3.42), (3.43) and (3.44)].

$$\tilde{T} = e^{-(H/\hat{d})\tilde{\tau}}\, U(\tilde{t}-\tilde{\tau}) \tag{3.50}$$

Both the solutions (3.49) and (3.50) are plotted in Fig. 3.3 for $H/\hat{d} = 10$ and for various values of $\tilde{t}$. The dashed lines in Fig. 3.3 are obtained with (3.49) and the solid line is obtained with (3.50). To interpret the results of Fig. 3.3 in terms of real times, the following data may be used as an example:

$$C_w = 4.1 * 10^6 \quad \left[\frac{kg}{ms^2K^0}\right]$$

$$C = 2.5 * 10^6 \quad \left[\frac{kg}{ms^2K^0}\right]$$

$$\hat{C} = 2 * 10^6 \left[\frac{kg}{ms^2K^0}\right]$$

$$\hat{\lambda} = 1 \quad \left[\frac{kgm}{s^3K^0}\right] \tag{3.51}$$

$$H = 10 \quad [m]$$

$$\hat{d} = 1 \quad [m]$$

$$n = 0.3 \quad [-]$$

so that it follows, for $\tilde{t}$ and $\tilde{\tau}$,

$$\tilde{t} = 0.01 \quad ; \quad t \simeq 1 \text{ month}$$

$$\tilde{\tau} = 0.021 \quad ; \quad \tau \simeq 1 \text{ month} \tag{3.52}$$

Therefore, in Fig. 3.3, the time since heat injection extends to almost two years.

Improved Approximate Heat Loss Mechanism

It may be observed from Fig. 3.3 that the exact solution indeed converges toward the approximate solution, provided some time has elapsed after the heat front has passed. However, in terms of total heat loss, the approximate solution systematically underestimates the heat loss through the aquifer boundary. This underestimation of the total heat loss is due partly to the negligence of heat storage in the aquifer boundaries. The heat loss mechanism, therefore, may be improved by incorporating heat storage in the aquifer boundary in some approximate fashion. The rate of heat storage in the upper aquifer boundary is denoted by $\hat{S}$ and is given by

$$\hat{S} = \hat{C}\frac{\partial}{\partial t}\int_H^{H+\hat{d}} \hat{T}dz \tag{3.53}$$

If a linear temperature distribution in the aquifer boundary is assumed, from $\hat{T} = T$ at $z = H$ and $\hat{T} = 0$ at $z = H + \hat{d}$, expression (3.53) yields

$$\hat{S} = \hat{C}\frac{\hat{d}}{2}\frac{\partial T}{\partial t} \tag{3.54}$$

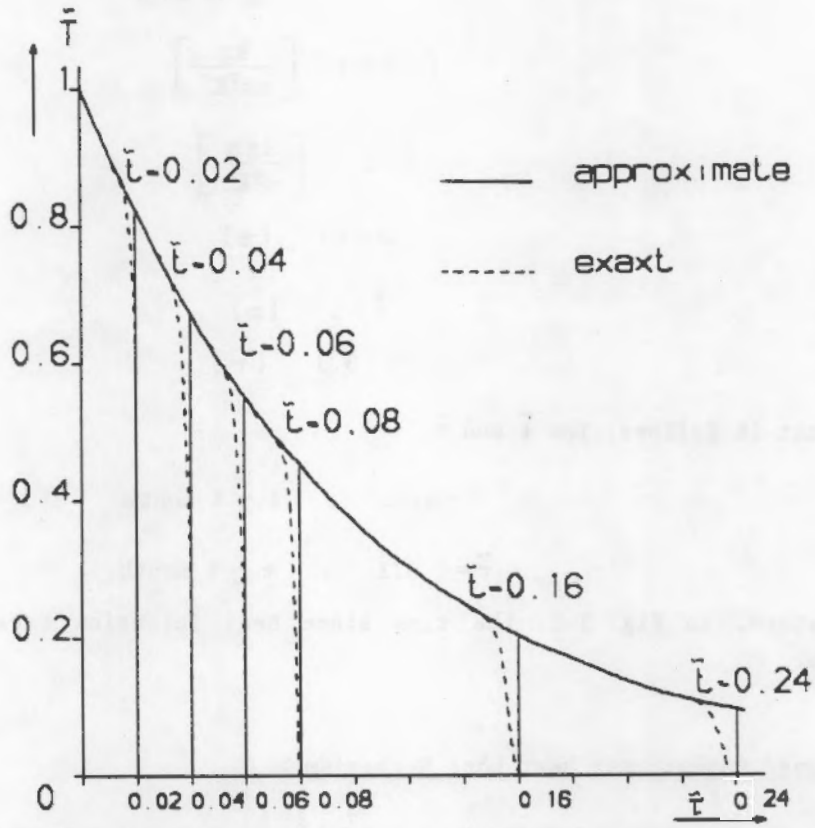

Fig. 3.3. Temperature Distribution in the Aquifer for $H/\hat{d}=10$, with Both the Exact and the Approximate Heat Loss Mechanisms

Adding this storage term to the differential equation (3.2) yields

$$nC_w\phi v_i\frac{\partial T}{\partial x_i} + \{C\phi + \hat{C}\hat{d}/2\}\frac{\partial T}{\partial t} = -(\hat{\lambda}/\hat{d})T \qquad (i=1,2) \tag{3.55}$$

where heat loss through the aquifer base is disregarded. The solution to (3.55) may be obtained from the solution to (3.2) by replacing C with C′, where

$$C' = C + \frac{\hat{C}\hat{d}}{2\phi} \tag{3.56}$$

It is noted that C′ contains the saturated aquifer thickness ϕ, so that C′, in general, is a function of x_1, x_2 and t. For the case of confined flow, the parameter C′ is constant;

$$C' = C + \frac{\hat{C}\hat{d}}{2H} \tag{3.57}$$

The introduction of C' in the approximate solution affects the time parameter $\tilde{t}$, which will be replaced by $\tilde{t}'$;

$$\tilde{t}' = \frac{\lambda^2}{C'H^3} t \tag{3.58}$$

The same calculations as performed for Fig. 3.3 are repeated, but now with the improved approximate solution,

$$\tilde{T} = e^{-(H/\hat{d})\tilde{\tau}} U(\tilde{t}' - \tilde{\tau}) \tag{3.59}$$

The results are presented in Fig. 3.4. It may be observed that the approximate solution (3.59) still discretizes the curved heat front by a temperature discontinuity, but the systematic underestimation of the total heat loss has been reduced. In Fig. 3.5, the results of Fig. 3.4 are plotted in the form of $\tilde{T}$ versus the dimensionless radial distance $\tilde{r}$,

$$\tilde{r} = \frac{r}{H}\sqrt{\frac{\lambda^2 \pi H}{Q\, C_w}} = \sqrt{\tilde{\tau}} \tag{3.60}$$

where Q is the discharge of the injection well. That $\tilde{r}$ equals $\sqrt{\tilde{\tau}}$ may be seen by calculating the residence time of water by use of (3.3). Equation (3.59) becomes, with (3.60),

$$\tilde{T} = e^{-(H/\hat{d})\tilde{r}^2} U(\tilde{t}' - \tilde{r}^2) \tag{3.61}$$

In Fig. 3.6 and Fig. 3.7 the same comparison as presented in Fig. 3.5 is carried out, but now for values of $H/\hat{d} = 5$ and $H/\hat{d} = 20$, respectively.

It is seen from Fig. 3.4 through Fig. 3.7 that, in case some time has elapsed since the heat front has passed, the temperature distribution in the aquifer becomes stationary, a result from the boundary condition at $r = 0$ and the steady groundwater flow. Under these circumstances, and if horizontal heat conduction in the aquifer is disregarded, a linear temperature distribution will occur in the aquifer boundary (Verruijt 1969). The approximate solution (3.59) is based on such a linear temperature distribution, which explains why the exact and approximate solutions in Fig. 3.4 through Fig. 3.7 coincide at some distance behind the heat front. For transient flow, in general, no stationary temperature distribution in the aquifer will be obtained, so that the exact and approximate solutions do not become the same.

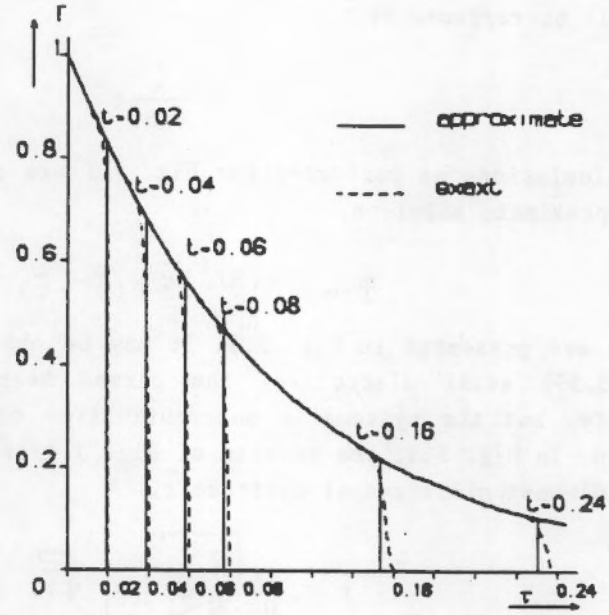

Fig. 3.4. Temperature Distribution in the Aquifer for $H/\hat{d}=10$, with Both the Exact and the Improved Approximate Heat Loss Mechanisms

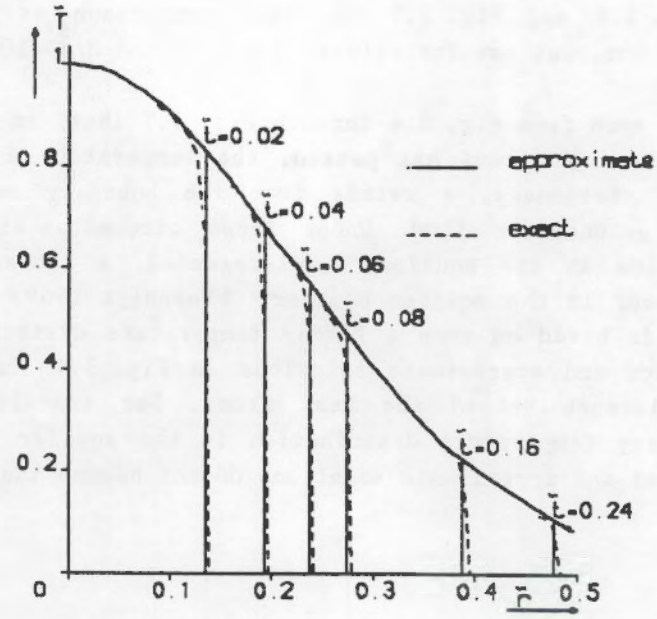

Fig. 3.5. Temperature Distribution in the Aquifer for $H/\hat{d}=10$ Plotted as a Function of the Dimensionless Radial Distance $\tilde{r}$

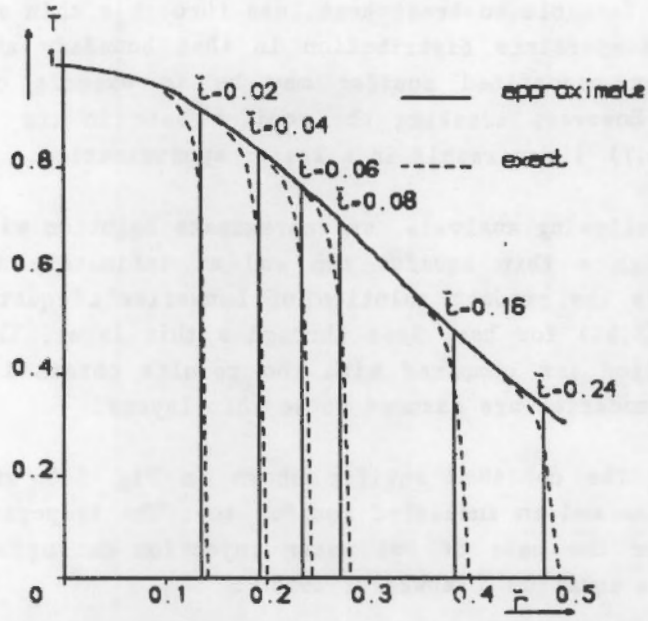

Fig. 3.6. Comparison Between Exact and Approximate Heat Loss Mechanism for $H/\bar{d}=5$

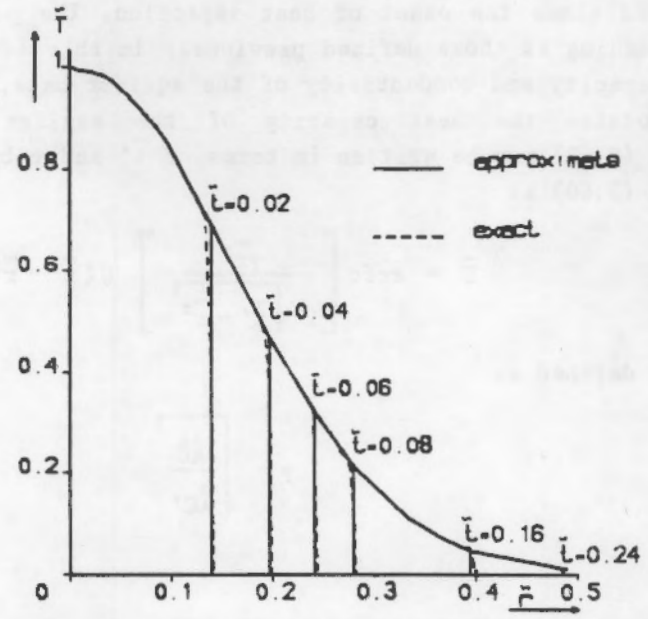

Fig. 3.7. Comparison Between Exact and Approximate Heat Loss Mechanism for $H/\bar{d}=20$

3.4 HEAT LOSS THROUGH AN INFINITELY THICK AQUIFER BASE AND A THIN AQUIFER TOP

It seems feasible to treat heat loss through a thin aquifer boundary assuming a linear temperature distribution in that boundary at all times. The vadose zone of an unconfined aquifer may be an example of such a thin aquifer boundary. However, treating the aquifer base in the same manner [see (3.1) through (3.7)] may result in a lesser approximation.

In the following analysis, an approximate solution will be presented for heat loss through a thin aquifer top and an infinitely thick aquifer base. The solution is the product solution of Lauwerier's equation and the approximate solution (3.61) for heat loss through a thin layer. The results obtained with this solution are compared with the results obtained from (3.7), where both aquifer boundaries are assumed to be thin layers.

Consider the confined aquifer shown in Fig. 3.8 with an infinitely thick aquifer base and an insulated aquifer top. The temperature distribution in the aquifer for the case of hot water injection during steady flow is given by Lauwerier's equation (Lauwerier 1955):

$$\frac{T}{T_o} = \operatorname{erfc}\left[\frac{(\overset{1}{\lambda}/H^2C_w n)\tau}{2\sqrt{\frac{C'}{\overset{1}{C}}\left[(\overset{1}{\lambda}/H^2C')t-(\overset{1}{\lambda}/H^2C_w n)\tau\right]}}\right] U\left[t-\frac{C'}{nC_w}\tau\right] \quad (3.62)$$

where τ is the residence time of the injected water and where t is the time that elapsed since the onset of heat injection. The parameters in (3.62) have the same meaning as those defined previously in this section, where $\overset{1}{C}$ and $\overset{1}{\lambda}$ are the heat capacity and conductivity of the aquifer base, respectively, and where C' incorporates the heat capacity of the aquifer top [see (3.57)]: Expression (3.62) may be written in terms of $\tilde{t}'$ and $\tilde{r}$ by use of (3.15), (3.18), (3.58) and (3.60) as

$$\tilde{T} = \operatorname{erfc}\left[\frac{\gamma\tilde{r}^2}{2\sqrt{\tilde{t}'-\tilde{r}^2}}\right] U(\tilde{t}'-\tilde{r}^2) \quad (3.63)$$

where γ is defined as

$$\gamma = \sqrt{\frac{\overset{1}{\lambda}\overset{1}{C}}{\overset{2}{\lambda}C'}} \quad (3.64)$$

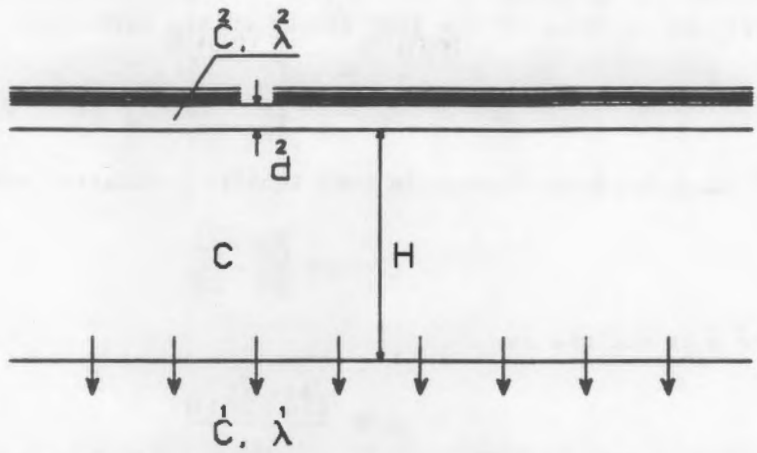

Fig. 3.8. Confined Aquifer with an Infinitely Thick Aquifer Base and Insulated Aquifer Top

In Fig. 3.9 an aquifer is depicted with an insulated aquifer base and a thin upper boundary of constant thickness $\overset{3}{d}$. An approximate solution for the temperature distribution in the aquifer of Fig. 3.9 is given by (3.61)

$$\tilde{T} = e^{-(H/\overset{3}{d})\tilde{r}^2}\, U(\tilde{t}' - \tilde{r}^2) \tag{3.65}$$

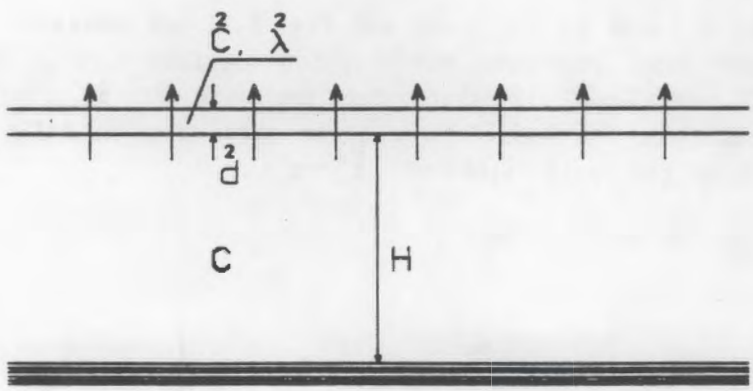

Fig. 3.9. Confined Aquifer With a Thin Upper Boundary and Insulated Base

The solution to the temperature distribution in a confined aquifer with both the infinitely thick base of Fig. 3.8 and the thin aquifer top of Fig. 3.9 is obtained as the product of the solutions (3.63) and (3.65) (see also Carslaw and Jaeger 1959, p. 33):

$$\tilde{T} = e^{-(H/\overset{3}{d})\tilde{r}^2}\, \mathrm{erfc}\left[\frac{\gamma\tilde{r}^2}{2\sqrt{\tilde{t}' - \tilde{r}^2}}\right] U(\tilde{t}' - \tilde{r}^2) \tag{3.66}$$

The solution (3.7), based on both a thin aquifer top and a thin aquifer base, may be written in terms of the same dimensionless parameters

$$\tilde{T} = e^{-\alpha\tilde{r}^2}\, U\left[\tilde{t}' - \frac{C^*}{C'}\tilde{r}^2\right] \tag{3.67}$$

where C^* includes heat storage in both aquifer boundaries and is defined as

$$C^* = C + \frac{\overset{1}{C}\overset{1}{d}}{2H} + \frac{\overset{2}{C}\overset{2}{d}}{2H} \tag{3.68}$$

and where α is defined as,

$$\alpha = \frac{(\overset{1}{\lambda}\overset{1}{d} + \overset{2}{\lambda}\overset{2}{d})\,H}{\overset{1}{d}\overset{2}{d}\overset{1}{\lambda}} \tag{3.69}$$

The temperature distributions as obtained from (3.66) and (3.67) have been compared by use of the data in (3.51) and with $\overset{1}{C} = \overset{2}{C}$ and $\overset{1}{\lambda} = \overset{2}{\lambda}$.

In Fig. 3.10 the temperature parameter $\tilde{T}$, obtained from both (3.66) and (3.67), is plotted as a function of $\tilde{r}$ for $H/\overset{1}{d} = H/\overset{2}{d} = 10$. The values for α, γ and C^*/C' for Fig. 3.10 are $\alpha = 20$, $\gamma = 0.8771$ and $C^*/C' = 1.03846$.

In Fig. 3.11 the plot is repeated for a somewhat thicker aquifer base in (3.67), $H/\overset{2}{d} = 5$, which results in values for α, γ and C^*/C' of $\alpha = 15$, $\gamma = 0.8771$ and $C^*/C' = 1.076923$.

The solid lines in Fig. 3.10 and Fig. 3.11 are obtained from (3.66), while the dashed lines represent the solution obtained from (3.67) It appears from Fig. 3.10 and Fig. 3.11 that, for the case of a thin aquifer base, the temperatures in the aquifer are below those for an infinitely thick aquifer base, except for small values of $(\tilde{t}' - \tilde{r}^2)$.

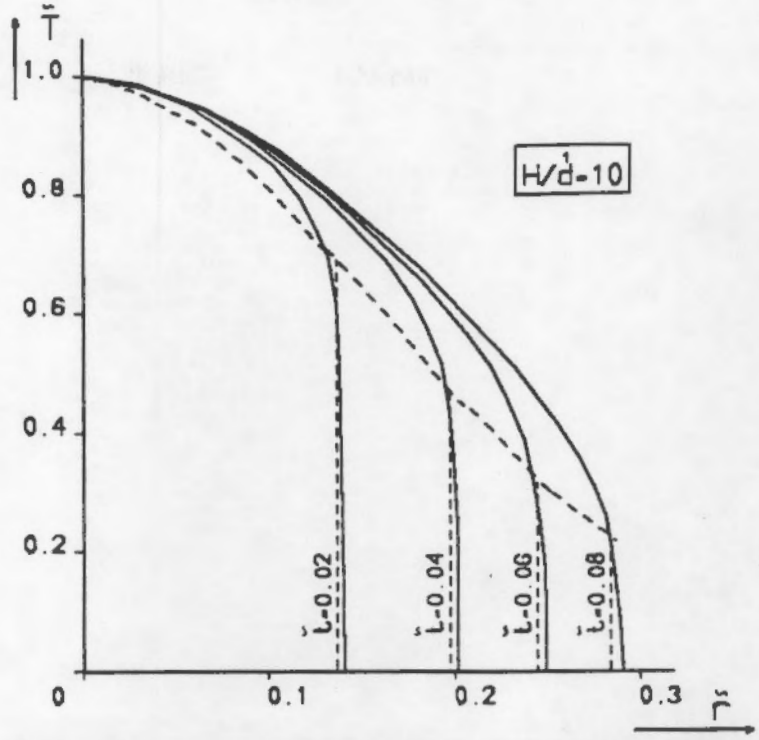

Fig. 3.10. Temperature Distribution in the Aquifer for a Thin Aquifer Top and Both a Thin ($H/\tilde{d}=10$) and an Infinitely Thick Aquifer Base

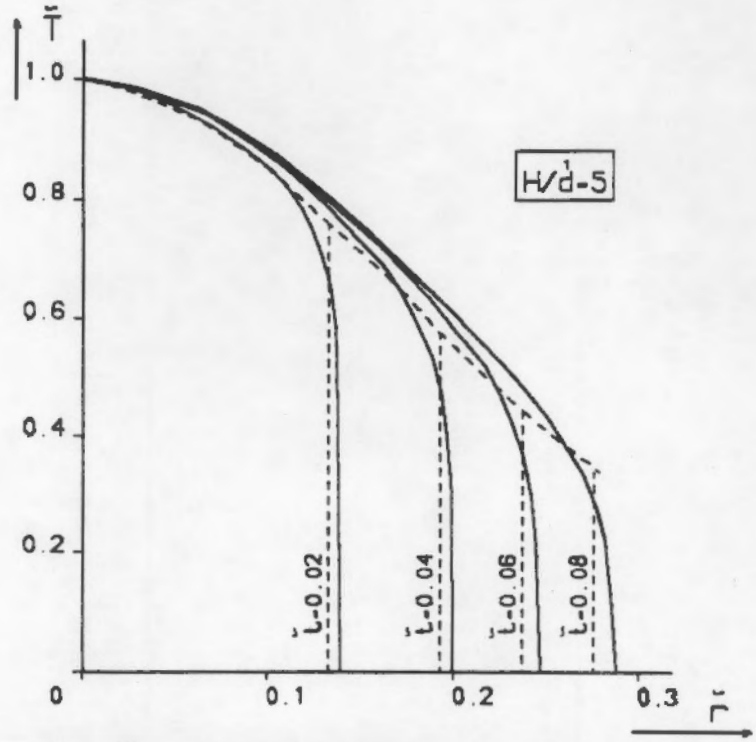

Fig. 3.11. Temperature Distribution in the Aquifer for a Thin Aquifer Top and both a Thin ($H/\tilde{d}=5$) and an Infinitely Thick Aquifer Base

4.0 THERMAL ENERGY STORAGE FOR THE CASE OF RADIAL FLOW

In this section some simple cases of thermal energy storage will be discussed, based on the heat transport equation derived in Section 2 and by use of the approximate heat loss mechanism discussed in Section 3, whereby both the aquifer top and aquifer base are assumed to be relatively thin. Thermal energy will be injected and recovered by a single well in both a confined and an unconfined aquifer. The groundwater flow conditions in the confined aquifer will be taken steady during injection and recovery, i.e., no elastic storage. In the unconfined aquifer, transient flow conditions will be taken into account. The analysis for a confined aquifer is included here for comparison.

The temperature distribution in the aquifer will be calculated for some key times: at the end of injection, at the end of storage, and at the end of recovery. During the recovery phase, the temperature in the well will be calculated as a function of the time since the start of the recovery. Finally, the thermal efficiency of the system will be determined.

4.1 CONFINED FLOW CONDITIONS

The temperature distribution for the case of confined flow, with heat loss through both aquifer boundaries, is given by (3.7) as

$$T = T_0 \, e^{-\beta t^*} \, U(t - t^*) \tag{4.1}$$

where β is defined by (3.6) after replacing C by C^*,

$$\beta = \frac{\overset{1}{\lambda}\overset{2}{d} + \overset{2}{\lambda}\overset{1}{d}}{C^* H \overset{1}{d}\overset{2}{d}} \tag{4.2}$$

The parameter C^* is obtained from the analysis of (3.53) through (3.56) by including heat storage in the lower aquifer boundary, and is defined by (3.68) as

$$C^* = C + \frac{\overset{1}{C}\overset{1}{d}}{2H} + \frac{\overset{2}{C}\overset{2}{d}}{2H} \tag{4.3}$$

The time t^* in (4.1) is the residence time of a thermal front.

A complete thermal energy storage cycle will consist of three phases: the injection phase of duration $(\Delta t)_i$, the storage phase of duration $(\Delta t)_s$ and the recovery phase of duration $(\Delta t)_r$. In this section, the duration of all three phases will be taken the same,

$$(\Delta t)_i = (\Delta t)_s = (\Delta t)_r = \Delta t \tag{4.4}$$

The elastic storage in the aquifer is assumed to be sufficiently small so that during each of the phases the flow may be treated as steady. The water velocity v_r in the aquifer, during injection, follows from

$$v_r = \frac{Q}{2\pi nHr} \tag{4.5}$$

where Q is the injection rate and where H is the aquifer thickness. The thermal velocity v_r^* is obtained from (3.3) with (4.5) as

$$v_r^* = \frac{C_w Q}{2\pi C^* Hr} \tag{4.6}$$

where C is replaced by C^*.
The residence time t^* of a thermal front is found from

$$t^* = \int_0^r \frac{dr}{v_r^*} = \frac{\pi C^* H}{C_w Q} r^2 \tag{4.7}$$

The following dimensionless parameters are introduced:

$$\tilde{T} = T/T_o \tag{4.8}$$

$$\bar{t} = \beta t \tag{4.9}$$

$$\bar{r} = r\sqrt{\frac{\pi C^* H\beta}{C_w Q}} \tag{4.10}$$

where β is defined by (4.2). With (4.1) and (4.7) through (4.10), the temperature in the confined aquifer becomes

$$\tilde{T} = e^{-\bar{r}^2}\, U(\bar{t} - \bar{r}^2) \tag{4.11}$$

<u>End of Injection</u>

The temperature distribution in the aquifer at the end of tbe injection period Δt follows from (4.11) as

$$\tilde{T} = e^{-\bar{r}^2}\, U(\beta\Delta t - \bar{r}^2) \tag{4.12}$$

The temperature parameter $\tilde{T}$ is plotted in Fig. 4.1 versus the radial distance parameter $\bar{r}$ for various values of $\beta\Delta t$.

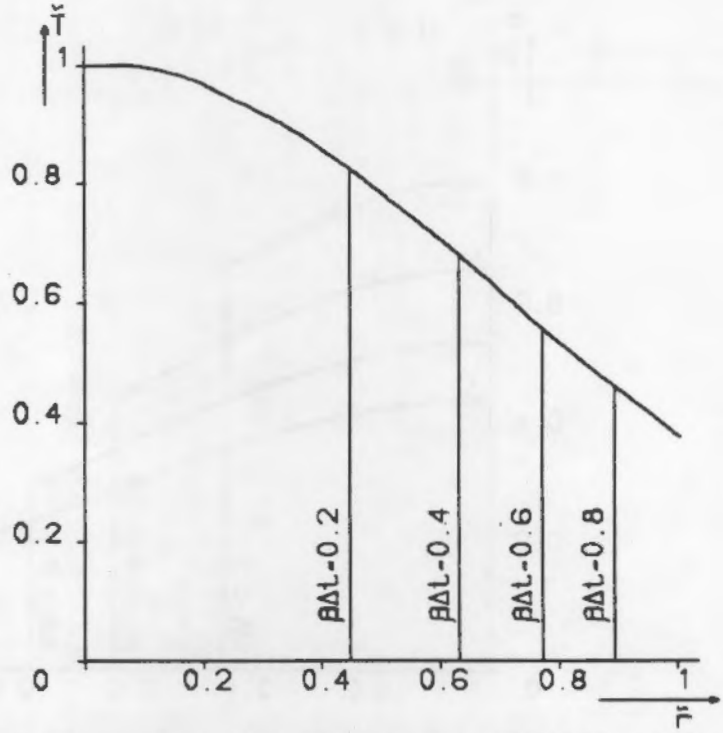

Fig. 4.1. Temperature Distribution in a Confined Aquifer at the End of Injection

End of Storage

The injection phase is followed by a storage phase of duration Δt. At the end of the storage phase, the residence time of any thermal front has increased by Δt. The temperature distribution at the end of the storage phase, therefore, may be found from (4.1) and (4.12) as

$$\tilde{T} = e^{-\beta\Delta t}\, e^{-\bar{r}^2}\, U(\beta\Delta t - \bar{r}^2) \qquad (4.13)$$

The argument of U in (4.13) remains the same as in (4.12), because it is assumed that the thermal velocity during the storage phase is zero. In Fig. 4.2 the temperature distribution (4.13) is plotted for various values of $\beta\Delta t$.

End of Recovery

If the rate of recovery is the same as the rate of injection, all infiltrated water will be pumped back. With the simplified heat transport mechanism applied in this study, no thermal energy remains stored in the aquifer at the end of recovery.

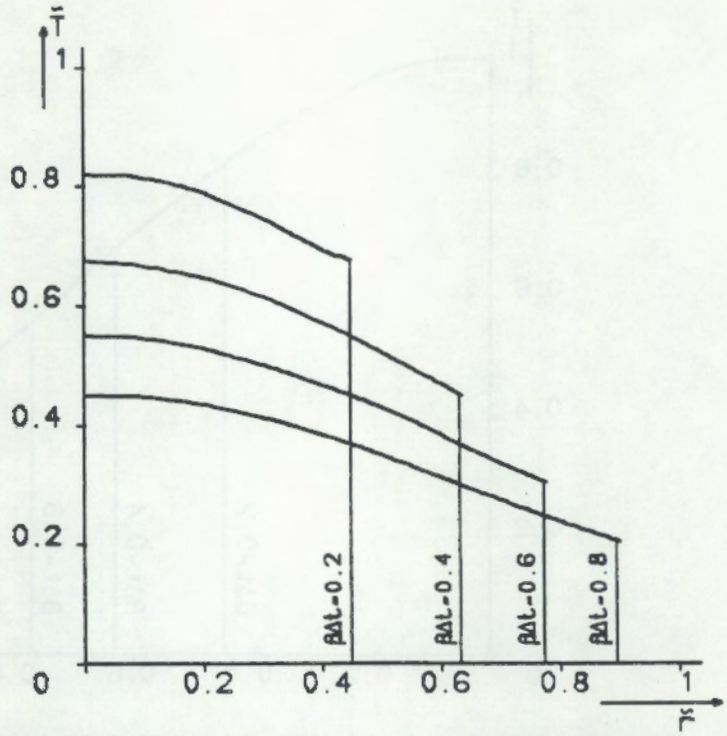

Fig. 4.2. Temperature Distribution in a Confined Aquifer at the End of Storage

Temperature Distribution in the Well

During injection the temperature in the well is kept constant,

$$\tilde{T} = 1 \qquad 0 < t < \Delta t \tag{4.14}$$

During recovery, the temperature in the well depends on the residence time of the thermal front that just enters the well. At the end of the recovery period, for instance, the thermal front that was injected at the start of the injection will be recovered: its residence time is $3\Delta t$. At the beginning of the recovery phase, a thermal front that was injected at the end of the injection cycle is recovered: its residence time is Δt. Therefore, the temperature distribution in the well is found from

$$\tilde{T} = e^{-\beta\{2t' + \Delta t\}} \tag{4.15}$$

where t' is the time since the start of recovery, so that

$$0 < t' < \Delta t \tag{4.16}$$

In Fig. 4.3 the temperature in the well is plotted as a function of the dimensionless time $\beta t'$ for various values of $\beta\Delta t$.

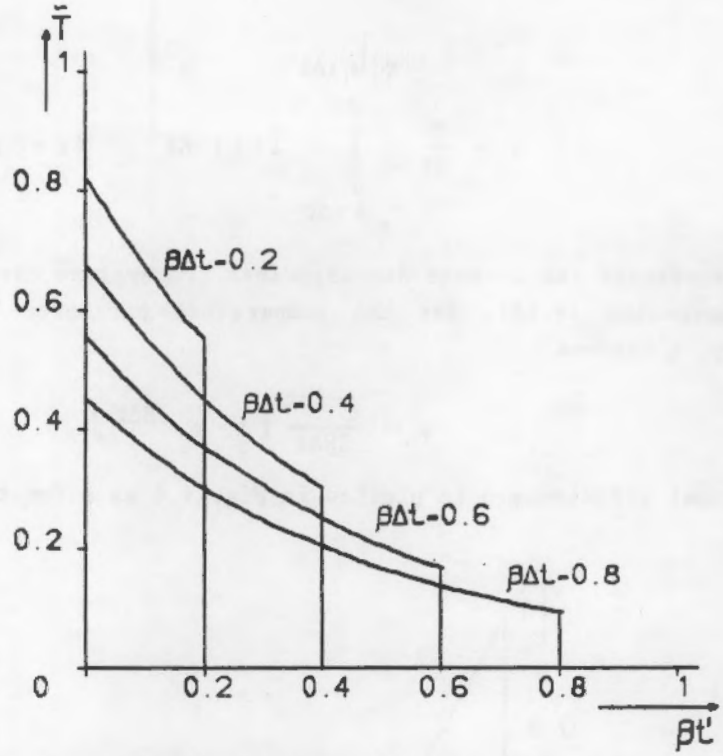

Fig. 4.3. Temperature Distribution in the Well During Recovery of Thermal Energy from a Confined Aquifer

<u>Thermal Efficiency</u>

The thermal efficiency, or recovery factor η, of the injection, storage and recovery system is defined as (Doughty et al. 1982)

$$\eta = \frac{\int_{t_0 + 2\Delta t}^{t_0 + 3\Delta t} C_w\, T(t)\, Q(t)\, dt}{\int_{t_0}^{t_0 + \Delta t} C_w\, T_0(t)\, Q_0(t)\, dt} \qquad (r=0) \qquad (4.17)$$

where the denominator represents the total amount of injected energy and the numerator represents the total amount of recovered energy. Injection starts at t_0 and the temperatures are measured in the source or sink. If the injection rate $Q_0(t)$ is constant and equal to the recovery rate $Q(t)$ and if $T_0(t) = T_0$, η becomes

$$\eta = \frac{1}{\Delta t} \int_{t_0 + 2\Delta t}^{t_0 + 3\Delta t} \tilde{T}(t)\, dt \qquad (r=0) \tag{4.18}$$

which represents the average dimensionless temperature during recovery. With expression (4.15), for the temperature parameter $\tilde{T}$ in the well during recovery, η becomes

$$\eta = \frac{e^{-\beta\Delta t}}{2\beta\Delta t}\left[1 - e^{-2\beta\Delta t}\right] \tag{4.19}$$

The thermal efficiency η is plotted in Fig. 4.4 as a function of $\beta\Delta t$.

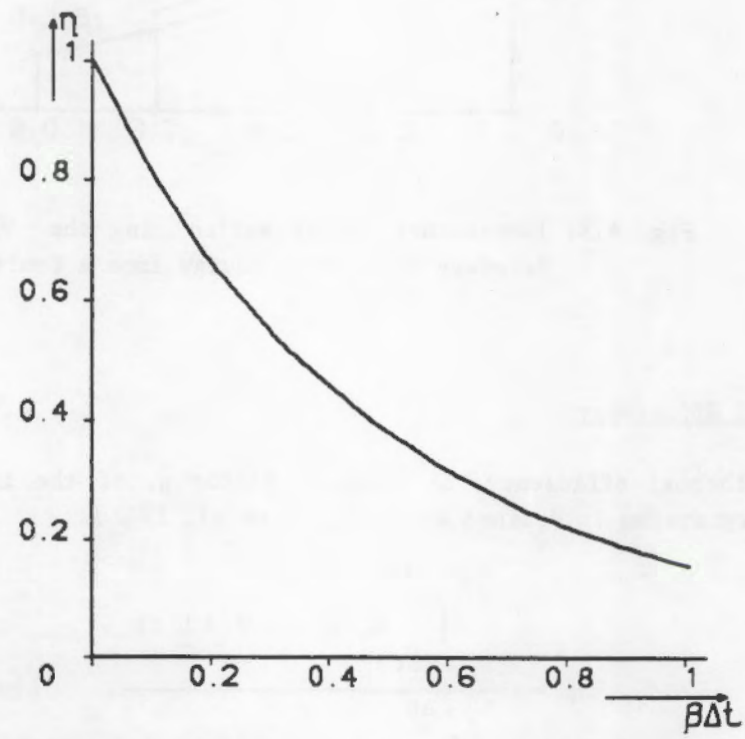

Fig. 4.4. Thermal Efficiency for a Storage System in a Confined Aquifer

4.2 UNCONFINED FLOW CONDITIONS

The differential equation for radial transient flow in an unconfined aquifer is, in terms of the discharge potential Φ,

$$\frac{\partial^2\Phi}{\partial r^2} + \frac{1}{r}\frac{\partial\Phi}{\partial r} = n\frac{\partial\phi}{\partial t} \tag{4.20}$$

The discharge potential Φ is defined as

$$\Phi = \frac{1}{2} k \phi^2 \tag{4.21}$$

where k is the aquifer permeability and where ϕ is the head in the aquifer, measured with respect to the aquifer base. For relatively small changes in ϕ, the right-hand side of (4.20) may be linearized, so that

$$\frac{\partial^2 \Phi}{\partial r^2} + \frac{1}{r}\frac{\partial \Phi}{\partial r} = \frac{n}{k\phi'}\frac{\partial \Phi}{\partial t} \tag{4.22}$$

where ϕ' represents some average head in the aquifer.
The solution to (4.22) is obtained through a Laplace transformation technique (Carslaw and Jaeger 1959, p. 263; Theis 1935);

$$\Phi = \Phi_0 + \frac{Q}{4\pi} E_1(u^2) \tag{4.23}$$

where Q is the discharge of the well during injection and where Φ_0 is the initial potential in the aquifer. The parameter u^2 is a function of r and t and is defined as

$$u^2 = \frac{nr^2}{4k\phi' t} \tag{4.24}$$

The exponential integral $E_1(u^2)$ is defined as

$$E_1(u^2) = \int_{u^2}^{\infty} \frac{e^{-\xi}}{\xi}\, d\xi \tag{4.25}$$

The radial velocity v_r follows from

$$v_r = -\frac{\partial \Phi / \partial r}{n\,\phi} = \frac{Q}{2\pi r n \phi} e^{-u^2} \tag{4.26}$$

where it is noted that v_r contains the head ϕ, which is a function of both r and t,

$$\phi = \sqrt{\frac{2}{k}}\ \sqrt{\Phi_0 + \frac{Q}{4\pi} E_1(u^2)} \tag{4.27}$$

A thermal front in the aquifer travels with a velocity v_r^*, which is given by [see also (3.3)]

$$v_r^* = \frac{n\, C_w}{C^*} v_r \tag{4.28}$$

where C^* follows from (4.3) by replacing H with ϕ,

$$C^* = C + \frac{\overset{11}{C}d}{2\phi} + \frac{\overset{22}{C}d}{2\phi} \tag{4.29}$$

Combining (4.26) with (4.28) and (4.29) yields

$$v_r^* = \frac{Q\, C_w\, e^{-u^2}}{2\pi\, C^*\, \phi\, r} \tag{4.30}$$

The temperature T in the aquifer is given by (3.5) as

$$\frac{\partial T}{\partial t^*} + \frac{\partial T}{\partial t} = -\beta T \tag{4.31}$$

where β follows from (3.4) as

$$\beta = \frac{\overset{12}{\lambda d} + \overset{21}{\lambda d}}{C^* \phi \overset{12}{d d}} \tag{4.32}$$

The following dimensionless parameters are introduced:

$$\alpha_o = \frac{n\, C_w}{C(1+\gamma_o)} \tag{4.33}$$

$$\gamma_o = \frac{\overset{11}{Cd} + \overset{22}{Cd}}{2C\phi_o} \tag{4.34}$$

$$\tilde{Q} = \frac{Q}{\pi k \phi_o^2} \tag{4.35}$$

$$\tilde{\phi} = \frac{\phi}{\phi_o} \tag{4.36}$$

$$\tilde{t} = t\beta_o \tag{4.37}$$

$$\tilde{r} = r\sqrt{\frac{n\beta_o}{\alpha_o \tilde{Q} k \phi_o}} \tag{4.38}$$

$$\tilde{\beta} = \frac{\beta}{\beta_o} = \frac{(1+\gamma_o)}{(\tilde{\phi}+\gamma_o)} \tag{4.39}$$

$$\tilde{T} = \frac{T}{T_o} \tag{4.40}$$

where β_o has the dimension of the inverse of time and is defined as

$$\beta_o = \frac{\overset{12}{\lambda d} + \overset{21}{\lambda d}}{C\phi_o(1+\gamma_o)\overset{12}{d d}} \qquad \left[\frac{1}{s}\right] \tag{4.41}$$

With (4.37) and (4.38) a dimensionless velocity $\tilde{v}_r^*$ is obtained

$$\tilde{v}_r^* = \sqrt{\frac{n}{\alpha_o \tilde{Q} k \phi_o \beta_o}}\; v_r^* \tag{4.42}$$

so that with (4.30), and with the dimensionless parameters defined above, it follows for $\tilde{v}_r^*$ that

$$\tilde{v}_r^* = \frac{\tilde{\beta}}{2\tilde{r}} e^{-u^2} \tag{4.43}$$

The parameter u^2 may be expressed in terms of the dimensionless parameters as [see (4.24)]

$$u^2 = \frac{\alpha_o \tilde{Q} \tilde{r}^2}{4\tilde{\phi}' \tilde{t}} \tag{4.44}$$

where $\tilde{\phi}'$ is some constant dimensionless head of the aquifer,

$$\tilde{\phi}' = \frac{\phi'}{\phi_o} \tag{4.45}$$

Selecting ϕ_o for ϕ' yields

$$\tilde{\phi}' = 1 \tag{4.46}$$

so that u^2 reduces to

$$u^2 = \frac{\alpha_o \tilde{Q} \tilde{r}^2}{4\tilde{t}} \tag{4.47}$$

The dimensionless head $\tilde{\phi}$ becomes, with (4.27) and the dimensionless parameters defined above,

$$\tilde{\phi} = \sqrt{1 + \frac{\tilde{Q}}{2} E_1(u^2)} \tag{4.48}$$

Care has to be taken in selecting values for $\tilde{Q}$. First, pumping rates should not become unrealistically high, so that the head in the well rises above the soil surface or sinks below the aquifer base. Furthermore, it should be kept in mind that the differential equation (4.22) has a linearized storage term, so that solutions are acceptable for only relatively small changes in the head ϕ. In this study, a value for $\tilde{Q}$ has been selected that is equal to 0.08,

$$\tilde{Q} = 0.08 \tag{4.49}$$

The dimensionless temperature $\tilde{T}$ follows from (4.31) after division by $\beta_o T_o$,

$$\frac{\partial \tilde{T}}{\partial \tilde{t}^*} + \frac{\partial \tilde{T}}{\partial \tilde{t}} = \tilde{\beta}\tilde{T} \tag{4.50}$$

It is not possible to write $\tilde{T}$ explicitly in terms of $\tilde{r}$, as has been done for the case of confined flow. For a given residence time $\tilde{t}^*$, $\tilde{r}$ becomes

$$\tilde{r} = \tilde{r}_o + \int_{\tilde{t}_o}^{\tilde{t}_o + \tilde{t}^*} \tilde{v}_r^* \, d\tilde{t} \tag{4.51}$$

where $\tilde{t}_o$ is the start of injection and where $\tilde{r}_o$ is the dimensionless radius of the injection well.

Expression (4.51) may be integrated numerically, for instance, by use of the following recursion formula,

$$\tilde{r}_{i+1} = \tilde{r}_i + \Delta\tilde{\tau} * \tilde{v}_r^*(\tilde{r}_i, \tilde{t}_i) \qquad (i = 0,1,2,\ldots\ldots N-1) \tag{4.52}$$

where

$$\tilde{t}_i = \tilde{t}_{i-1} + \Delta\tilde{\tau} \tag{4.53}$$

Expression (4.52) represents an explicit integration scheme for (4.51), where $\Delta\tilde{\tau}$ is the dimensionless time step,

$$\Delta\tilde{\tau} = \beta_o \, \Delta\tau \tag{4.54}$$

The temperature parameter $\tilde{T}$ may also be obtained through numerical integration of (4.50) by keeping $\tilde{\beta}$ constant during a small time step $\Delta\tilde{\tau}$, which leads to [compare (3.7)]

$$\tilde{T}_{i+1} = \tilde{T}_i \, e^{-\tilde{\beta}(\tilde{r}_i, \tilde{t}_i) * \Delta\tilde{\tau}} \tag{4.55}$$

where $U(\tilde{t} - \tilde{t}^*)$ is omitted, because thermal fronts are followed, so that $\tilde{t}$ will automatically satisfy

$$\tilde{t} \geqq \tilde{t}^* \tag{4.56}$$

<u>End of Injection</u>

With (4.52) and (4.55) the temperature distribution in the aquifer may be solved by tracing a number of thermal fronts during the injection phase. The thermal fronts to be traced will all start at the dimensionless well radius $\tilde{r}_o$,

but at different times $\tilde{t}_{j_0}$,

$$0 < \tilde{t}_{1_0} < \tilde{t}_{2_0} < \tilde{t}_{3_0} \ldots\ldots < \Delta\tilde{t} \tag{4.57}$$

where $\Delta\tilde{t}$ is the dimensionless duration of the injection cycle,

$$\Delta\tilde{t} = \beta_0 \, \Delta t \tag{4.58}$$

The temperature distribution in the aquifer, at the end of injection, will be obtained if the numerical integration with (4.52) through (4.55), for the jth thermal front, is aborted after the $N_j{}^{th}$ time step, where

$$\tilde{t}_j(N_j) = \Delta\tilde{t} \tag{4.59}$$

and whereby N_j follows from

$$N_j = (\Delta\tilde{t} - t_{j_0})/\Delta\tilde{\tau} \tag{4.60}$$

In Fig. 4.5 the temperature distribution is plotted for various values of $\beta_0 \Delta t$ and for fixed values of $\tilde{Q}$, α_0 and γ_0:

$$\tilde{Q} = 0.08$$

$$\alpha_0 = 0.455 \tag{4.61}$$

$$\gamma_0 = 0.08$$

<u>End of Storage</u>

The flow problem during the storage phase may be described by superimposing a sink onto the source at the end of injection, $t = \Delta t$. The discharge of the sink equals that of the source. The head $\tilde{\phi}$ takes the form

$$\tilde{\phi} = \sqrt{1 + \frac{\tilde{Q}}{2}\left[E_1(u^2) - E_1(u_1^2)\right]} \qquad (t > \Delta t) \tag{4.62}$$

where u_1^2 is defined as

$$u_1^2 = \frac{\alpha_0 \tilde{Q} \tilde{r}^2}{4(\tilde{t} - \Delta\tilde{t})} \qquad (\tilde{t} > \Delta\tilde{t}) \tag{4.63}$$

Similarly, the velocity $\tilde{v}^*_r$ now becomes

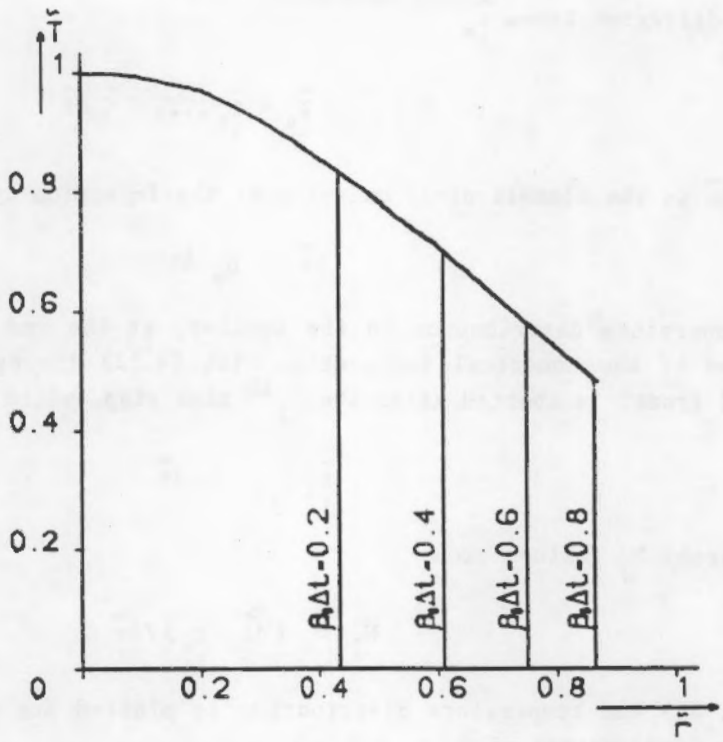

Fig. 4.5. Temperature Distribution in an Unconfined Aquifer at the End of Injection

$$\tilde{v}_r^* = \frac{\tilde{\beta}}{2\tilde{r}}\left[e^{-u^2} - e^{-u_1^2}\right] \qquad (\tilde{t} > \Delta\tilde{t}) \tag{4.64}$$

The integration with (4.52) through (4.55) for each thermal front is continued with (4.62) through (4.64) for M time steps, until the end of storage, so that

$$\tilde{t}_{j(M)} = 2\,\Delta\tilde{t} \tag{4.65}$$

whereby M is given by

$$M = \Delta\tilde{t}/\Delta\tilde{\tau} \tag{4.66}$$

It is noted that, as for the case of confined flow, all three phases are chosen of equal length Δt [see (4.4)] . The temperature distribution in the aquifer is plotted in Fig. 4.6 for various values of $\beta_o\Delta t$.

End of Recovery

The approach adopted above can be extended to the recovery phase by once more adding a sink, now at the end of the storage period. The head $\tilde{\phi}$ and thermal velocity $\tilde{v}_r^*$ will now become

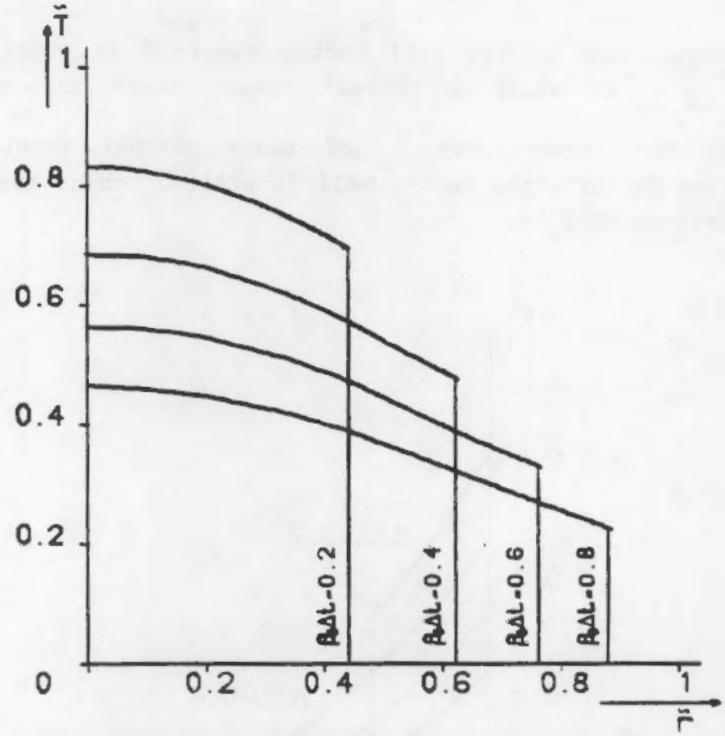

Fig. 4.6. Temperature Distribution in an Unconfined Aquifer at the End of Storage

$$\tilde{\phi} = \sqrt{1 + \frac{\tilde{Q}}{2}\left[E_1(u^2) - E_1(u_1^2) - E_1(u_2^2) \right]} \qquad (\tilde{t} > 2\Delta\tilde{t}) \qquad (4.67)$$

and

$$\tilde{v}_r^* = \frac{\tilde{\beta}}{2\tilde{r}}\left[e^{-u^2} - e^{-u_1^2} - e^{-u_2^2} \right] \qquad (\tilde{t} > 2\Delta\tilde{t}) \qquad (4.68)$$

respectively, where u_2^2 is defined as

$$u_2^2 = \frac{\alpha_0 \tilde{Q}\tilde{r}^2}{4[\tilde{t} - 2\Delta\tilde{t}]} \qquad (\tilde{t} > 2\Delta\tilde{t}) \qquad (4.69)$$

Executing (4.52) with (4.68) will result in the tracing of thermal fronts back to the well. The process for the jth heat front is aborted after the K_j^{th} time step, when it enters the well; hence,

$$\tilde{r}_j(K_j) \leq \tilde{r}_o \qquad (4.70)$$

It appears that, as for the case of confined flow, no thermal energy remains stored in the aquifer after recovery is completed.

Temperature Distribution in the Well

The temperature in the well during recovery is obtained by recording all times $\tilde{t}_j(K_j)$ at which a thermal front enters the recovery well and by recording the temperatures $\tilde{T}_j$ of those thermal fronts. In Fig. 4.7 this temperature distribution in the well is plotted versus the recovery time t' for various values of $\beta_o \Delta t$.

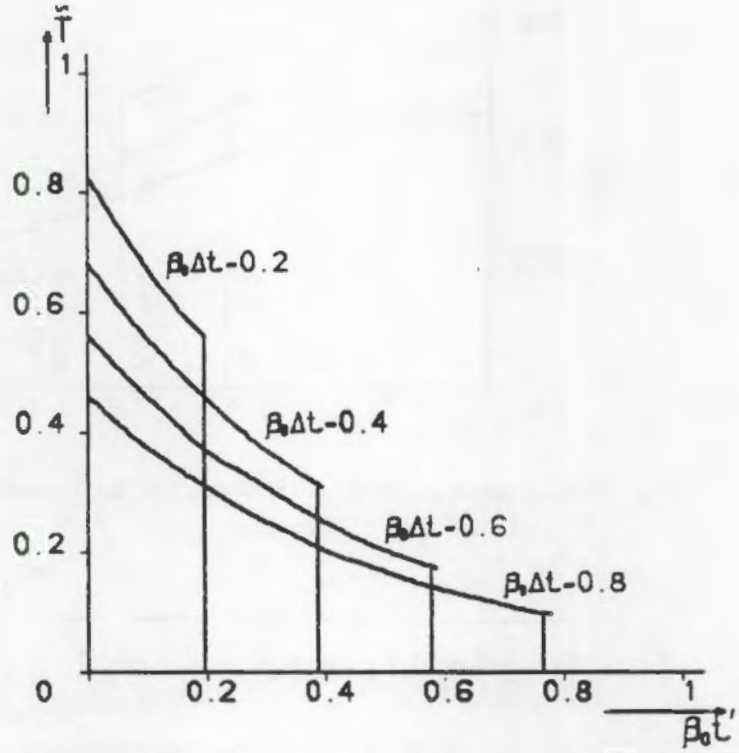

Fig. 4.7. Temperature Distribution in the Well During Recovery of Thermal Energy from an Unconfined Aquifer

Thermal Efficiency

The thermal efficiency η has been calculated for the four different values of $\beta_o \Delta t$ used in the previous plots. The values of η are obtained by numerically integrating (4.18). The results are given in Table 4.1

TABLE 4.1. Thermal efficiency for storage in an unconfined aquifer

$\beta_o \Delta t \rightarrow$	0.2	0.4	0.6	0.8
η	0.67	0.47	0.34	0.22

4.3 REMARKS

Small differences exist between the results obtained for confined flow and unconfined flow. The temperature distribution penetrates slightly more into the confined aquifer than into the unconfined aquifer. The thermal efficiency of the injection, storage and recovery scheme, however, is approximately the same for both flow cases.

In comparing the results in this section with those of other studies, it appears that the thermal efficiency η (4.19) is low, especially for larger values of Δt (Doughty et al. 1982). A reason for this low efficiency may be the rather crude way in which heat loss through the aquifer boundaries is modeled. Especially the assumption of a thin aquifer base with a constant outer temperature, shown in Fig. 3.1, may lead to an overestimation of the heat loss, as was found in Section 3.

5.0 MODELING THERMAL ENERGY STORAGE IN UNCONFINED AQUIFERS

In Section 4, the injection, storage and recovery of thermal energy has been discussed for the simple case of radial flow. In general, however, the flow pattern loses its symmetry due to such features as uniform flow, creeks, canals and wells. As a result of this asymmetry, a significant portion of the injected hot or cold water may not be recovered. Hence, the flow conditions in the aquifer may have a significant impact on the thermal efficiency of an ATES system.

A computer program UCATES (UnConfined Aquifer Thermal Energy Storage) has been written that solves the general problem of transient groundwater flow and heat transport in unconfined aquifers through the superposition of elementary analytic solutions.

The program is intended to be a first step toward a comprehensive screening tool for projected ATES systems in unconfined aquifers. In its present form, it treats the heat loss through the aquifer base and vadose zone in a rather crude manner, but is designed to provide a detailed solution to the heat convection in the aquifer, including flow toward, for instance, canals or creeks.

In this section the solution techniques employed by UCATES will be discussed and the main structure of the program will be outlined. At the end of this section some program validations and demonstrations will be presented.

5.1 SOLVING THE HEAT TRANSPORT PROBLEM

The differential equation for heat transport in unconfined aquifers is given by (2.18) as

$$nC_w\phi v_\alpha \frac{\partial T}{\partial x_\alpha} + C\phi\frac{\partial T}{\partial t} = \overset{1}{F} + \overset{2}{F} \qquad (\alpha = 1,2) \tag{5.1}$$

The heat fluxes $\overset{1}{F}$ and $\overset{2}{F}$ through the aquifer base and vadose zone, respectively, will be approximated by [see (3.1)]

$$\overset{1}{F} = -\frac{\overset{1}{\lambda}}{\overset{1}{d}}T \quad ; \quad \overset{2}{F} = -\frac{\overset{2}{\lambda}}{\overset{2}{d}}T \tag{5.2}$$

where $\overset{1}{\lambda}$ and $\overset{1}{d}$ are the thermal conductivity and thickness of the aquifer base, respectively, and where $\overset{2}{\lambda}$ and $\overset{2}{d}$ are the same properties for the vadose zone. It

has been shown in Section 3 that this heat loss mechanism may be improved upon by incorporating heat storage in the aquifer boundaries. In doing so, C must be replaced by C^* [see also (3.68)]:

$$C^* = C + \frac{\overset{11}{\rho d}}{2\phi} + \frac{\overset{22}{\rho d}}{2\phi} \tag{5.3}$$

whereby it is noted that C^* depends on the head ϕ, which is a function of both location and time. Expression (5.1) may be written in the form

$$v_\alpha^* \frac{\partial T}{\partial x_\alpha} + \frac{\partial T}{\partial t} = -\beta T \tag{5.4}$$

where the thermal velocity v_α^* is defined by [see also (3.3)]

$$v_\alpha^* = \frac{nC_w}{C^*} v_\alpha \tag{5.5}$$

and where β is defined by

$$\beta = \frac{\overset{12}{\lambda d} + \overset{21}{\lambda d}}{C^* \phi \overset{12}{d d}} \tag{5.6}$$

Equation (5.4) may also be written as

$$\frac{\partial T}{\partial t^*} + \frac{\partial T}{\partial t} = -\beta T \tag{5.7}$$

where t^* is the residence time of a thermal front. Expression (5.7) is identical to (3.5), however β is dependent on ϕ and therefore on x_α and t. Equation (5.7) therefore, in general, cannot be evaluated by use of standard Laplace transforms, as has been done in section 3 with β being constant, see (3.6). However, if β is taken to be constant during a small increment Δt^* of the residence time t^*, then (5.7) can be evaluated incrementally, leading to

$$T_{i+1} = T_i e^{-\beta_i (t^*_{i+1} - t^*_i)} \; U(t_{i+1} - t^*_{i+1}) \tag{5.8}$$

where β_i is evaluated at time t_i and kept constant between t^*_i and t^*_{i+1}, see also (3.7). If, in evaluating (5.8), thermal fronts are followed, then t^* may be replaced by the time t, leading to

$$T_{i+1} = T_i \; e^{-\beta_i (t_{i+1} - t_i)} \tag{5.9}$$

<u>Temperature Distribution in the Aquifer</u>

The location x_α^* of a thermal front is found by integrating

$$\frac{dx_\alpha^*}{dt} = \frac{nC_w}{C^*(x_\alpha^*,t)} v_\alpha(x_\alpha^*,t) \qquad (\alpha=1,2) \tag{5.10}$$

whereby the temperature of the thermal front is obtained from (5.9):

$$T_{i+1} = T_i e^{-\beta(x_\alpha^*,t_i)[t_{i+1}-t_i]} \tag{5.11}$$

The differential equations (5.10) are solved in program UCATES by the classical fourth order Runge-Kutta method (Forsyth et al. 1977).

Because expressions (5.10) and (5.11) involve both the groundwater velocity v_α and the head ϕ [see also (5.3) and (5.6)], the solution to the transient groundwater flow problem must either be known in advance or constructed simultaneously in solving (5.10) and (5.11). In program UCATES, the solution to the groundwater flow problem is solved and stored for one phase of the ATES cycle at a time: the injection, the storage, or the recovery phase.

5.2 SOLVING THE TRANSIENT GROUNDWATER FLOW PROBLEM

The differential equstion for transient flow in an unconfined aquifer, based on the Dupuit-Forchheimer assumption, is

$$\nabla^2\Phi = \frac{n}{k\phi}\frac{\partial\Phi}{\partial t} \tag{5.12}$$

The discharge potential Φ is defined as

$$\Phi = \frac{1}{2}k\phi^2 \tag{5.13}$$

where k is the aquifer permeability and ϕ is the head meaaured with respect to the aquifer base. The storage term on the right-hand side of (5.1) may be viewed as an areal sink distribution, the strength of which depends on both location and time;

$$\frac{n}{k\phi}\frac{\partial\Phi}{\partial t} = \sigma(x_\alpha,t) \qquad (\alpha=1,2) \tag{5.14}$$

The areal sink distribution strength σ may be approximated by a network of triangles, each with a linear strength distribution. The solution in terms of Φ and velocity v_α for such a triangular areal sink was provided by Strack, who also suggested its use for solving transient flow.

The potential at an arbitrary point x_α and at a time t in the aquifer may be written in the form

$$\Phi(x_\alpha,t) = \sum_{m=1}^{M} \overset{ls}{F}_m(x_\alpha)Q_m^{(t)} + \sum_{j=1}^{J} \overset{tr}{F}_j(x_\alpha)\sigma_j^{(t)} + G(x_\alpha) + \overset{c}{\Phi} \qquad (5.15)$$

The function G represents all known contributions to the potential Φ as generated, for instance, by uniform flow and discharge specified wells. The functions $\overset{ls}{F}_m$ represent the contributions of all M flow features with unknown strength parameters $Q_m^{(t)}$. In this study $\overset{ls}{F}_m$ represents line sinks only, which may be used to model creeks, canals, or lake boundaries (Strack and Haitjema 1981). The functions $\overset{tr}{F}_j$ represent the contributions of the areal sink distribution, with J nodal strengths $\sigma_j^{(t)}$, which are also unknown. The potential $\overset{c}{\Phi}$ is independent of the location and time. The M+J unknown strength parameters and the constant $\overset{c}{\Phi}$ may be obtained as follows. At each element with unknown $Q_m^{(t)}$ the potential is given and assumed constant, which leads to the following M equations:

$$\Phi_i = \overset{ls}{F}_{im}Q_m^{(t)} + \overset{tr}{F}_{ij}\sigma_j^{(t)} + G_i + \overset{c}{\Phi} \qquad (i=1,2,\ldots.M) \qquad (5.16)$$

$$(m=1,2,\ldots..M)$$
$$(j=1,2,\ldots..J)$$

At the jth nodal point of the triangle network, the strength σ_j may be expressed in terms of the potential Φ [see (5.14)]

$$\left[\frac{n}{k\phi}\frac{\partial\Phi}{\partial t}\right]_j = \sigma_j \qquad (5.17)$$

If a linear strength distribution is assumed over a time span Δt, (5.17) leads to the following J equations at the J nodal points of the triangle network:

$$\frac{n}{k\phi^{(t)}}\frac{\Phi_j^{(t+\Delta t)} - \Phi_j^{(t)}}{\Delta t} = \frac{\sigma_j^{(t)} + \sigma_j^{(t+\Delta t)}}{2} \qquad (j=1,2,\ldots..J) \quad (5.18)$$

Finally a continuity condition is to be satisfied requiring that all discharge variations, at each time step, together are zero. This condition implies that water is obtained from storage and not from infinity. Consequently, when a well is switched on and left pumping for a long time its entire discharge is supplied by line sinks (creeks) in the domain; the strengths of the triangular surface distributions will have vanished.

Before the above equations can be solved, a solution is required for t=0. This steady state solution can be obtained from (5.15) by omitting the terms of the triangles. Like for the transient case potentials are specified at the line sink centers to solve for the strength's $Q_m^{(o)}$. The constant $\overset{c}{\Phi}$ is obtained by specifying the potential at a reference point outside the domain of interest.

This procedure is identical to the one applied by Strack and Haitjema [1981].

The approach outlined here was proposed by Strack and first tested by Debbarh (1982) for the case of one-dimensional flow. Debbarh employed sink distributions over a line element instead of triangles. Good agreement was obtained in comparison with exact solutions, except during the early time steps. Debbarh identified that problem as related to a poor estimate of the initial areal sink distribution. Tests conducted during this study for the two-dimensional flow case confirmed his findings. However, after improving the initial areal strength distribution, by locally refining the network and using small initial time steps, good agreement with an exact solution could be obtained.

Alternative Solution Procedure

When the transient flow conditions in the aquifer are due mainly to discharge specified wells, as may be the case when dealing with injection and recovery systems for thermal energy, the efficiency of the above approach may be improved upon as follows.

The potential Φ is written as the sum of N+1 potentials,

$$\Phi = \overset{e}{\Phi} + \sum_{i=1}^{N} \overset{w}{\Phi}_{(i)} \tag{5.19}$$

With (5.19) the differential equation (5.12) may be written as

$$\nabla^2\Phi = \frac{n}{k\phi}\frac{\partial\overset{e}{\Phi}}{\partial t} + \sum_{i=1}^{N}\frac{n}{k\phi}\frac{\partial\overset{w}{\Phi}_{(i)}}{\partial t} \tag{5.20}$$

The second term on the right-hand side of (5.20) is written as

$$\sum_{i=1}^{N}\frac{n}{k\phi}\frac{\partial\overset{w}{\Phi}_{(i)}}{\partial t} = \sum_{i=1}^{N}\left[\frac{n}{k\bar{\phi}_{(i)}}\frac{\partial\overset{w}{\Phi}_{(i)}}{\partial t} - \frac{n\Delta\phi_{(i)}}{k\phi\bar{\phi}_{(i)}}\frac{\partial\overset{w}{\Phi}_{(i)}}{\partial t}\right] \tag{5.21}$$

where the head $\bar{\phi}_{(i)}$ is chosen independent of both location and time and is defined as

$$\bar{\phi}_{(i)} = \phi - \Delta\phi_{(i)} \tag{5.22}$$

Expressions (5.20) and (5.21) are combined to form the following N+1 differential equations:

$$\nabla^2\overset{e}{\Phi} = \frac{n}{k\phi}\frac{\partial\overset{e}{\Phi}}{\partial t} - \sum_{i=1}^{N}\frac{n\Delta\phi_{(i)}}{k\phi\bar{\phi}_{(i)}}\frac{\partial\overset{w}{\Phi}_{(i)}}{\partial t} \tag{5.23}$$

$$\nabla^2 \overset{w}{\Phi}_{(i)} = \frac{n}{k\bar{\phi}_{(i)}} \frac{\partial \overset{w}{\Phi}_{(i)}}{\partial t} \qquad (i = 1,2,3,\ldots\ldots,N) \tag{5.24}$$

If a solution is found for $\overset{e}{\Phi}$, which satisfies (5.23), and solutions are found for $\overset{w}{\Phi}_{(i)}$, which satisfy (5.24), then the sum of these solutions, Φ [see (5.19)], will satisfy (5.20) and therefore (5.12). It is noted that the equations (5.24) are linear, since $\bar{\phi}_{(i)}$ is a constant. The differential equations (5.24) are of the same form as (4.22) for the case of radial flow. The potentials $\overset{w}{\Phi}_{(i)}$, therefore, may be chosen as the solutions to (5.24) for flow due to the injection and recovery wells. The potential $\overset{w}{\Phi}_{(i)}$ is then generated by the ith well, located at $\overset{w}{x}_{i\alpha}$ and pumping with a discharge $Q_{(i)}$ since time $t_{(i)}$:

$$\overset{w}{\Phi}_{(i)}(x_\alpha, t) = -\frac{Q_{(i)}}{4\pi} E_1(\overset{i}{u}^2) \tag{5.25}$$

where $\overset{i}{u}^2$ is defined as

$$\overset{i}{u}^2 = \frac{n\left[\overset{w}{x}_{i\alpha} - x_\alpha\right]\left[\overset{w}{x}_{i\alpha} - x_\alpha\right]}{4k\bar{\phi}_{(i)}\left[t - t_{(i)}\right]} \qquad (i \text{ no sum}) \tag{5.26}$$

It is noted that the use of (5.25) requires finite injection or extraction periods, as (5.25) does not approach a steady state solution when t becomes infinite. In the present case of seasonal thermal energy storage, however, periodic injection and extraction is automatically implied. The potential $\overset{e}{\Phi}$ is now used to represent all remaining flow features in the aquifer, such as uniform flow, wells (that are not switched on or off) and creeks. The potential $\overset{e}{\Phi}$ also contains contributions from the transient wells, which are introduced by means of the areal sink or source distributions represented by the second term on the right-hand side of (5.23). This latter term accounts for the nonlinearity of the original differential equation (5.20).

Equation (5.23) may be solved in the same way as was proposed for solving (5.12) [i.e. see (5.12) through (5.18)]. However, instead of a single strength distribution σ, the right-hand side of (5.23) is now replaced by two areal sink or source distributions, $\overset{e}{\sigma}$ and $\overset{w}{\sigma}$,

$$\nabla^2 \overset{e}{\Phi} = \overset{e}{\sigma}(x_\alpha, t) - \overset{w}{\sigma}(x_\alpha, t) \tag{5.27}$$

where

$$\overset{e}{\sigma} = \frac{n}{k\phi}\frac{\partial\overset{e}{\Phi}}{\partial t} \tag{5.28}$$

$$\overset{w}{\sigma} = \sum_{i=1}^{N} \frac{n\Delta\phi_{(i)}}{k\phi\bar{\phi}_{(i)}}\frac{\partial\overset{w}{\Phi}_{(i)}}{\partial t} \tag{5.29}$$

Both strength distributions (5.28) and (5.29) may be approximated by the same network of triangles as was proposed for representing distribution (5.14). The strength distribution (5.29) is known, provided that $\Delta\phi_{(i)}$ or, for that matter, ϕ is known. The unknown strengths $\overset{e}{\sigma}_j$, Q_m and the unknown constant $\overset{c}{\Phi}$ are obtained from a continuity equation and from the following J + M equations; see also (5.16) through (5.18):

$$\overset{o}{\Phi}_i(t) = \overset{ls}{F}_{im}Q_m(t) + \overset{tr}{F}_{ij}\left[\overset{e}{\sigma}_j(t) - \overset{w}{\sigma}_j(t)\right] + G_i + \overset{c}{\Phi} \tag{5.30}$$

and

$$\frac{n}{k\phi(t)}\frac{\overset{o}{\Phi}_j(t+\Delta t) - \overset{o}{\Phi}_j(t)}{\Delta t} = \frac{\overset{e}{\sigma}_j(t) + \overset{o}{\sigma}_j(t+\Delta t)}{2} \tag{5.31}$$

whereby

$$(i = 1,2,3,\ldots,M)$$
$$(m = 1,2,3,\ldots,M)$$
$$(j = 1,2,3,\ldots,J)$$

As indicated in (5.31), in solving for the unknowns at time $t+\Delta t$, the head ϕ in (5.31) is obtained from the solution at time t. The potentials $\overset{o}{\Phi}_i(t)$ at the line sink centers are obtained from the known and constant potentials Φ_i at those points by

$$\overset{o}{\Phi}_i(t) = \Phi_i - \sum_{j=1}^{N}\left[\overset{w}{\Phi}_{(j)}(t)\right]_i \quad (i = 1,2,\ldots,M) \tag{5.32}$$

where $\left[\overset{w}{\Phi}_{(j)}(t)\right]$ are the potentials at the line sink centers obtained from (5.25) with (5.26). Because the most dominant transient effects are already incorporated in the potentials $\overset{w}{\Phi}_{(i)}$, a solution to (5.27) may be constructed with larger time steps then would be feasible when solving (5.12) with (5.14). The sensitivity of the solution to the initial areal strength distribution, mentioned before, may also be avoided by making proper choices for the heads $\bar{\phi}_{(i)}$. At the onset of pumping, the derivative of the potential with respect to time, $\partial\overset{w}{\Phi}_{(i)}/\partial t$, is zero everywhere except at the well. If $\bar{\phi}_{(i)}$ is

selected equal to the head at the well that occurs at the onset of pumping, the corresponding term in (5.29) vanishes. Expression (5.29) vanishes altogether (initially) if this procedure is adopted for all transient wells. Expression (5.28) is also zero initially, since the remaining flow features in the aquifer do not cause transient effects until affected by the transient wells.

The above solution procedure is implemented in program UCATES. Solutions to the groundwater flow problem are constructed and stored for a complete phase of the ATES cycle at a time: injection, storage, or recovery. The solution is stored by storing the following parameters for I time steps:

$$\begin{bmatrix} \overset{e}{\sigma}_j - \overset{w}{\sigma}_j \end{bmatrix}^{(t_i)}$$

$$Q_m^{(t_i)} \tag{5.33}$$

$$\overset{c}{\Phi}(t_i)$$

where

$$(j = 1,2,3,\ldots,J)$$
$$(m = 1,2,3,\ldots,M)$$
$$(i = 1,2,3,\ldots,I)$$

The coefficient function $\overset{ls}{F}$ for the line sink is given below as the real part of a complex potential function,

$$\overset{ls}{F}(x_\alpha) = \mathrm{Re}\left[\overset{ls}{\Omega}(z)\right] \tag{5.34}$$

where $\Omega(z)$ is given by (see Strack and Haitjema 1981)

$$\overset{ls}{\Omega}(z) = \frac{Q\,|z_2 - z_1|}{2\pi(z_2 - z_1)} \cdot$$

$$\left[(z - z_2)\ln(z - z_2) - (z - z_1)\ln(z - z_1) + (z_2 - z_1) \right] \tag{5.35}$$

The argument z in (5.34) is the complex coordinate

$$z = x_1 + ix_2 \tag{5.36}$$

and z_1 and z_2 in (5.35) are the complex endpoints of the line sink. The form of the coefficient function for the areal source distribution $\overset{tr}{F}$ is presented in Appendix A.

6.0 PROGRAM UCATES

A new program UCATES (UnConfined Aquifer Thermal Energy Storage) has been designed to solve the heat transport problem in unconfined aquifers under transient flow conditions. The program is developed on a Perkin Elmer 3220 computer and written in Fortran. Program UCATES is equipped with free format input rontines, which allows the introduction of data in random order by command words and parameters. Commands may be entered from a file or a terminal or from both by a SWITCH command. Two types of binary data files can be created; one file containa all data stored in common, while the other file contains data for generating contour plots of heads, isotherms, or temperature distributions in the recovery wells. The data files make it possible to preserve intermediate results or to save complete ATES simulations for later interpretation. Error checking routines are included that protect the user against illegal input and array overflow. Two debugging facilities are provided. First, most routines in the program check essential parameters prior to execution. Second, a DEBUG command is available, which lets the user inspect the contents of all common blocks and arrays through free format commands. In addition, each individual function in the program may also be tested using the DEBUG command. A user manual is provided that may be accessed via a HELP command. Typing HELP displays a summary of all available commands and parameters, while typing HELP followed by a command word displays an explanation of the use of that command.

6.1 MATRIX EQUATIONS

The groundwater flow problem is solved with (5.30) and (5.31) at various times during a phase of the ATES cycle. The equations (5.30) with (5.32) and (5.31) may be written in matrix form as

$$A_{ij}x_j = y_i \tag{6.1}$$

where the matrix coefficients A_{ij} are defined as follows:

For $i = 1,2,\ldots,J+M$ and $j = 1,2,\ldots,J$:

$$A_{ij} = \overset{tr}{F}_{ij} - \delta_{ij}\frac{n}{k\phi_{(j)}^{(t)}} \tag{6.2}$$

For $i = 1,2,\ldots,J+M$ and $j = J+1,J+2,\ldots,J+M$:

$$A_{ij} = \overset{ls}{F}_{ij} \tag{6.3}$$

For $i = 1,2,\ldots J+M$ and $j = J+M+1$:

$$A_{ij} = 1.0 \tag{6.4}$$

For $i = J + M + 1$ and $j = 1,2,\ldots,J$

$$A_{ij} = \frac{1}{3}\sum \overset{tr}{O} \tag{6.5}$$

For $i = J + M + 1$ and $j = J + 1,\ldots,J + M$

$$A_{ij} = \overset{ls}{L}_j \tag{6.6}$$

For $i = J + M + 1$ and $j = J + M + 1$

$$A_{ij} = 0 \tag{6.7}$$

where the right hand side of (6.5) represents the total area of the triangles associated with the j th triangle node and where the rigth hand side of (6.6) represents the length of the j th line sink. The solution vector x_j is defined as

$$x_j = \overset{e}{\sigma}_j(t + \Delta t) - \overset{e}{\sigma}_j(t) \qquad (j = 1,2\ldots,J) \tag{6.8}$$

$$x_j = Q_j^{(t + \Delta t)} - Q_j^{(t)} \qquad (j = J + 1,\ldots,J + M) \tag{6.9}$$

$$x_j = \overset{c}{\Phi}(t + \Delta t) - \overset{c}{\Phi}(t) \qquad (j = J + M + 1) \tag{6.10}$$

The last equation implies that the constant $\overset{c}{\Phi}$ is recomputed at every time step. However, $\overset{c}{\Phi}$ does not vary with time, so (6.10) should yield zero. The recomputed constant $\overset{c}{\Phi}$ is stored for every time step and may be used to verify the accuracy with which the differential equation is satisfied in the farfield. The known vector y_i is defined as

$$y_i = \frac{k\phi_{(i)}^{(t)}\Delta t}{n}\,\overset{e}{\sigma}_i(t) + \sum_{j=1}^{J} \overset{tr}{F}_{ij}\left[\overset{w}{\sigma}_j(t + \Delta t) - \overset{w}{\sigma}_j(t)\right] \qquad (i = 1,2,\ldots J) \tag{6.11}$$

$$y_i = \Phi_i - \Phi_i^{(t)} - \sum_{j=1}^{N}\left[\overset{w}{\Phi}_{(j)}(t + \Delta t) - \overset{w}{\Phi}_{(j)}(t)\right]_i + \sum_{j=1}^{J} \overset{tr}{F}_{ij}\left[\overset{w}{\sigma}_j(t + \Delta t) - \overset{w}{\sigma}_j(t)\right] \qquad (i = J + 1,\ldots,J + M) \tag{6.12}$$

$$y_i = -\sum\left[\overset{e}{\sigma}_j(t) - \overset{w}{\sigma}_j(t)\right]\frac{1}{3}\sum\overset{tr}{0} - \sum Q_j(t)\overset{ls}{L}_j \quad (i = J + M + 1) \tag{6.13}$$

The potential Φ_i is given and follows from the heads specified at line sink centers. It is noted that the strength $\overset{w}{\sigma}_j(t+\Delta t)$ involves the unknown head $\phi_{(j)}^{(t+\Delta t)}$ [see (5.29) and (5.22)]:

$$\overset{w}{\sigma}_j(t+\Delta t) = \sum_{i=1}^{N} \frac{n[\bar{\phi}_{(j)} - \phi_{(j)}^{(t+\Delta t)}]}{k\phi_{(j)}^{(t+\Delta t)}\bar{\phi}_{(i)}} \frac{\partial\overset{w}{\Phi}_{(i)}}{\partial t} \tag{6.14}$$

The head $\phi^{(t+\Delta t)}$ in UCATES is estimated by use of $\overset{e}{\Phi}(t)$ and $\overset{w}{\Phi}_{(i)}^{(t+\Delta t)}$, both of which are known at time t, so that

$$\phi^{(t+\Delta t)} \simeq \sqrt{\frac{2}{k}\left[\overset{e}{\Phi}(t) + \sum_{i=1}^{N}\overset{w}{\Phi}_{(i)}^{(t+\Delta t)}\right]} \tag{6.15}$$

The matrix equations (6.1) are solved by use of LU decomposition and back substitution (Forsythe et al. 1977). Because some of the matrix coefficients A_{ij} depend on ϕ [see (6.2)], the LU decomposition has to be repeated for each time step Δt.

6.2 THERMAL MARKERS

The temperature distribution in the aquifer as a function of both location and time is represented by sets of thermal markers, which are released at the injection well(s) at certain time intervals and which are traveling through the aquifer with the thermal velocity, (5.5). The position of each thermal marker is calculated with (5.10) and its temperature is found from (5.11). Since β in (5.11) depends on both location and time, the equations (5.10) and (5.12) are evaluated simultaneously under control of the routine TRACE. The markers are released at time intervals that are selected in such a way that the temperature intervals between markers are approximately the same. This is accomplished by estimating the subsequent release times t_r by using (5.11) with a constant value $\bar{\beta}$ for β.

$$t_{r+1} = t_r - \frac{1}{\bar{\beta}}\ln\left[1 - \frac{\Delta T}{T_r}\right] \tag{6.16}$$

The parameter ΔT is the desired temperature increment and T_r is the temperature at time t_r. The locations and release times of thermal markers are generated by the rontine GENCHR. An isotherm of a given temperature is generated by a set of points in the aquifer. Each point is obtained by linear interpolation between markers released from the same location at the same well, but at different

times.

During recovery, thermal markers may enter a recovery well, influencing the temperature in that well. A recovery well is subdivided into a number of sectors. At the onset of recovery the temperature in each sector is the same and determined by the temperature distribution in the aquifer that occurs at the end of storage. The program requires the specification of this initial temperature as user-provided input. When a single marker enters a sector during a time step, the temperature in that sector is set equal to the temperature of that thermal marker. When more than one marker enters the same sector during the same time step, the temperatures of the markers are averaged and assigned to that sector. At the end of each time step, the temperature in the well is defined as the average of the temperatures in the sectors. Each sector, however, maintains its own temperature, unless new thermal markers enter that sector. When a thermal marker that was released at the onset of the injection cycle enters a sector, it is assumed that the temperature in that sector is zero (equals the initial temperature in the aquifer) during all subsequent time steps. The temperature in a sector is also maintained at zero, if a 'zero marker' enters that sector. The latter markers, with a temperature zero, are distributed just outside the warm water domain at the beginning of the recovery cycle. The bookkeeping discussed above is performed in routine WELTEM. It is clear that a smooth temperature distribution in the well can be obtained only if the temperature in the aquifer is defined by a sufficient amount of thermal markers.

The thermal efficiency η of an ATES cycle is finally obtained by calculating the average temperature in all recovery wells for the recovery phase; see also (4.18).

7.0 VALIDATIONS

The elementary functions used in program UCATES, such as those that generate the potential due to line sinks or triangular area sinks, have been tested individually. The line sink function has been used before in modeling steady flow (Strack and Haitjema 1981). The triangular areal sinks were tested and validated as part of this study. The capability of program UCATES to model transient flow in unconfined aquifers is tested by use of two validation problems. The first problem deals with a well at the center of a circular island, which starts pumping at time t_0. The solution obtained from program UCATES is compared with a finite difference solution. The second problem deals with a well near the center of a long, but finite, canal. The solution in the vicinity of the well and the canal is compared with a solution obtained with UCATES, whereby the conditions along the canal are modeled by use of an image well. A third validation problem deals with heat transport. In order to test the use of thermal markers for solving the heat transport in the aquifer, the results of an ATES simulation presented in Section 4.2 are reproduced with program UCATES.

7.1 WELL AT THE CENTER OF A CIRCULAR ISLAND

The objective of this validation is to verify whether the effects of the nonlinear storage term in (5.12) are properly incorporated in program UCATES. To induce significant head variations in the aquifer, an unrealistically large diameter r_0 of the well is used, so that a large well discharge can be obtained. In using (5.25) to represent the well in program UCATES, the discharge at the well is not constant in time, but is given by

$$Q_{(t)} = Q_0 e^{-u_0^2} \tag{7.1}$$

where u_0^2 follows from (5.26) as

$$u_0^2 = \frac{n\, r_0^2}{4k\phi_0 (t - t_0)} \tag{7.2}$$

The head ϕ_0 is taken equal to the initial head in the aquifer. The following dimensionless parameters are introduced:

$$\tilde{x} = x/\phi_o \quad ; \quad \tilde{y} = y/\phi_o \quad ; \quad \tilde{r} = r/\phi_o$$

$$\tilde{\phi} = \frac{\phi}{\phi_o}$$

$$\tilde{t} = \frac{k}{\phi_o} t \tag{7.3}$$

$$\tilde{Q} = \frac{Q}{k\phi^2}$$

$$\tilde{\Phi} = \frac{\Phi}{k\phi_o^2}$$

In program UCATES a triangle network is used, as indicated in Fig. 7.1. The side $\tilde{a}$ of the square net is $\tilde{a}=20$. The lower left corner of the network is located at $\tilde{x}=\tilde{y}=0$. The well with radius $\tilde{r}_o=2$ and discharge $\tilde{Q}_o=1.5$, is located at the center of the network: $\tilde{x}=\tilde{y}=10$. A reference point is selected at $\tilde{x}=\tilde{y}=21$, where the head is maintained at $\tilde{\phi}=1$. Solutions to (5.30) and (5.31) are generated at times $\tilde{t}=0.05$, 0.1, 0.2, 0.3, 0.5, 0.7, 1, 2, 3, 5, 7, 10, 15, 20, 25, and 30. Heads are evaluated along the dashed line in Fig. 7.1

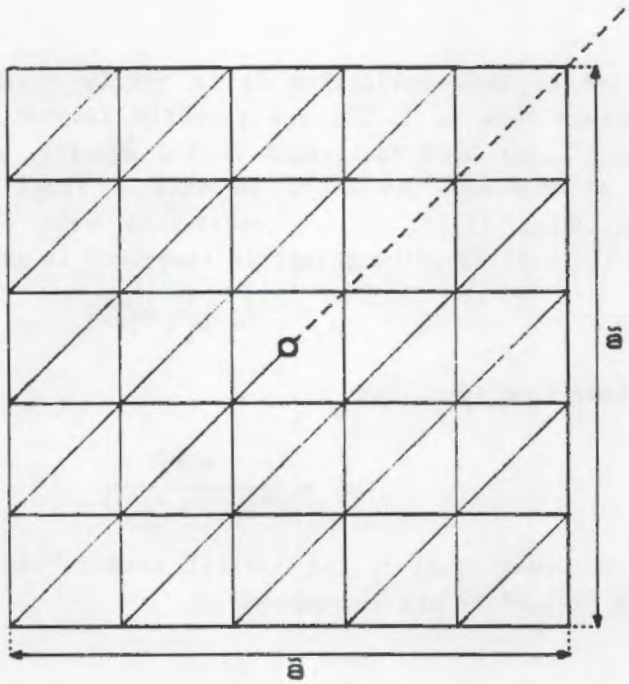

Fig. 7.1. Well at the Center of a Triangle Network

for comparison with the results of a finite difference program.

The finite difference program solves radial flow in a grid of constant

spacing Δr. The potential $\Phi_i^{(t+\Delta t)}$ at the ith grid point is found from

$$\Phi_i^{(t+\Delta t)} = \Phi_i^{(t)} + \frac{k\phi^{(t)}\Delta t}{n(\Delta r)^2} \cdot$$

$$\left[\left[1+\frac{\Delta r}{2r_i}\right]\Phi_{i+1}^{(t)} + \left[1-\frac{\Delta r}{2r_i}\right]\Phi_{i-1}^{(t)} - 2\Phi_i^{(t)}\right] \qquad (i=2,3,\ldots,N-1) \tag{7.4}$$

The potential at the Nth grid point is kept constant and the potential at the first grid point $(i=1)$ is obtained using equation (7.1), from

$$\Phi_1^{(t+\Delta t)} = \Phi_2^{(t+\Delta t)} - \frac{\Delta r Q_0 e^{-u_1^2}}{2\pi(r_1+\frac{\Delta r}{2})} \tag{7.5}$$

where u_1^2 is defined by

$$u_1^2 = \frac{n(r_1+\frac{\Delta r}{2})^2}{4k\phi_0(t+\Delta t-t_0)} \tag{7.6}$$

The finite difference program has been validated by comparison with expression (5.25) whereby $\phi^{(t)}$ in (7.4) was replaced by ϕ_0. The latter comparison was carried out for times that were chosen sufficiently small so that the effect of a constant potential at the last grid point $(i=N)$ can be neglected.

In comparing (7.4) and (7.5) with the results obtained from UCATES, a grid spacing and time step were used of

$$\Delta\tilde{r} = 0.2$$
$$\Delta\tilde{t} = 0.001 \tag{7.7}$$

The results are plotted in Fig. 7.2. The solid lines in Fig. 7.2 represent the head distributions along the dashed line in Fig. 7.1 for times $\tilde{t}=1$, 10, 20 and 30 as obtained from program UCATES. The line for $\tilde{t}=\infty$ has been obtained from a steady-state solution and is added for comparison, although the solution obtained from UCATES will not converge to a steady state solution due to the use of (7.1). lines in Fig. 7.2 are obtained from the finite difference program with a nonlinear storage term. The dotted lines are also obtained from the finite difference program, but now with a linearized storage term, whereby $\phi^{(t)}$ in (7.4) equals ϕ_0.

It may be observed from Fig. 7.2 that the nonlinearity of the storage term,

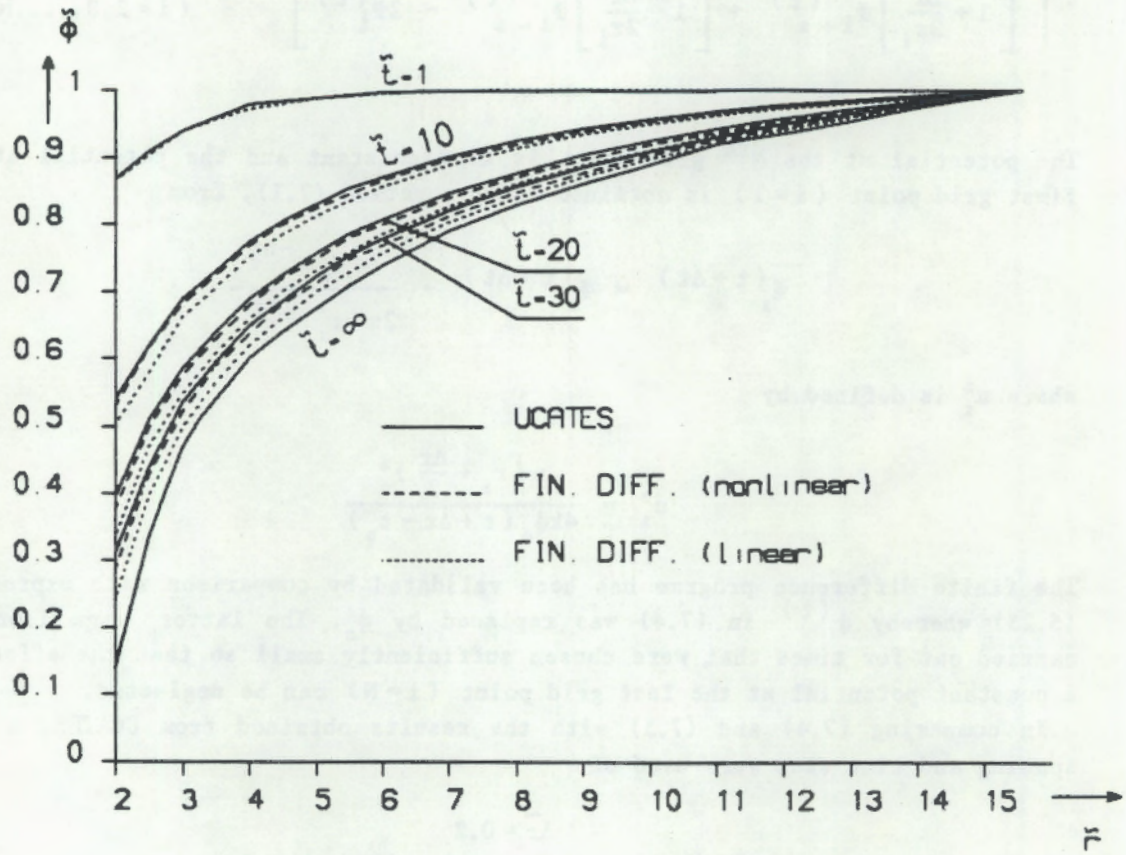

Fig. 7.2. Drawdowns Obtained with Program UCATES Compared with Finite Difference Solutions

even for this case of large drawdowns, does not have a dominant effect.

7.2 WELL NEAR A CANAL

The areal sink distribution with strength $(\overset{e}{\sigma}-\overset{w}{\sigma})_{(x_\alpha,t)}$ in general, not only represents the effects of the nonlinear storage terms in (5.12), but also includes the transient effects due to line sinks in the domain. These line sinks are used in UCATES to maintain head-specified boundary conditions along, for example, creeks and canals, during the injection or recovery of thermal energy. To test the capabilitiy of program UCATES to satisfy these

boundary conditions under transient flow conditions, the following problem is solved.

In Fig. 7.3, a finite canal is located in the upper section of a network of triangles. The sides of the network are $\tilde{a}=30$ and $\tilde{b}=20$. The lower left corner

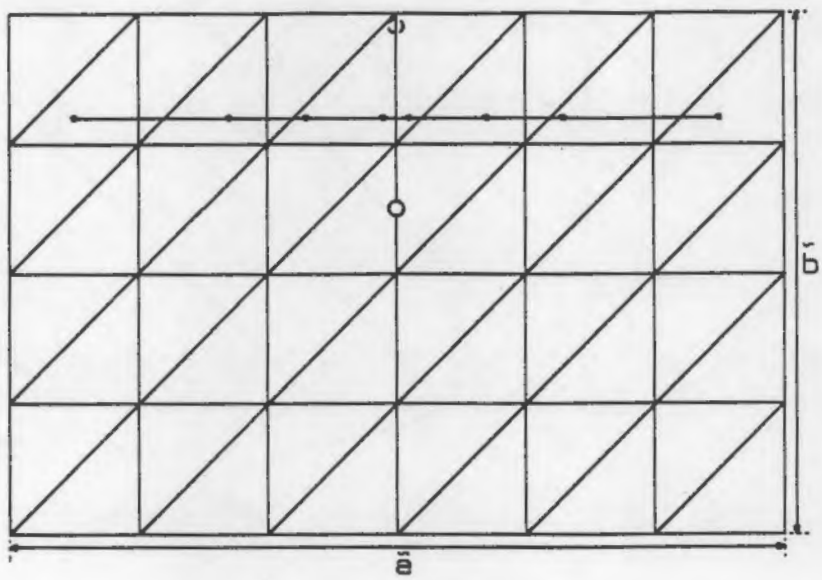

Fig. 7.3. Well near a Finite Canal

of the network is located at $(\tilde{x}=-2.5,\ \tilde{y}=5)$. A well, with radius $\tilde{r}_0=0.02$ and discharge $\tilde{Q}=0.5$, is located at $(\tilde{x}=12.5,\ \tilde{y}=17.5)$. The canal has its end points at $(\tilde{x}=0,\ \tilde{y}=21)$ and $(\tilde{x}=25,\ \tilde{y}=21)$ and is represented by means of seven line sinks as indicated in Fig. 7.3. At a reference point $(\tilde{x}=12.5,\ \tilde{y}=0)$ the head is specified as $\tilde{\phi}=1$. Contour plots of heads are produced at times $\tilde{t}=2$ and $\tilde{t}=10$ since the onset of pumping and are represented in Fig. 7.4 and Fig. 7.5, respectively, by solid lines. A second run with UCATES is performed whereby the canal is eliminated and a well is located at $(\tilde{x}=12.5,\ \tilde{y}=24.5)$. The latter well has the same discharge as the original well, but of opposite sign $(\tilde{Q}=-0.5)$ and forms the image of the well in Fig. 7.3 with respect to the canal. The well and its image should produce the same head distibution on the side of the canal where the well is located, provided the influence of the well and its image do not extend too far beyond the ends of the canal in Fig. 7.3. The latter condition will be met for a limited time period after the onset of pumping. Contour plots of piezometric heads are produced for time $t=2$ and $t=10$ in Fig. 7.4 and Fig. 7.5,

respectively. The dashed contour plots in Fig. 7.4 and Fig. 7.5 are obtained from UCATES by use of the image well instead of the canal. Solutions to (5.30) and (5.31) have been generated at times $\tilde{t} = 0.05$, 0.1, 0.2, 0.3, 0.5, 0.7, 1, 2, 3, 5, 7 and 10. It is noted, that at the centers of line sinks and at the reference point, the boundary conditions are satisfied indentically at the above specified times. At other times the heads at these control points exhibited a maximum error of about 1 percent.

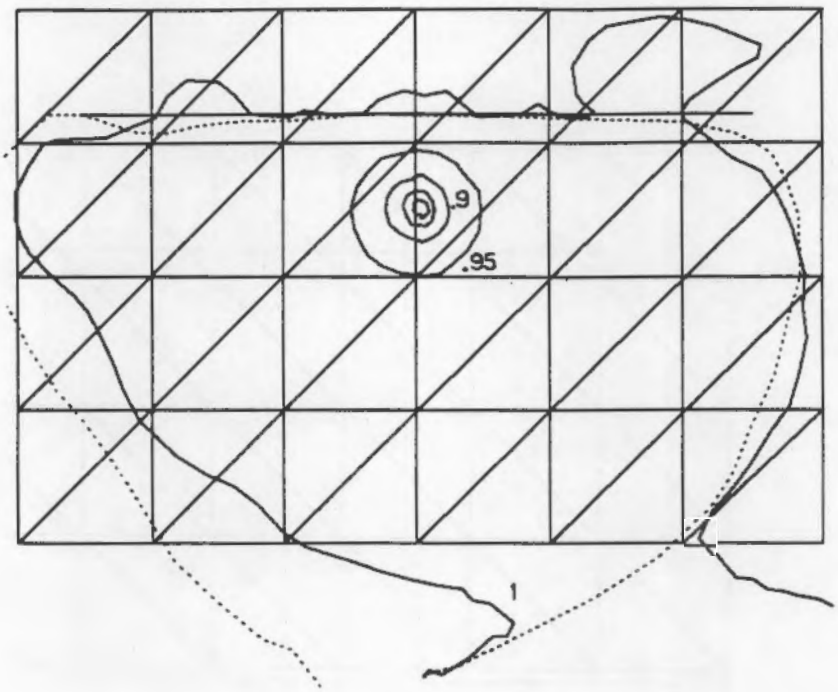

Fig. 7.4. Contour Plot of Piezometric Heads for t = 2

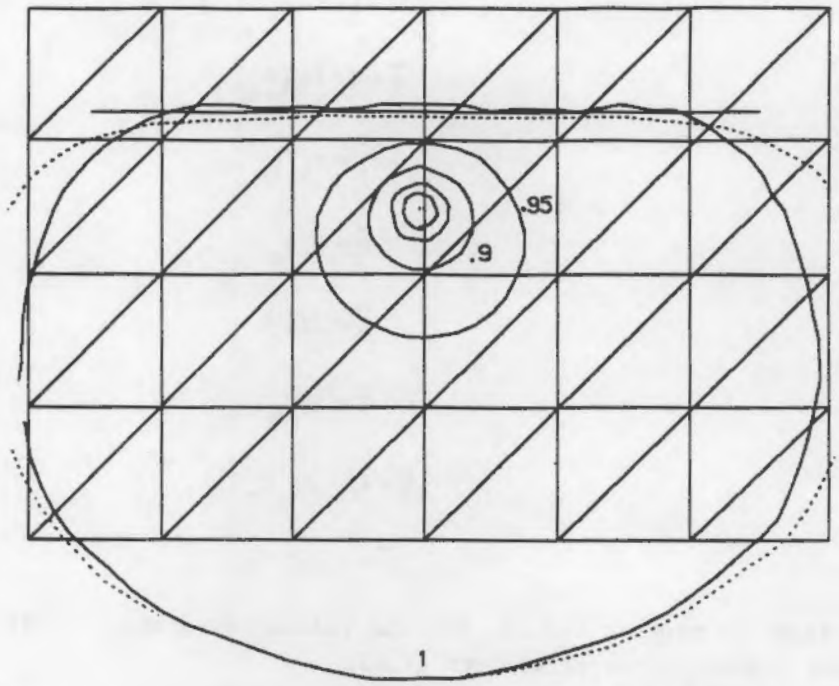

Fig. 7.5. Contour Plot of Piezometric Heads for t = 10

7.3 THERMAL ENERGY STORAGE FOR THE CASE OF RADIAL FLOW

The example of thermal energy storage in an unconfined aquifer presented in Section 4.2 is repeated here by use of program UCATES. The comparison is aimed at verifying the program logic dealing with the thermal markers. The input data is the same as used in Section 4.2, whereby $\Delta\tilde{t}$ as defined in Section 4.2 is chosen to be

$$\Delta\tilde{t} = 0.8 \tag{7.8}$$

Input in program UCATES may be given in terms of any coherent units system or in terms of dimensionless parameters by specifying

$$\begin{aligned} C_w &= 1 \\ k &= 1 \\ \phi_o &= 1 \end{aligned} \tag{7.9}$$

The other input parameters then are of the following dimensionless form:

$$\tilde{\phi} = \phi/\phi_o$$

$$\tilde{Q} = Q/(k\phi_o^2)$$

$$\tilde{\Phi} = \Phi/(k\phi_o^2)$$

$$\tilde{x}_i = x_i/\phi_o$$

$$\tilde{r} = r/\phi_o \qquad (7.10)$$

$$\tilde{d} = d/\phi_o$$

$$\tilde{C} = C/C_w$$

$$\tilde{\lambda} = \lambda/(k\phi_o C_w)$$

$$\tilde{t} = (k/\phi_o)\,t$$

The input in program UCATES, for the validation problem (7.8), becomes in terms of the dimensionless parameters (7.10),

$$\tilde{C} = 0.609756$$

$$\tilde{C}_1 = \tilde{C}_2 = 0.487805$$

$$\tilde{\lambda}_1 = \tilde{\lambda}_2 = 0.0002107$$

$$\tilde{d}_1 = \tilde{d}_2 = 0.1$$

$$\tilde{r}_o = 0.02$$

$$|\tilde{Q}| = 0.251327$$

$$\tilde{\Delta t} = 125$$

Due to symmetry, it would be sufficient to solve the heat transport problem along only one of the radial flow paths. In this simulation, however, four flow paths are traced and the well is subdivided into four sectors during the recovery phase. Similar to the radial flow case in Section 4.2, no nonlinearity of the storage term is included in the modeling.

The temperature distributions in the aquifer, at the end of injection and at the end of storage, are presented in Fig. 7.6 and Fig. 7.7, respectively. The solid lines represent the solution obtained with UCATES and the dashed lines

are obtained from Section 4.2. The discrepancies, visible in Fig. 7.7, are due to the linear interpolations between thermal markers, as carried out in UCATES.

The thermal efficiency predicted by the program was approximately the same ($\eta = 0.22$) as in Section 4.2, Table 4.1.

The temperature distribution in the well is presented in Fig. 7.8. The temperature distribution in Fig. 7.8, as produced by UCATES, is aborted somewhat earlier than the one obtained in Section 4.2 due to a difference in program logic. In Section 4.2 the temperature in the well becomes zero if the last thermal marker arrives within the well radius r_0. In UCATES, this boundary has been set at $3 * r_0$, in order to avoid possible overshoot under conditions of high groundwater velocities.

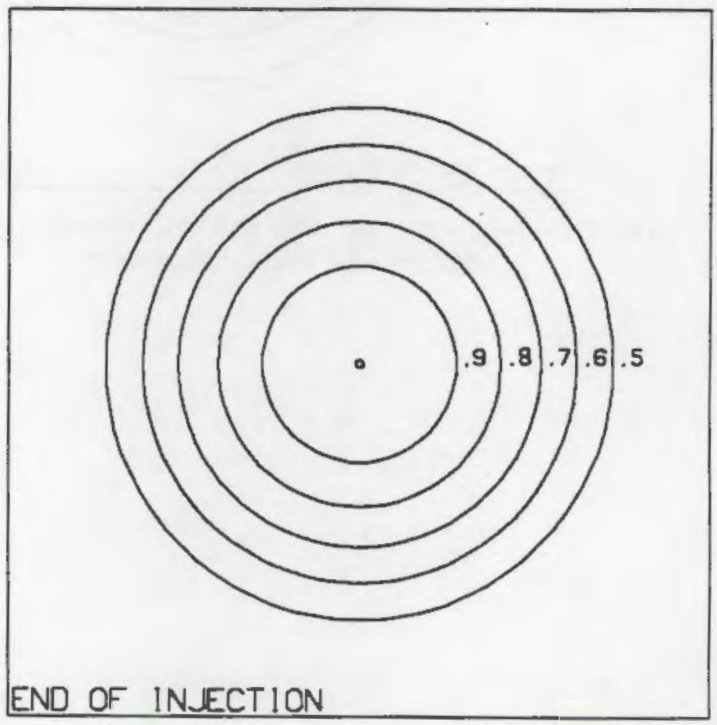

Fig. 7.6. Isotherms at the End of Injection Obtained with UCATES for the Radial Flow Case

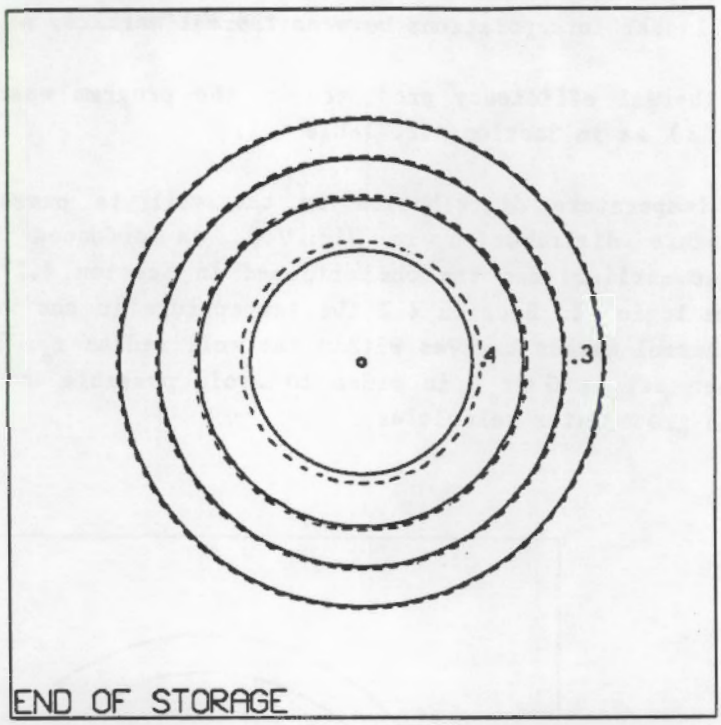

Fig. 7.7. Isotherms at the End of Storage Obtained with UCATES for the Radial Flow Case

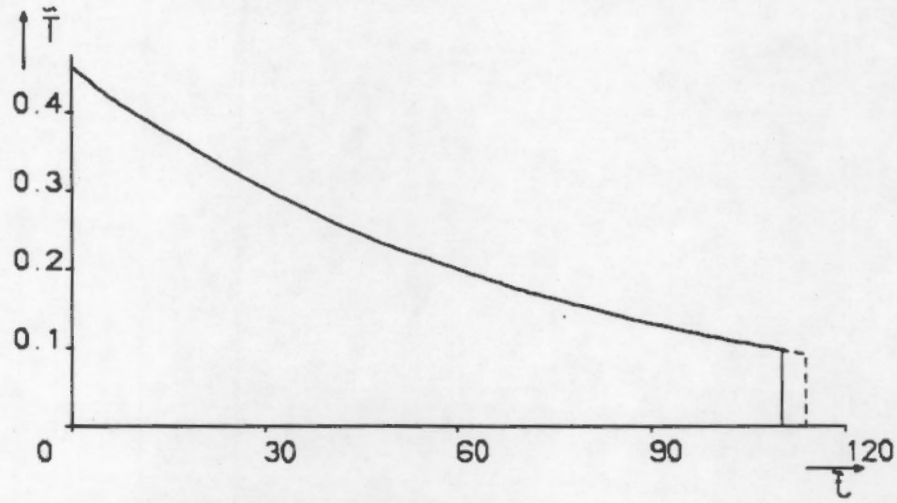

Fig. 7.8. Temperature Distribution in the Well During Recovery Obtained with UCATES

8.0 EXAMPLES

Two examples are presented of ATES simulations with program UCATES. The first example deals with a single well in a uniform flow field. The solution (5.25) is adopted for flow from or toward the well so that the nonlinear storage term in (5.12) is diaregarded. The second example simulates an ATES system near creeks and a domestic well; the groundwater flow solution incorporates the nonlinear storage term.

8.1 A SINGLE WELL ATES SYSTEM IN A UNIFORM FLOW FIELD

Injection, storage and recovery are first simulated under circumstances of zero uniform flow rates. The single well ATES system is located at $\tilde{x}=\tilde{y}=0$ and the dimensionless well discharge is $|\tilde{Q}|=0.5$. The injection, storage, and recovery periods are denoted by $\Delta\tilde{t}_i$, $\Delta\tilde{t}_s$, and $\Delta\tilde{t}_r$, respectively, whereby

$$\Delta\tilde{t}_i=\Delta\tilde{t}_r=120$$
$$\Delta\tilde{t}_s=60 \tag{8.1}$$

The thicknesses $\tilde{d}^1$ and $\tilde{d}^2$ for the aquifer base and vadose zone, respectively, are selected as $\tilde{d}_1=0.2$ and $\tilde{d}_2=0.1$. With the permeability $k=1.1574\ 10^{-4}$ m/s and an initital head ϕ_0 of $\phi_0=10$ m, the periods in (8.1) are 120 days and 60 days, respectively. In Fig. 8.1 isotherms in the aquifer are plotted at the end of injection, storage, and recovery. The dashed lines indicate where the aquifer temperature $\tilde{T}$ becomes zero. The temperature distribution in the well during recovery is plotted in Fig. 8.2. The dots in Fig. 8.2 are generated by the program, the solid lines are hand-drawn. The symmetrical isotherm patterns give the system a thermal efficiency of $\eta=0.45$. In Fig. 8.3 the isotherm plots of Fig. 8.1 are repeated bnt now for the case of uniform flow with a discharge vector given by

$$\tilde{Q}_x=\tilde{Q}_y=0.09 \tag{8.2}$$

The markings on the isotherms in Fig. 8.3 indicate data points generated by the program, the isotherms are hand-drawn. The thermal efficiency of the latter system is significantly lower: $\eta=0.29$. The temperature distribution in the well is plotted in Fig. 8.4. The scatter in the data points in Fig. 8.4, and in subsequent temperature distributions in the recovery well, is a consequence of the poor definition of the temperature in the aquifer due to a limited number of thermal markers. An increased number of thermal markers will reduce the observed scatter.

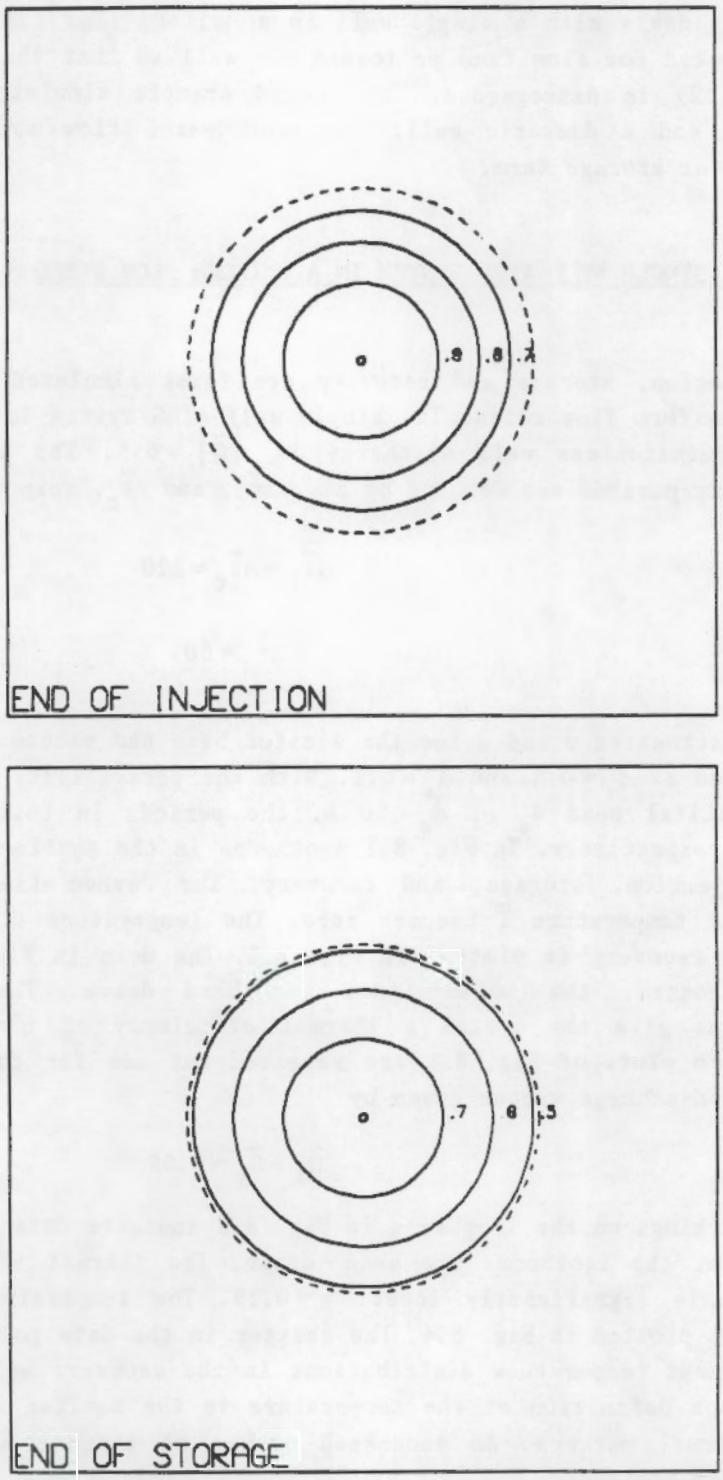

Fig. 8.1. Predicted Isotherms at the End of the ATES Phases for the Case of a Zero Uniform Flow Rate

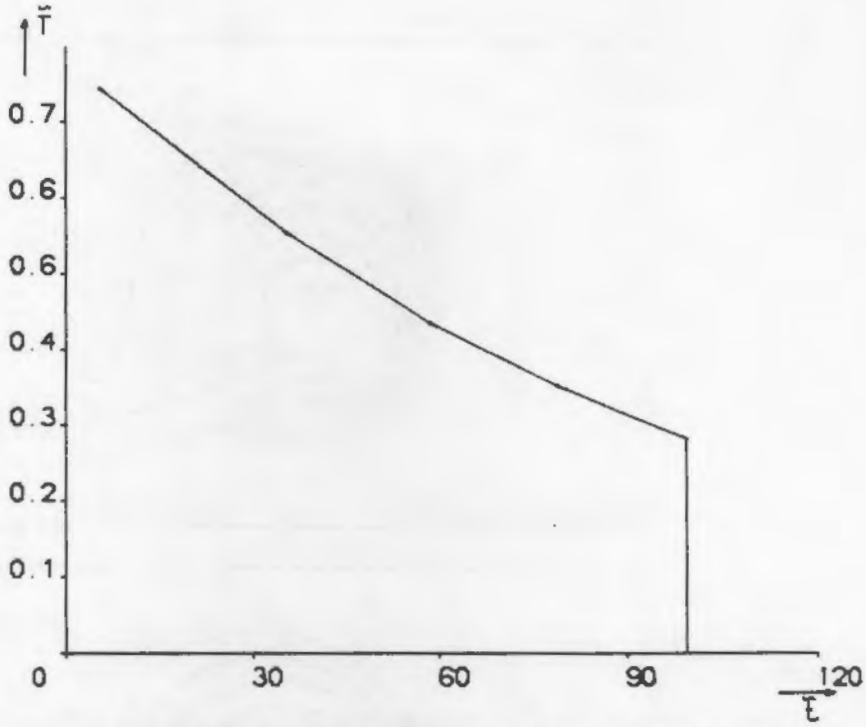

Fig. 8.2. Predicted Temperatures in the Well During Recovery for the Case of a Zero Uniform Flow

As may be observed from the isotherms at the end of storage and at the end of recovery, a significant portion of the injected hot water is flowing outside the reach of the recovery well. Based on the results presented in Fig. 8.3, a separate recovery well is simulated, located at $\tilde{x}=\tilde{y}=2.2$. The isotherms at the end of recovery and the temperature distribution in the well are plotted in Fig. 8.5. The thermal efficiency of the system is now restored to $\eta=0.44$.

8.2 A SINGLE WELL ATES SYSTEM NEAR CREEKS AND A DOMESTIC WELL

In Fig. 8.6 the predicted isotherms at the end of an injection phase are presented for a fictitious ATES system surrounded by creeks and canals and near a domestic well which pumps continuously at $\tilde{Q}=0.2$. The well used for injection of hot water has a discharge of $|\tilde{Q}|=0.5$. The transient flow in the domain caused by the ATES cycle is solved for 10 different times during each of the phases: injection, storage, and recovery. The domain of Fig. 8.6 is covered by a rectangular grid of 72 triangles, which are not depicted in Fig. 8.6. The triangle network extends well beyond the domain depicted in Fig. 8.6 through Fig. 8.8. For the exact input data for this example reference is made to appendix B. The dimensions of the domain shown in Fig. 8.6 are, in terms of

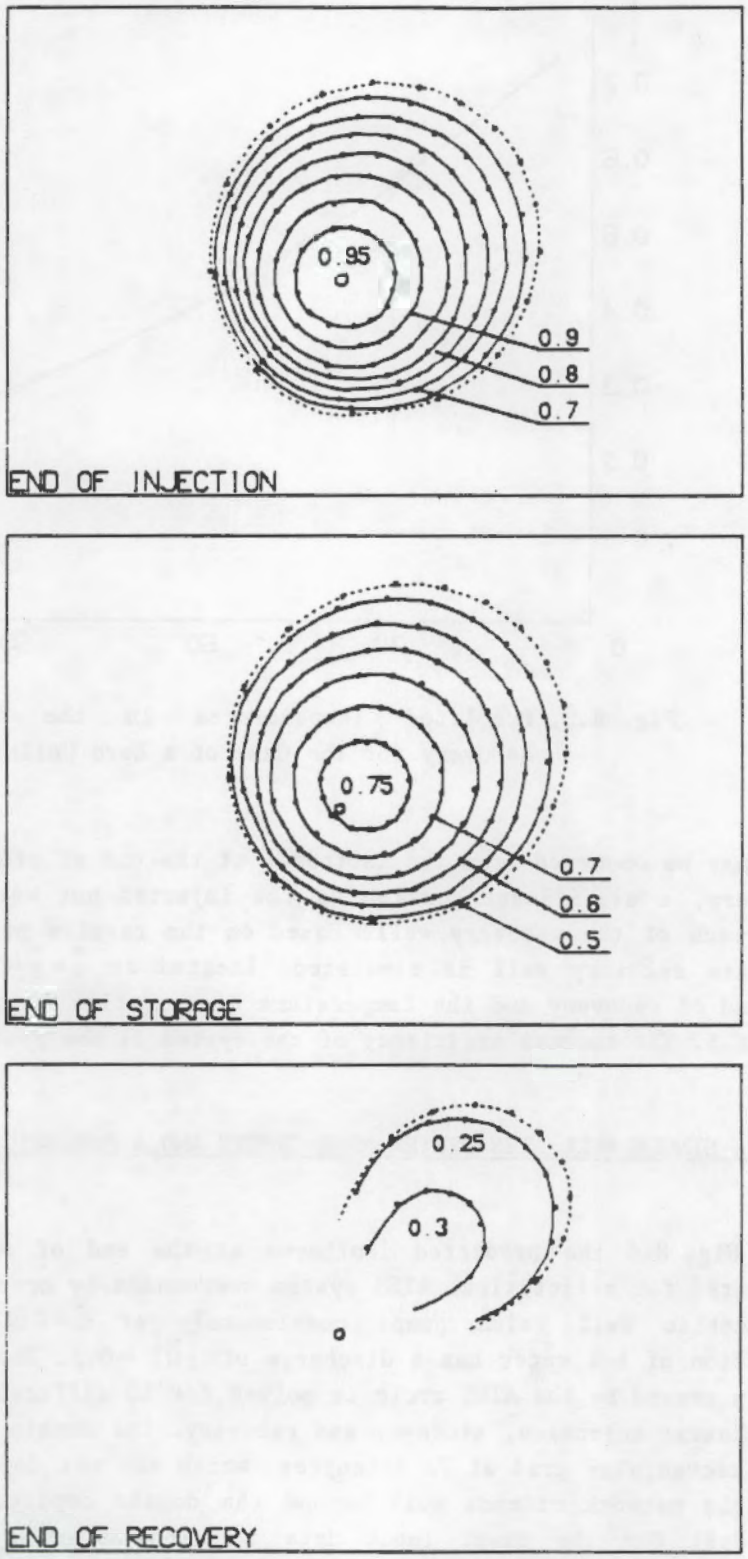

Fig. 8.3. Predicted Isotherms at the End of the ATES Phases for the Case of Uniform Flow

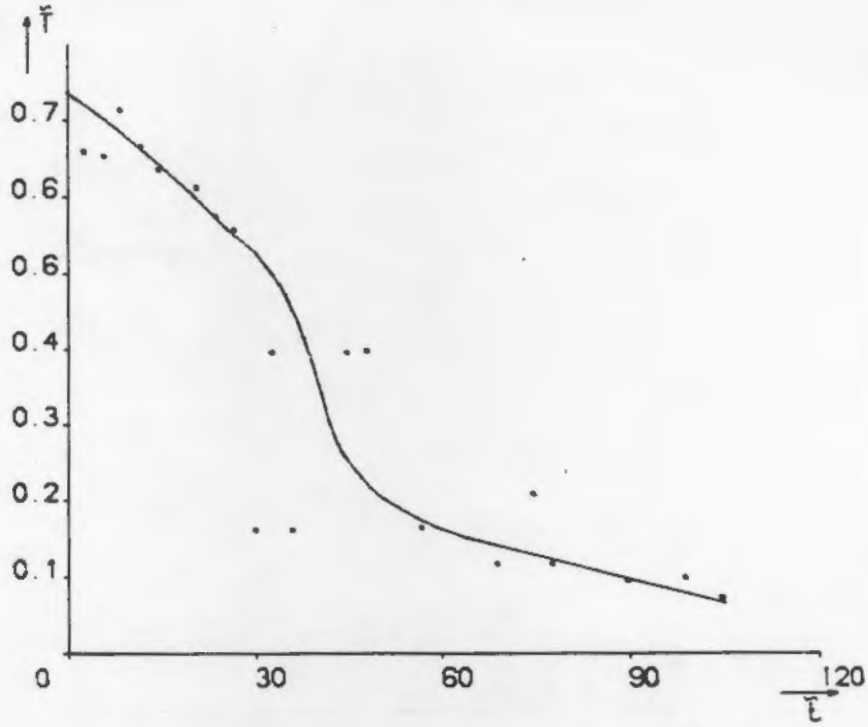

Fig. 8.4. Predicted Temperatures in the Well During Recovery for the Case of Uniform Flow

dimensionless lengths [see (7.10)], 22 by 22. It may be observed from Fig. 8.6 that part of the injected thermal energy is entering the domestic well. Another part of the injected hot water passes underneath a nearby creek. Because the creek is producing, i.e., adding water to the aquifer, mixing is assumed in program UCATES between the cold water infiltrated by the creek and the hot water passing underneath; the temperatures show a sharp decline across the creek. In Fig. 8.7 isotherms are plotted at the end of both the storage and the recovery phase. Similar to the previous example, a separate recovery well has been introduced somewhat downstream of the injection well. Its location is chosen after inspection of the isotherm plot at the end of storage in Fig. 8.7. The temperature distribution in the recovery well is given in Fig. 8.8. The thermal efficiency η for this system was estimated by program UCATES as $\eta = 0.4$.

8.3 REMARKS

Program UCATES, in its present form, is designed to handle the effect of heat convection in an unconfined aquifer. The heat losses through the vadose zone

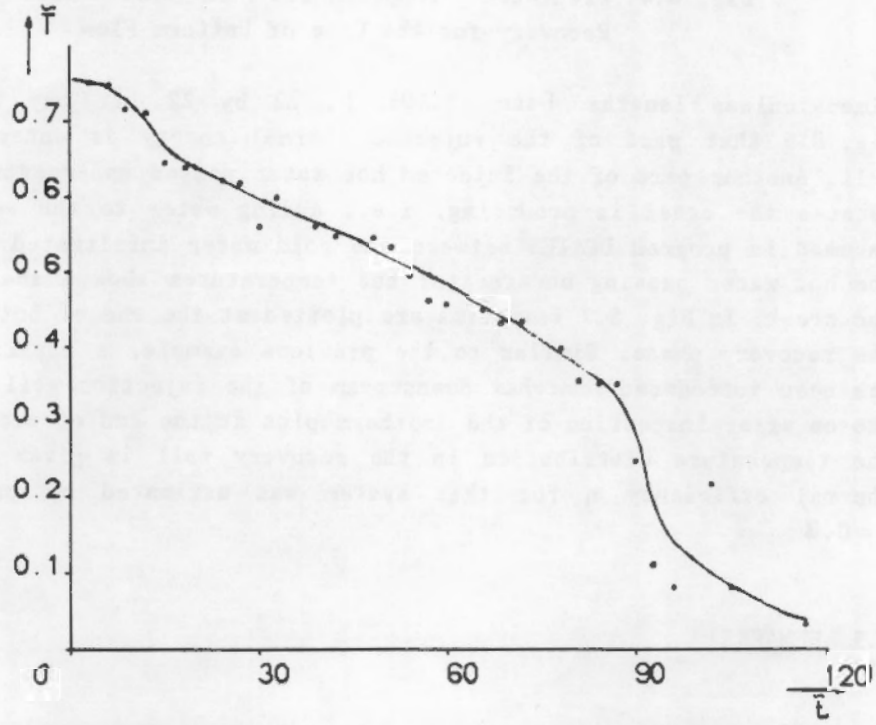

Fig. 8.5. Predicted Isotherms at the End of Recovery and Temperatures in the Well for the Case of a Separate Recovery Well in a Uniform Flow Field

and aquifer base, however, are not yet modeled realistically. The transient heat conduction through these aquifer boundaries, as occurs in reality, must be incorporated in the modeling before the absolute values of predicted isotherms and thermal efficiencies can be relied upon. UCATES, therefore, must be regarded as a research tool that needs further development. However, it may already aid in ATES design studies when significant convective heat losses are anticipated.

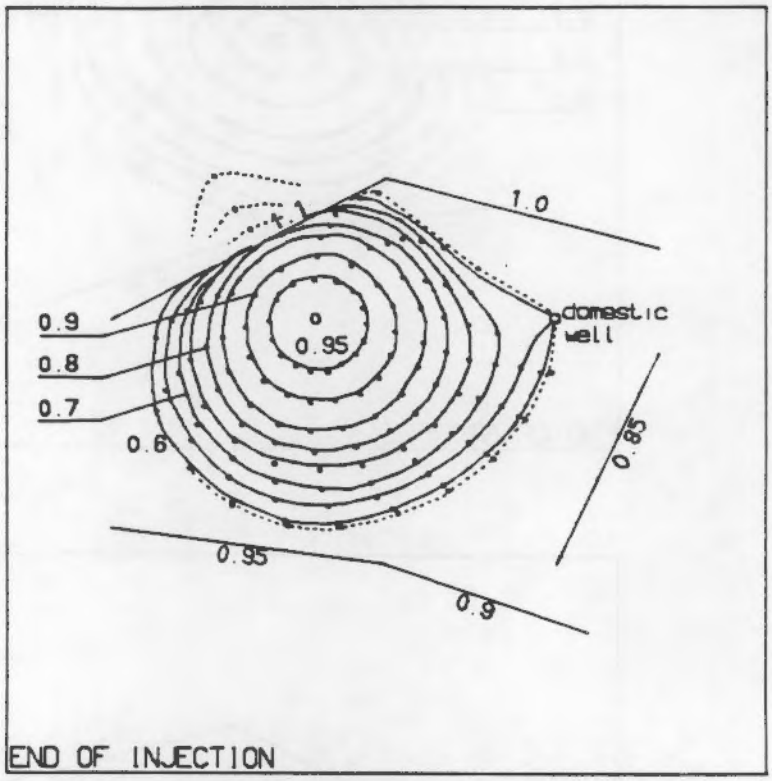

Fig. 8.6. Predicted Isotherms at a Site Surrounded by Creeks and Canals, and Including a Domestic Well

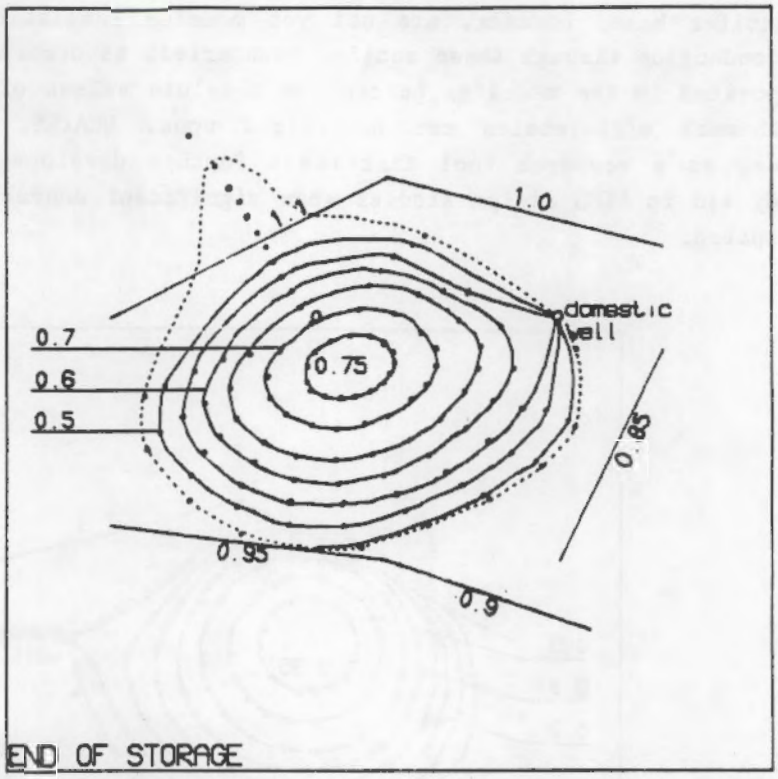

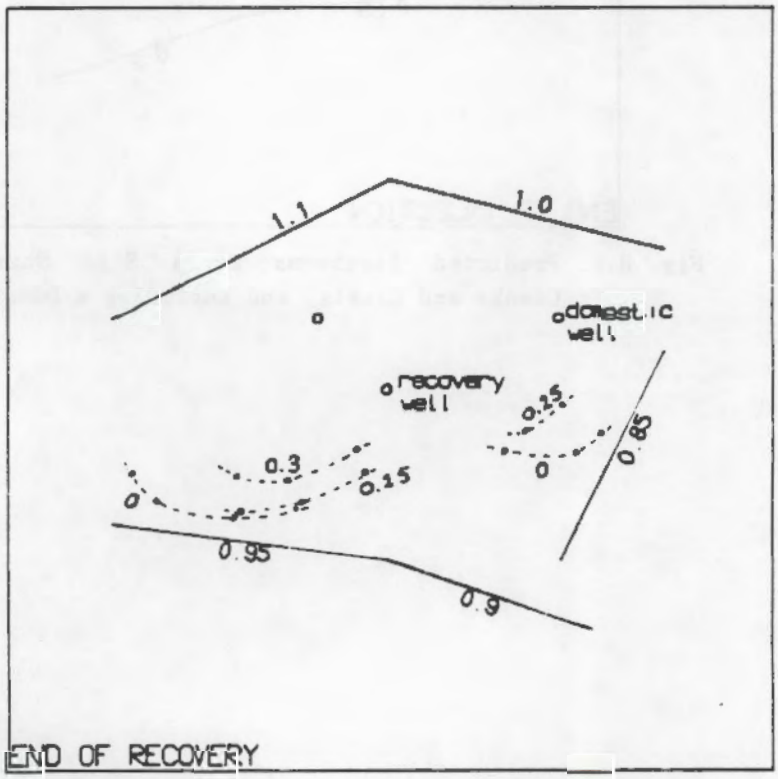

Fig. 8.7. Predicted Isotherms at the End of the Storage and Recovery Phases at a Site Surrounded by Creeks, Canals, and Including a Domestic Well

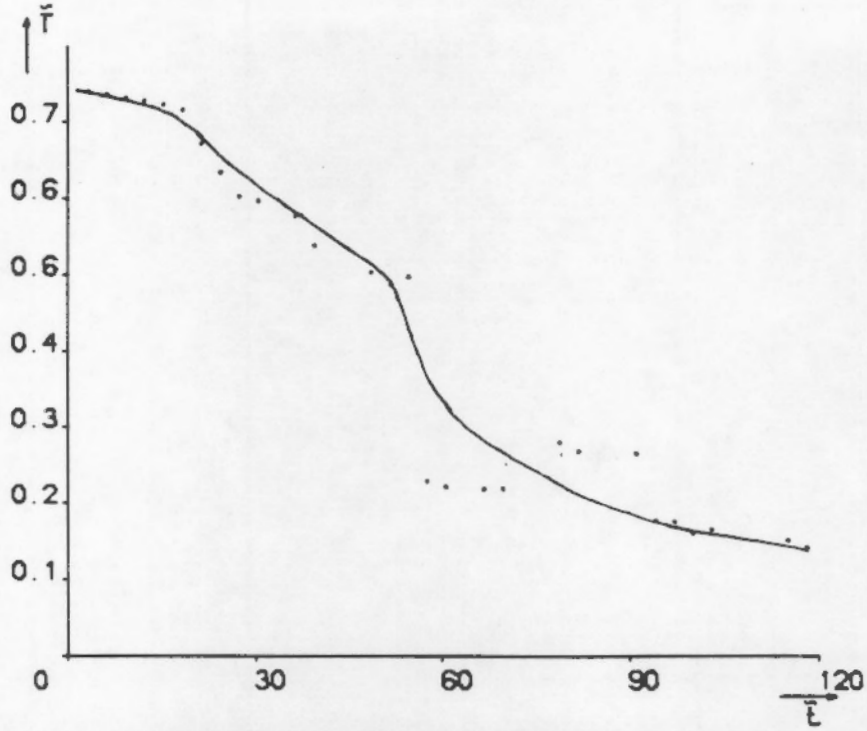

Fig. 8.8. Predicted Temperatures in the Recovery Well at a Site Surrounded by Creeks and Canals, and Including a Domestic Well

REFERENCES

Avdonin, N.A. 1964. Some Formulas for Calculating the Temperature Field of a Formation during Thermal Injection, Izv. Vysshiks Uchebn. Zavedennii, Neft i Gaz 7(3), 37 - 41.

Bellman, R.E., R.E. Kalaba and J.A. Lockett. 1966. Numerical Inversion of the Laplace Transform, Modern Analytic and Computational Methods in Science and Mathematics, New York: American Elsevier Publishing Company, Inc.

Brandes, M.C., and G.J.M. Uffink. 1977. De berekening van de temperatuursverhoging in het grondwater ten gevolge van een koelwaterinjectie, R.I.D. - Mededeling, Rijksinstituut voor drinkwater, Voorburg, The Netherlands.

Carslaw, H.S., and J.C. Jaeger. 1959. Conduction of Heat in Solids, Oxford University Press, England.

Childs, S.W., and G. Malstaff. 1982. Final Report: Heat and Mass Transfer in Unsaturated Porous Media, PNL - 4036, Pacific Northwest Laboratory, Richland, Washington.

Claesson, J. 1980. Tilting Rate of a Wide Thermal Front, Notice 1980/4, Mathematical Physics Dept. Lund Insitute of Technology, Lund, Sweden.

Claesson, J., and G. Hellström. 1980. Heat Storage in Aquifers, Thermohydraulic Considerations, Lund Institute of Technology, Lund, Sweden.

Debbarh, A. 1982. Preliminary Written Examination for the Ph.D Degree, Civil Engineering Department University of Minnesota, Minneapolis, Minnesota.

Dietz, D.N., and F. Lehner. 1969. Letter to the Editor, Appl.Sci.Res. 20, 309 - 311.

Doughty, C., G. Hellström, C.F. Tsang and J. Claesson. 1982. A Dimensionless Parameter Approach to the Thermal Behavior of an Aquifer Thermal Energy Storage System, Water Resour. Res., 18(3): 571 - 587.

Forsythe, G.E., M.A. Malcolm and C.B. Moler. 1977. Computer Methods for Mathematical Computations, Prentice Hall Inc., Englewood Cliffs, New Jersey.

Gringarten, A.C., and J.P.Sauty. 1975. A Theoretical Study of Heat Extraction from Aquifers with Uniform Regional Flow, J. of Geophysical Research, 80(35), 4956 - 4962.

Güven, O., J.G. Melville and F.J. Molz. 1983. An Analysis of the Effect of Surface Heat Exchange on the Thermal Behavior of an Idealized Aquifer Thermal Energy Storage System, Water Resour. Res., 19(3): 860 - 864.

Hantush, M.S., and C.E. Jacob. 1955. Non-Steady Green's Function for an Infinite Strip of Leaky Aquifer, Trans. Amer. Geophys. Union., 36 (1), 101-112.

Hellström, G., and J. Claesson. 1978. Heat Losses and Temperature Fields for Heat Storage Aquifers, A Computational Model with a Simplified Linear Water Flow, Lund Institute of Technology, Lund, Sweden.

Huisman, L. 1972. Groundwater Recovery, MacMillan, London, England.

Lamant, D. 1982. Stockage D'Eau Chaude En Nappe Aquifere, Etude Des Transferts De Chaleur Modelisations, Principaux Parametres Pour Une Etude De Sensibilite, Commisariat a l'Energie Atomique.

Lauwerier, H.A. 1955. The Transport of Heat in an Oil Layer Caused by the Injection of Hot Fluid, Appl. Sci. Res., A(5), 145-150.

Mercer J.W., C.R. Faust, W.J. Miller and F.J. Pearson, Jr., 1982. Review of Simulation Techniques for Aquifer Thermal Energy Storage (ATES) in Advances in Hydroscience, edited by Ven Te Chow, Academic Press, New York, Volume 13, pp 1-129.

Moench, A.F. 1973. Analytical Solutions to the One-Dimensional Nonlinear Diffusion Equation for Flow through Porona Media, Water Resour. Res., 9(5), 1378-1384.

Neuman, S.P., 1975. Analysis of Pumping Test Data from Anisotropic Unconfined Aquifers Considering Delayed Gravity Response, Water Resour. Res., 11(2) 329-342.

Noyer, M.L. 1977. Simulation de Transferts Thermiques dans les Aquiferes, Conditions de Validite des Solutions Analytiques, Bureau de Recherches Geologiques et Mineres, Orleans Cedex, France

Olsthoorn, T.N. 1977. In Nederlandse zandformaties zijn de totale en de effectieve porositeit aan elkaar gelijk (In Netherlands' sand formations the total and effective porosity are the same), H_2O, 10(5), 118-122.

Sauty, J.P., A.C. Gringarten and P.A. Landel. 1978. The Effect of Thermal Dispersion on Injection of Hot Water in Aquifers, in Proceedings Second Invitational Well Testing Symposium, LBL-8883, pp 122-131 Berkeley, California.

Sauty, J.P., A.C. Gringarten, A. Menjoz and P.A. Landel, 1982. Sensible Energy Storage in Aquifers, I. Theoretical Study, Water Resour. Res., 18(2), 245-265.

Strack, O.D.L., and H.M. Haitjema. 1981a. Modeling Double Aquifer Flow Using a

Comprehensive Potential and Distributed Singularities I. Solution for Homogeneous Permeability, Water Resour. Res., 17(5), 1535-1549.

Strack, O.D.L., and H.M. Haitjema. 1981b. Modeling Double Aquifer Flow Using a Comprehensive Potential and Distributed Singularities II. Solution for Inhomogeneous Permeabilities, Water Resour. Res., 17(5), 1551-1560.

Strack, O.D.L. 1983. Three-Dimensional Streamlines in Dupuit-Forchheimer Models, Water Resour. Res., Accepted for publication.

Theis, C.V. 1935. The Relation Between the Lowering of the Piezometric Surface and the Rate and Duration of Discharge of a Well Using Ground-water Storage, Reports and Papers, Hydrology.

Tsang, C.F., D. Hopkins and G. Hellström. 1980. Aquifer Thermal Energy Storage - A Survey, LBL-10441, Lawrence Berkeley Laboratory, Berkeley, California.

Vail, L.W., and C.T. Kincaid. 1983. A Simple Areal Flow Model. A Screening Tool for Managing Aquifer Thermal Energy Storage Systems. in Proceedings of International Conference on subsurface Heat Storage in Theory and Practice, Appendix, Part II, pp. 530-535. Swedish Council for Building Research, Stockholm, Sweden.

Verruijt, A. 1969. Stationary Heat Transport by Plane Groundwater Movement in a Thin or a Thick Layer, Fundamentals of Transport Phenomens in Porous Media. Elsevier, Amsterdam, The Netherlands.

Verruijt, A. 1970. Theory of Groundwater Flow, MacMillan, London, England.

APPENDIX A

FLOW DUE TO A TRIANGULAR AREAL SOURCE WITH LINEARLY VARYING STRENGTH

APPENDIX A

FLOW DUE TO A TRIANGULAR AREAL SOURCE WITH LINEARLY VARYING STRENGTH

In this appendix the expressions are presented for generating the potential distribution and flow field due to a triangular areal sink or source distribution. The expressions and variables are presented here for the purpose

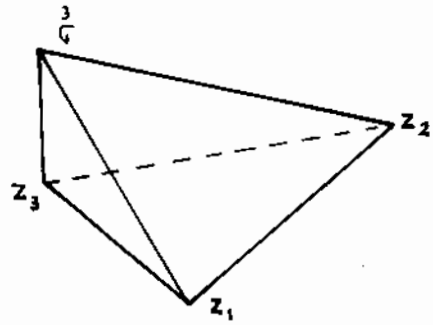

Fig. A.1. Linearly Varying Source Distribution Over a Triangle

of interpreting program UCATES.

Consider the triangle with its corners defined by the complex coordinates z_1, z_2 and z_3 as sketched in Fig. A.1. A linearly varying source distribution exists over the triangle with a strength $\overset{3}{\sigma}$ in z_3 and a zero strength in points z_1 and z_2. The potential $\Phi_{(z)}$ for this source distribution is here written in the form

$$\Phi_{(z)} = \overset{3}{\sigma}\, F(z, z_1, z_2, z_3) \tag{A.1}$$

where $\overset{3}{\sigma}$ is the strength at the point z_3 and where the complex coordinate z is defined as

$$z = x_1 + ix_2 \tag{A.2}$$

The function F is given by

$$F(z, z_1, z_2, z_3) = \mathrm{Re}\left[A_3\chi_1^3 + A_2 + iA_1K_1^2\Lambda_1 \right] \ln\frac{\chi_1 - c}{\chi_1 + a} +$$

$$\left[\beta_2\chi_2^3 + \beta_1\chi_2^2 + iA_1K_1^2\Lambda_1 \right] \ln\frac{\chi_2}{\chi_2 + 1} + \left[\gamma_2\chi_3^3 + \gamma_1\chi_3^2 + iA_1K_1^2\Lambda_1 \right] \ln\frac{\chi_3 - 1}{\chi_3} +$$

$$B \ln\left[(\chi_1 - c)L \right] - P(z, z_1, z_2, z_3) \tag{A.3}$$

The last term in (A.3) represents a farfield correction which will be presented later in this section. The parameters in (A.3) are defined as follows (see also Fig. A.2):

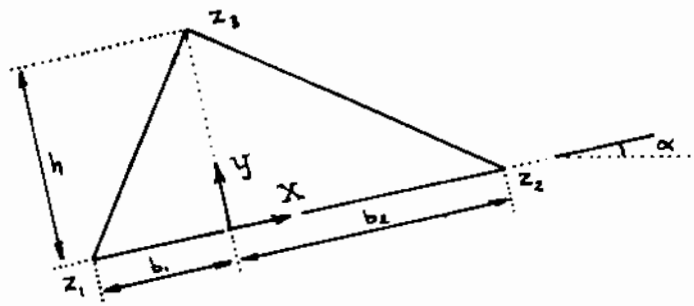

Fig. A.2. Local Coordinate System for a Triangle

$$a + ib = \frac{z_3 - z_1}{z_2 - z_1} \tag{A.4}$$

$$c = 1 - a \tag{A.5}$$

$$A_1 = \frac{1}{4}\frac{L^2}{\pi b} \tag{A.6}$$

$$L = \left| z_2 - z_1 \right| \tag{A.7}$$

$$A_2 = \frac{1}{12}\frac{abL^2}{\pi} \tag{A.8}$$

$$A_3 = -\frac{1}{12}\frac{L^2}{\pi b} \tag{A.9}$$

$$B = \frac{-L^2 b}{12\pi} \tag{A.10}$$

$$\beta_1 = \frac{L^2}{4\pi} ci\,(-c + ib) \tag{A.11}$$

$$\beta_2 = \frac{L^2}{12\pi b} c\,(-c + 2ib)\,(-c + ib) \tag{A.12}$$

$$\gamma_1 = -\frac{L^2}{4\pi} ai\,(a + ib) \tag{A.13}$$

$$\gamma_2 = \frac{L^2}{12\pi b} a\,(a + 2ib)\,(a + ib) \tag{A.14}$$

$$\chi_1 = K_1 + i\,\Lambda_1 = \frac{z - z_1}{z_2 - z_1} - a \tag{A.15}$$

$$\lambda_2 = \frac{z - z_3}{z_3 - z_2} \tag{A.16}$$

$$\lambda_3 = \frac{z - z_2}{z_1 - z_2} \tag{A.17}$$

It is noted that λ_i $(i=1,2,3)$ are complex coordinates with respect to the local coordinate systems (K_1, Λ_1), $(K_2 \Lambda_2)$ and (K_3, Λ_3), each of which originates at a side of the triangle (see Fig. A.3). The complex potential $\Phi(z)$ due to the strength parameter σ in a network of triangles is given by

$$\Phi(z) = \sigma \overset{tr}{F}(z, z_3, N) \tag{A.18}$$

where $\overset{tr}{F}(z, z_3, N)$ is the sum of those N triangles in the network that have the corner point z_3 in common,

$$\overset{tr}{F}(z, z_3, N) = \sum_{i=1}^{N} \overset{i}{F}(z, \overset{i}{z}_1, \overset{i}{z}_2, z_3) \tag{A.19}$$

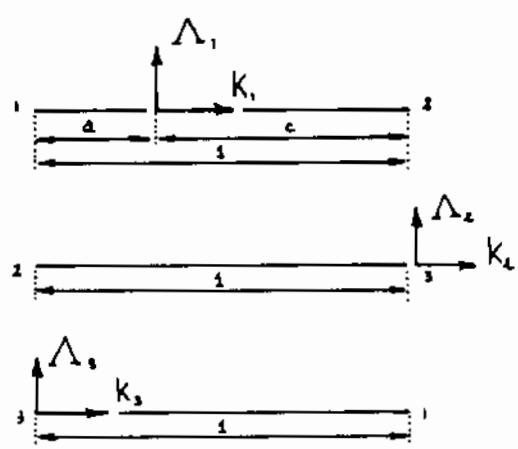

Fig. A.3. Local Coordinate Systems at Normalized Triangle Sides

The function F as given by (A.3) and (A.4) through (A.17) is programmed in the routine CFTRIP. The coefficients (A.4) through (A.14) are generated only once

for each triangle and are stored in common COE. These coefficients are generated by the routines DRIVCO and GENCOE.

Farfield Solutions

In case the potential is evaluated at a large distance outside the triangle, expression (A.3) is inappropriate due to the inaccurate way in which the imaginary parts of the complex logarithms of (A.3) are evaluated. Therefore, and for reasons of computational efficiency, a farfield expansion has been derived for (A.3),

$$F(z,z_1,z_2,z_3) = \frac{1}{2\pi h}\left[\sum_{n=4}^{N} c_n \zeta^{3-n} + C_1 \ln(\zeta-\zeta_1) + + C_2 \ln(\zeta-\zeta_2) - i(C_1+C_2)\alpha\right] \tag{A.20}$$

where ζ is defined as

$$\zeta = z - \tfrac{1}{3}(z_1+z_2+z_3) \tag{A.21}$$

The coefficients C_n are defined as,

$$c_n = \sum_{i=1}^{3} \overset{i}{b}_n \tag{A.22}$$

with $\overset{i}{b}_n$ defined as

$$\begin{aligned}
\overset{1}{b}_n &= \sum_{j=0}^{3} \frac{\zeta_1^{\,n-j} - \zeta_2^{\,n-j}}{n-j}\,\overset{1}{a}_{3-j} \\
\overset{2}{b}_n &= \sum_{j=0}^{3} \frac{\zeta_2^{\,n-j} - \zeta_3^{\,n-j}}{n-j}\,\overset{2}{a}_{3-j} \\
\overset{3}{b}_n &= \sum_{j=0}^{3} \frac{\zeta_3^{\,n-j} - \zeta_1^{\,n-j}}{n-j}\,\overset{3}{a}_{3-j}
\end{aligned} \tag{A.23}$$

and $\overset{i}{a}_j$ defined as

$$
\begin{aligned}
\overset{1}{a}_0 &= \frac{e^{-i3\alpha}\,\overset{1}{\zeta}{}_0^3}{6} \\
\overset{1}{a}_1 &= -\frac{e^{i3\alpha}\,\overset{1}{\zeta}{}_0^2}{2} \\
\overset{1}{a}_2 &= \frac{e^{-i3\alpha}\,\overset{1}{\zeta}_0}{2} \\
\overset{1}{a}_3 &= -\frac{e^{-i3\alpha}}{6}
\end{aligned}
\tag{A.24}
$$

and

$$
\begin{aligned}
\overset{i}{a}_0 &= -\frac{\overset{i}{\Gamma}_1\zeta_3^3}{6} + \frac{\overset{i}{\Gamma}_2\zeta_3^2}{2} \\
\overset{i}{a}_1 &= \frac{\overset{i}{\Gamma}_1\zeta_3^2}{2} - \overset{i}{\Gamma}_2\zeta_3 \\
\overset{i}{a}_2 &= -\frac{\overset{i}{\Gamma}_1\zeta_3}{2} + \frac{\overset{i}{\Gamma}_2}{2} \\
\overset{i}{a}_3 &= \frac{\overset{i}{\Gamma}_1}{6}
\end{aligned}
\qquad (i=2,3) \tag{A.25}
$$

The coefficients $\overset{i}{\Gamma}_i$ are given by

$$
\begin{aligned}
\overset{3}{\Gamma}_1 &= \frac{(\zeta_2-\overset{1}{\zeta}_0)(2\zeta_2-\overset{1}{\zeta}_0-\zeta_2)}{(\zeta_3-\zeta_2)^2\,e^{3i\alpha}} \\
\overset{3}{\Gamma}_2 &= \frac{\zeta_3-\overset{1}{\zeta}_0)(\zeta_2-\overset{1}{\zeta}_0)}{(\zeta_3-\zeta_2)\,e^{3i\alpha}} \\
\overset{3}{\Gamma}_1 &= \frac{(\zeta_1-\overset{1}{\zeta}_0)(2\zeta_3-\overset{1}{\zeta}_0-\zeta_2)}{(\zeta_3-\zeta_1)^2\,e^{3i\alpha}} \\
\overset{3}{\Gamma}_2 &= \frac{\zeta_3-\overset{1}{\zeta}_0)(\zeta_1-\overset{1}{\zeta}_0)}{(\zeta_3-\zeta_1)\,e^{3i\alpha}}
\end{aligned}
\tag{A.26}
$$

The coefficients c_n are calculated by the routines DRIVCC and GENCC, whereas

the coefficients a_n and b_n are calculated by GENCA and GENB. The latter two coefficients are not stored permanently. The points ζ_i $(i=1,2,3)$ reflect the corner points of the triangle (see (A.21)), while ζ_0 is defined as

$$\zeta_0 = \tfrac{1}{2}(z_1+z_2) - \tfrac{1}{3}(z_1+z_2+z_3) \tag{A.27}$$

The constants C_1, C_2 and α are given by

$$C_1 = -\tfrac{1}{6}h^2 b_1 \tag{A.28}$$

$$C_2 = -\tfrac{1}{6}h^2 b_2 \tag{A.29}$$

$$\alpha = \arg\{z_2 - z_1\} \tag{A.30}$$

The farfield solution (A.20) is included in the routine CFTRIP and is used with $N=10,7,5$ and 3 at distances from the center of the triangle, of 2,4,8 and 16 times the length of side z_1, z_2, respectively. The farfield correction $P(z,z_1,z_2,z_3)$ in (A.3) becomes, in terms of ζ,

$$p(z,z_1,z_2,z_3) = p^*(\zeta) = \sum_{n=1}^{3} c_n \zeta^{3-n} \tag{A.31}$$

The function (A.31) is implemented in the routine CFARCO.

Discharge Function

The discharge vector Q_x, Q_y may be obtained from the complex discharge function $W(z)$,

$$W(z) = -\frac{\overline{d\Omega}}{dz} = Q_x + iQ_y \tag{A.32}$$

The discharge function W for the triangular areal distribution of Fig. A.1 is given by

$$\begin{aligned} W(z) = -\frac{3\sigma}{z_2 - z_1} \Bigg[& 3A_3(\chi_1^2 - K_1^2)\ln\frac{\chi_1 - c}{\chi_1 + a} + \left[3\tilde{\beta}_2\chi_2^2 + 2\tilde{\beta}_1\chi_2 - 3A_3K_1^2\right]\ln\frac{\chi_2}{\chi_2+1} + \\ & \left[3\tilde{\gamma}_2\chi_3^2 + 2\tilde{\gamma}_1\chi_3 - 3A_3K_1^2\right]\ln\frac{\chi_3 - 1}{\chi_3} + \left[A_3\chi_1^3 + A_2\right]\left[\frac{1}{\chi_1 - c} - \frac{1}{\chi_1 + a}\right] + \\ & \left[\tilde{\beta}_2\chi_2^3 + \tilde{\beta}_1\chi_2^2\right]\left[\frac{1}{\chi_2} - \frac{1}{\chi_2+1}\right] + \left[\tilde{\gamma}_2\chi_3^3 + \tilde{\gamma}_1\chi_3^2\right]\left[\frac{1}{\chi_3 - 1} - \frac{1}{\chi_3}\right] + \\ & \frac{B}{(\chi_1 - c)} - \frac{dP^*(\zeta)}{d\zeta}\frac{d\zeta}{dz}\frac{(z_2 - z_1)}{2\pi h}\Bigg] \end{aligned} \tag{A.33}$$

where

$$\tilde{\beta}_i = \beta_i \frac{z_3 - z_1}{z_3 - z_2}$$

$$(i = 1,2) \qquad (A.34)$$

$$\tilde{\gamma}_i = \gamma_i \frac{z_3 - z_1}{z_1 - z_3}$$

The last term in (A.33) represents the farfield correction, which is obtained by differentiating (A.31) with respect to ζ and (A.21) with respect to z,

$$\frac{dP^*(\zeta)}{d\zeta}\frac{d\zeta}{dz} = \sum_{n=1}^{2} (3-n)c_n\zeta^{2-n} \qquad (A.35)$$

The farfield expression (A.20) may be differentiated also to yield a farfield expression for the discharge function,

$$W(\zeta) = -\frac{\sigma}{2\pi h}\left[\sum_{n=4}^{\infty}(3-n)c_n\zeta^{2-n} + \frac{C_1}{\zeta-\zeta_1} + \frac{C_2}{\zeta-\zeta_2}\right] \qquad (A.36)$$

The components v_x and v_y of the groundwater velocity vector are obtained from W as,

$$v_x(z) = \frac{Q_x(z)}{n\phi} = \mathrm{Re}\{W(z)\}/(n\phi)$$

$$v_y(z) = \frac{Q_y(z)}{n\phi} = -\mathrm{Im}\{W(z)\}/(n\phi) \qquad (A.37)$$

where n is the porosity of the aquifer and where ϕ is the saturated aquifer thickness, hence the bead in a Dupuit-Forchheimer model.
Similarly as for the case of the potential function, evaluation of v_x and v_y at a point z, and therefore of W(z), will be performed by the nearfield solution (A.33) or by the farfield solution (A.34) depending on the distance of z from the center of the triangle.

APPENDIX B

MANUAL FOR PROGRAM UCATES

APPENDIX B

MANUAL FOR PROGRAM UCATES

Program input and output is controlled by command words and parameters. Each command and parameter may be abbreviated, provided it remains unique. An explanation of each command word and its parameters may be obtained under program control by typing HELP followed by the command word to be explained. If only HELP is typed a summary of the command words and their parameters is displayed. This summary and the command word explanations are stored in a file UCATES.MAN, which is listed in this Appendix.

Command Sequence

Even though there exists no fixed order in which commands must be given, some restrictions apply to ensure proper program execution. The AQUIFER command must preceed all other data input commands, unless its parameters are retrieved from a file by use of the GET command. Obviously, output commands are only legal if relevant output data have been generated.

File Handling

There are four commands for storing and retrieving data from file: SAVE, GET WRITE and READ. The SAVE and GET commands store and retrieve all data in main common, respectively. Since the program generates a solution to the groundwater flow problem for each phase of an ATES cycle at the time, three data files are necessary to store the complete flow problem for an ATES cycle: injection, storage and recovery.

Piezometric head distributions in the aquifer, as obtained by use of the GRID command, and temperature distributions in the aquifer or recovery wells, as obtained by use of the SOLVE TEMPERATURES command, may be stored on a file by use of the WRITE command. They may be retrieved at any time by use of the READ command, after which a PLOT ISOTHERMS or a PLOT WELL command may be given. Therefore, three more data files are necessary to store the three temperature distributions in the aquifer; at the end of injection, at the end of storage and at the end of recovery. The temperature distributions in the recovery wells are automatically stored with the temperature data at the end of the recovery phase.

NOTE: Core storage for piezometric head distributions and temperature distributions is shared with storage for the matrix operations necessary for a groundwater flow solution. Therefore, a SAVE or WRITE command must be given prior to a new SOLVE or GRID command if the generated data is to be stored.

Instead of operating the program interactively, it is often convenient to store all data input commands on a file and let the program read that input file by use of the SWITCH command. A SWITCH CON: at the end of the file will switch control back to the terminal (Consol). This procedure avoids retyping everything in case of an error in the input data.

Debugging

It is noted that program UCATES, in its present form, is not yet an operational screening tool for ATES systems, but a research tool awaiting further development. In view of this, extensive debugging facilities are incorporated in the program. The contents of all variables in common and all arrays can be displayed at any point in the command sequence by typing DEBUG. The debugging routine has its own command structure, a summary of which may be displayed by typing HELP after a DEBUG command has been executed. For more extensive debugging, the DEBUG subroutine may be called at any point in the program, to provide an opportunity to display intermediate results. A RETURN command will exit the debugging routine and cause program execution to continue.

Example

As an example of the program operation, the commands given for the ATES simulation near creeks and a domestic well in section 8.2, is listed below. Note that the program is stopped and restarted three times in order to allow for data interpretation.

```
AQUI 1 0.25 0.05
REFE 22 0 0.85
WELL 14 11 0.2
LINE 1 11 9 15 1.1
LINE 9 15 17 13 1
LINE 1 5 9 4 0.95
LINE 9 4 15 2 0.9
LINE 14 4 17 10 0.85
TRIA -50 -50 80 80 72
THERM
0.6097561 0.0002107 1
0.4878049 0.0002107 0.1
0.4878049 0.0002107 0.2
WINDOW -2 -2 20 20
SAVE UCATES00.RST
SOLVE GROU
7 11 -0.5 0

0.1
0.5
1
5
10
20
50
80
120
0
SAVE UCATES01.RST
WRITE UCATES01.GRD
ST
```

```
GET UCATES01.RST
SOLVE TEM
INJ
1 0.1 16 3
SAVE UCATES01.RST
WRITE UCATES01.GRD
SOLVE GROUN
7 11 0.5 120

120.5
121
125
130
140
160
170
180
0
READ UCATES01.GRD
SOLVE TEM
STO
3
SAVE UCATES02.RST
WRITE UCATES02.GRD
ST


GET UCATES02.RST
SOLVE GROUND
9 9 0.5 180

180.1
180.5
181
185
190
200
230
260
300
0
SAVE UCATES03.RST
READ UCATES02.GRD
SOLVE TEM
REC
4 3
0.75
```

```
WRITE UCATES03.GRD
SAVE UCATES03.RST
ST
```

```
*HBUCATES.MAN
                USER MANUAL OF PROGRAM -UCATES-
-
Command summary:
-
HELP          [command word]
AQUIFER       (rperm) (rpor) (r0)
THERMAL
RESET
UNIFLO        (x) (y) (Qx) (Qy)
WELL          (x) (y) (Q)
LINESINK      (x1) (y1) (x2) (y2) (h)
TRIANGLES     (x1) (y1) (x2) (y2) (ntt)
REFERENCE     (x) (y) (h)
POTENTIAL     (x) (y) (t)
DISCHARGE     (x) (y) (t)
LAYOUT
WINDOW        (x1) (y1) (x2) (y2)
GRID          (nincx) (t)
PLOT          (heads/isotherms/well)
SOLVE         (groundwater/temperatures)
DEBUG
SAVE          (filename.ext)
GET           (filename.ext)
LOG           (on/off)
EFFICIENCY
STOP
-
-
AQUIFER          (rperm) (rpor) (r0)
-
rperm            permeability (=1 for dimensionless input)
rpor             porosity of the aquifer
r0               radius for all wells
-
In case of a new problem, this command should preceed all other
data input commands.
-
-
REFERENCE        (x) (y) (H)
-
x,y              Location of a reference point where heads
                 are assumed unaffected
H                head at the reference point (initial head if
                 only transient wells are introduced)
                 Select H=1 for dimensionless input
-
-
WELL             (x) (y) (Q)
-
x,y              location of steady state well
Q                discharge
-
Note:  Transient wells are prompted for upon giving the
       command SOLVE GROUNDWATER
```

```
-
-
LINESINKS       (x1) (y1) (x2) (y2) (H)
-
x1,y1           starting point of a line sink
x2,y2           end point of a line sink
H               head at the center of a line sink
-
Note:  If line sinks are introduced, a triangle network
       must be added by using the command TRIANGLE
-
-
UNIFLO          (x) (y) (Qx) (Qy)
-
x,y             point where head remains unaffected
                by uniform flow
Qx,Qy           uniform flow vector
-
-
TRIANGLE        (x1) (y1) (x2) (y2) (NT)
-
x1,y1           lower left-hand corner of network
x2,y2           upper right-hand corner of network
NT              approximate number of triangles
-
Note:  Triangles are produced with approximately equal
       rectangular sides, which may lead to less than
       NT triangles for a given domain
-
-
THERMAL
-
                Routine prompts for thermal constants and the
                thicknesses of the vadose zone and the aquifer base.
                (Recommended values for the thicknesses of
                the aquifer base d1 and vadose zone d2 are:
                d1=0.2   and    d2=0.1)
-
-
WINDOW          (x1) (y1) (x2) (y2)
-
x1,y1           lower left-hand corner of domain to be plotted
x2,y2           upper right-hand corner of domain to be plotted
-
-
DEBUG
-
                Enters debugging program, which has its own
                command summary display. The debugging program
                allows every common block and every array
                element to be examined. Every function in
                UCATES may be examined separately under control
                of the DEBUG program
-
-
```

```
LOG             (on/off)
-
on              echo's all output from program DEBUG to
                logical unit ILU4 (see DEFAUL routine)
                and plots the tracing of thermal markers
off             prevents above actions
-
-
SWITCH          (file name/device name)
-
                Input is read from the specified device
                or file. Default: consol
-
-
RESET
-
                Command reinitializes the data base
-
-
SAVE            (file name)
-
                Creates a file and writes all common blocks
                to that file
-
-
GET             (file name)
-
                Reads all common blocks from a file
-
-
WRITE           (file name)
-
                Creates a file and writes grid data for
                contour plots of heads or isotherm data
                to that file
-
-
READ            (file name)
-
                Reads grid data for contour plots of
                heads or isotherm data from file
-
-
LAYOUT
-
                Plots a layout of all elements in the
                flow domain, including the triangle network
-
-
SOLVE           (Groundwater/temperatures)
Groundwater     prompts for new transient wells,
                prompts for times at which to calculate
                a solution.
                message: Groundwater solution is ready
Temperatures    prompts for end of injection/storage/
```

```
                    recovery
                    injection: prompts for temperature increments
                               along flow paths, number of flow
                               paths per well and approximate
                               time step (for Runga-Kutta routine)
                    storage  : prompts for approximate time step
                    recovery : prompts for number of sectors per
                               well and approximate time step.
                               prompts for temperature in the well
                               at the onset of recovery (data to be
                               obtained from the isotherms at the
                               end of storage)
-
-
POTENTIAL           (x) (y) (t)
-
x,y                 location where potential will be calculated
t                   time from which potential will be calculated
-
Note:  t must be with the time span for which a groundwater
       flow solution has been generated
-
-
DISCHARGE           (x) (y) (t)
-
x,y                 location where the discharge vector Qx+iQy
                    will be calculated
t                   time for which the discharge will be calculated
-
Note:  t must be with the time span for which a groundwater
       flow solution has been generated
-
-
GRID                (NX) (T)
-
(NX)                number of increments along the horizontal
                    base of the window (see also WINDOW command)
(T)                 time for which heads are to be plotted
-
Note:  generates a grid of heads to be contoured by use
       of the command PLOT (heads). NX determines the
       resolution (limited to 40)
-
-
PLOT                (heads/isotherms/well)
-
heads:              must have been preceded by a GRID command
                    or an appropriate READ command.
                    displays minumum and maximum level in the
                    grid and prompts for the min. level and
                    increment for contours
isotherms:          prompts for the temperatures to be displayed.
                    plots dots in the domain for each temperature
                    and reports which temperatures were
                    plotted
```

```
well:          prompts for a recovery well number and plots
               the temperature distribution versus the
               recovery time
-
-
EFFICIENCY
-
               Command may only be given after a recovery
               cycle has been solved by use of SOLVE
               TEMPERATUREs command. The thermal efficiency
               of the ATES simulation is displayed
-
-
STOP
-
               terminates program execution.
```

DISTRIBUTION

No of Copies

OFFSITE

US Department of Energy
Attn: E. Reimers
Office of Energy Systems Res.
Forrestal Bldg, CE-141 5E-052
Washington, DC 20585

US Department of Energy
Attn: K. Klein
Office of Energy Systems Res.
Forrestal Bldg, CE-141 5E-052
Washington, DC 20585

5 DOE Technical Information Center

Imre Gyuk
1201 Lyndale Drive
Alexandria, VA 22308

5 Dr. H. Haitjema
2323 Rock Creek Drive
Bloomington, IN 47401

Lawrence Berkeley Laboratory
Attn: C-F. Tsang
University of California
Bldg. 90, Room 1012-H
1 Cyclotron Road
Berkeley, CA 94720

Public Works Canada
Attn: E. Morofsky
C456 Sir Charles Tupper Bldg.
Riverside Drive and Heron Rd.
Ottawa, Ontario
K1A OM2 Canada

University of Alabama
Attn: C. Brett
School of Mines & Energy Development
Box 6282
University, AL 35486

No of Copies

3 University of Minnesota
Attn: Otto Strack
Dept. of Civil and Mineral Eng.
122 Civil and Mineral Eng Bldg
500 Pillsbury Drive S.E.
Minneapolis, MN 55455-D22D

US Dept. of Interior
Attn: Lucy Howton
Natural Resources Library
Serial Branch
Gifts and Exchange Div.
Washington, DC 20240

ONSITE

DOE Richland Operations Office

D. R. Segna

18 Pacific Northwest Laboratory

L. D. Kannberg (10)
L. W. Vail
Technical Information (5)
Publishing Coordination (2)